Modern, equatorial carbonates from Kepulauan Seribu, Indonesia: Facies, isotope geochemistry, and microplastic as a sedimentary component

Von der Fakultät für Georessourcen und Materialtechnik
der Rheinisch-Westfälischen Technischen Hochschule Aachen

zur Erlangung des akademischen Grades einer

Doktorin der Naturwissenschaften

genehmigte Dissertation

vorgelegt von **M.Sc.**

Dwi Amanda Utami

aus Jakarta, Indonesien

Berichter: Prof. Peter Kukla
Prof. Miriam Pfeiffer

Tag der mündlichen Prüfung: 31. März 2021

Abstract

Carbonates in the humid equatorial zone have characteristics that distinguishes them from their sub-tropical counterparts and therefore should be re-examined as a distinct depositional system. Equatorial carbonates are also known to share some similarities with cool water systems that can complicate the distinction between non-tropical and equatorial carbonates. Kepulauan Seribu is an isolated patch reef complex situated in the Java Sea (Indonesia) and is a typical example for a humid, equatorial carbonate system.

Microplastic pollution recently has been reported from coral reef systems all over the tropics, including Indonesia which is known as the second-largest contributor of mismanaged plastic waste to the ocean. Exposure to microplastics has negative impacts on coral health that in the long run threaten its ability to act as framework builders in coral reef systems. This study aims to investigate the processes that control the distribution of sedimentary and environmental facies of modern carbonate in Kepulauan Seribu. The study further evaluates the differences between humid equatorial carbonates and other carbonate systems, using isotope geochemistry in combination with XRD and SEM analysis. Additionally, to analyzes the controlling processes for microplastic dispersion and accumulation in reefs sediments. Surface sediment from the reef platforms of Pramuka, Panggang, and Semak Daun in the Kepulauan Seribu complex serve as the basis of this study.

Statistical analysis based on texture and composition reveal that there are four sedimentary facies; coral grainstone, coral packstone/grainstone, coral-mollusc packstone, and mollusc wackestone. The occurrence of mollusc wackestone in the lagoon is controlled by water depth, while sand apron and reef front do not show significant facies separation with water depth. The cooccurrence of these different facies in the same depth window is contrary to the common thought that changes in bathymetry should be reflected in facies changes. A satellite derived environmental facies map generated by an image analysis algorithm indicates that environmental facies distribution is mainly controlled by water depth, density of seagrass cover and coral abundance. The sand apron can be subdivided into three environmental facies with no, sparse and dense seagrass cover. The deeper water zone can be separated into shallow and deep subtidal parts of lagoons and platform margins. In the lagoon, satellite derived environmental facies directly correlates with sedimentary facies. No direct correlation of environmental facies to sedimentary facies was possible in the sand apron due to the heterogeneity and complexity of the environment. However, the mean sediment grain size is significantly smaller in areas of the sand apron colonized by dense seagrass.

A characteristic property of shallow water (<20 m) sediments from Kepulauan Seribu is their increased low-Mg calcite (LMC) content (~10%) derived from some genera of rotaliid foraminifers and bivalves. The relative abundance of these faunal elements in shallow waters might be related to at least temporary turbid conditions caused by sediment laden river runoff. This influence is also evidenced by the presence of low amounts of siliciclastic minerals below the regional wave base. Kepulauan Seribu carbonates are characterized by very low $\delta^{13}C$ and $\delta^{18}O$ values. This is related to the isotopically depleted riverine input. The $\delta^{13}C_{DIC}$ in riverine water is reduced by the contribution of ^{12}C from riverside mangroves. The depleted $\delta^{13}C$ signature in carbonates is further enhanced by the lack of green algae and inorganic carbonates and the abundance of coral debris. Low $\delta^{18}O$ values in carbonates are favored by the high water-temperatures in the equatorial setting. Deep atmospheric convection and intensive rains further contribute ^{18}O depleted freshwater in the river catchments, finally reducing salinity in the Java Sea. Since equatorial carbonates in SE Asia, including the Java Sea, are typically influenced by high turbidity and/or river runoff, the observed distinctively low isotope values likely are characteristic for equatorial carbonate systems in the region.

Microplastics are present as a sedimentary component in Kepulauan Seribu. Microplastics were concentrated using density floatation and characterized by light and scanning electron microscopy. Some particles were identified as polypropylene using micro Fourier transform infrared (μFT-IR) spectroscopy. Phthalates, a common plastic additive, was detected on the surface of microplastic particles which demonstrates that contaminants associated with microplastics could become bioavailable to corals after ingestion. All recovered microplastics were classified as secondary microplastics, likely derived from marine and local sources, with fibers as the most abundant type. Microplastics are showing similar transport and accumulation behaviour as fine siliciclastic grains. Abundance of microplastic is controlled by the proximity to the source area of larger plastic debris and hydrodynamic processes. Microplastics are not only present in low energy environment but also in high energy settings such as e.g. the reef crest. Processes that contribute to accumulation in reef sediments are biofouling, interlocking, and the creation of compound grains. Microplastics are present in sediment close to the seafloor (0-3.5 cm) but also in a depth between 3.5 and 7 cm. Microplastic particles below 3.5 cm are unlikely to be remobilized under modal weather conditions in the studied equatorial reefs. Therefore, microplastics in subtidal reef environments from the equatorial zone can be a good practical indicator of Anthropocene strata.

Zusammenfassung

Karbonate in der feuchten äquatorialen Zone weisen Merkmale auf, die sie von ihren subtropischen Gegenstücken unterscheiden, und sollten daher als eigenständiges Ablagerungssystem erneut untersucht werden. Es ist auch bekannt, dass äquatoriale Karbonate einige Gemeinsamkeiten mit Kaltwassersystemen aufweisen, die die Unterscheidung zwischen nicht-tropischen und äquatorialen Karbonaten erschweren können. Kepulauan Seribu ist ein isolierter Flecken-Riffkomplex in der Javasee (Indonesien) und ist ein typisches Beispiel für ein feuchtes, äquatoriales Karbonatsystem.

In jüngster Zeit wurde über Verschmutzung durch Mikroplastik aus Korallenriffsystemen im kompletten tropischen Bereich berichtet, darunter auch aus Indonesien, das als zweitgrößter Emittent schlecht gemanagter Kunststoffabfälle im Ozean bekannt ist. Die Exposition gegenüber Mikroplastik hat negative Auswirkungen auf die Gesundheit der Korallen, die langfristig ihre Fähigkeit bedrohen, als Gerüstbildner in Korallenriffsystemen zu wirken. Ziel dieser Studie ist es, die Prozesse zu untersuchen, die die Verteilung der Sediment- und Umweltfazies des modernen Karbonats in Kepulauan Seribu kontrollieren. Die Studie evaluiert ferner die Unterschiede zwischen feuchten äquatorialen Karbonaten und anderen Karbonatsystemen, wobei die Isotopengeochemie in Kombination mit RDS- und REM-Analysen verwendet wird. Zusätzlich analysiert die Studie die Kontrollprozesse für die Dispersion und Akkumulation von Mikroplastik in Riffsedimenten. Oberflächensedimente von den Riffplattformen von Pramuka, Panggang und Semak Daun im Kepulauan-Seribu-Komplex dienten als Grundlage dieser Studie.

Statistische Analysen auf der Grundlage von Textur und Zusammensetzung zeigen, dass es vier sedimentäre Fazies gibt: coral grainstone, coral packstone/grainstone, coral-mollusc packstone, and mollusc wackestone. Das Vorkommen von mollusc wackestone in der Lagune wird durch die Wassertiefe kontrolliert, während Sandflächen und die Rifffront keine signifikante Faziestrennung mit der Wassertiefe zeigen. Das Zusammentreffen dieser verschiedenen Fazies im gleichen Tiefenfenster widerspricht der allgemeinen Auffassung, dass Veränderungen in der Bathymetrie sich in Veränderungen der Fazies widerspiegeln sollten. Eine von Satellitendaten abgeleitete Karte der Umweltfazies, die durch einen Bildanalyse-Algorithmus erstellt wurde, zeigt, dass die Verteilung der Umweltfazies hauptsächlich durch die Wassertiefe, die Dichte der Seegrasbedeckung und den Korallenreichtum gesteuert wird. Das Sandflächen kann in drei Umweltfazies mit keiner, spärlicher und dichter Seegrasbedeckung unterteilt werden. Die tiefere Wasserzone kann in flache und tiefe subtidale Teile von Lagunen und Plattformrändern unterteilt werden. In der Lagune korreliert die von Satelliten abgeleitete Umweltfazies direkt mit der sedimentären Fazies. In Sandflächen war aufgrund der Heterogenität und Komplexität der Umwelt keine direkte Korrelation der Umweltfazies mit der sedimentären Fazies

möglich. Allerdings ist die mittlere Sedimentkorngröße in Bereichen der Sandflächen, die von dichtem Seegras besiedelt sind, deutlich geringer.

Eine charakteristische Eigenschaft von Flachwassersedimenten (<20 m) aus Kepulauan Seribu ist ihr erhöhter Gehalt (~10%) an niedrig Mg Kalzit (LMC), der von einigen Gattungen rotaliider Foraminiferen und Muscheln stammt. Die relative Häufigkeit dieser Faunenelemente im seichten Wasser könnte mit zumindest vorübergehenden trüben Bedingungen zusammenhängen, die durch sedimentbelasteten Flusseintrag verursacht werden. Dieser Einfluss wird auch durch das Vorhandensein geringer Mengen an siliziklastischen Mineralien unterhalb der regionalen Wellenbasis belegt. Karbonate aus Kepulauan Seribu zeichnen sich durch sehr niedrige $\delta^{13}C$ und $\delta^{18}O$ Werte aus. Dies hängt mit dem Flusseintrag zusammen. Der Wert von $\delta^{13}C_{DIC}$ im Flusswasser wird durch den Beitrag von ^{12}C aus Ufer-Mangroven reduziert. Die niedrige $\delta^{13}C$ Signatur in den Karbonaten wird durch das Fehlen von Grünalgen und anorganischen Karbonaten und den hohen Anteil an Korallenschutt noch verstärkt. Niedrige $\delta^{18}O$ Werte in Karbonaten werden durch die hohen Wassertemperaturen in der äquatorialen Umgebung begünstigt. Tiefe atmosphärische Konvektion und intensive Regenfälle tragen weiter dazu bei, dass der Niederschlag in den Flusseinzugsgebieten niedrige $\delta^{18}O$ Werte aufweist. Da äquatoriale Karbonate in Südostasien, einschließlich der Javasee, typischerweise durch hohe Trübung und/oder Flusseintrag beeinflusst werden, sind die beobachteten ausgesprochen niedrigen Isotopenwerte wahrscheinlich charakteristisch für äquatoriale Karbonatsysteme in der Region.

Mikroplastik-Partikel sind als sedimentäre Komponente in Kepulauan Seribu vorhanden. Die Mikroplastik-Partikel wurden mittels Dichteflotation konzentriert und durch Licht- und Rasterelektronenmikroskopie charakterisiert. Einige Partikel wurden mittels Mikro-Fourier-Transformations-Infrarotspektroskopie (µFT-IR) als Polypropylen identifiziert. Phthalate, ein gebräuchliches Plastikadditiv, wurde auf der Oberfläche von Mikroplastikpartikeln nachgewiesen, was zeigt, dass Verunreinigungen, die mit Mikroplastiken assoziiert sind, nach der Aufnahme für Korallen bioverfügbar werden könnten. Alle zurückgewonnenen Mikroplastikteile wurden als sekundäre Mikroplastikteile klassifiziert, die wahrscheinlich aus marinen und lokalen Quellen stammen, wobei Fasern am häufigsten vorkommenden. Mikroplastik-Partikel zeigen ein ähnliches Transport- und Akkumulationsverhalten wie feine silikatische Körner. Die Häufigkeit von Mikroplastik wird durch die Nähe zum Quellgebiet von größeren Kunststofffragmenten und hydrodynamischen Prozessen gesteuert. Mikroplastik findet sich nicht nur in Ablagerungsbereichen mit niedriger, sondern auch mit hoher Energie, wie z.B. den Riffkamm. Prozesse, die zur Akkumulation in Riffsedimenten beitragen, sind Biofouling, Verzahnung und die Bildung von Verbundkörnern. Mikroplastik-Partikel sind in Sedimenten in der Nähe des Meeresbodens (0-3,5 cm), aber auch in einer Tiefe zwischen 3,5 und 7 cm vorhanden. Es ist unwahrscheinlich, dass Mikroplastikpartikel unterhalb von 3,5 cm während modalen Wetterbedingungen in den untersuchten äquatorialen Riffen remobilisiert werden. Daher können Mikroplastikpartikel in subtidalen Riffumgebungen aus der äquatorialen Zone ein guter praktischer Indikator für Schichten des Anthropozän sein.

Contents

Acknowledgements

I am forever grateful to Lars Reuning, without his guidance writing this thesis would not be possible. I am thankful to Peter Kukla for his support in any respect during all the years. My gratitude to Miriam Pfeiffer for her endless support and her willingness to review my works. My special thanks to Stefan Back for always being supportive.

I highly acknowledge Lembaga Pengelola Dana Pendidikan for funding my study and thesis. My special appreciation to Geotechnology Research Center, LIPI for all the support during my study years.

I thank Philipp Binger and Uwe Wollenberg for their help with sample preparation and measurement. Mykhaylo Anokhin is thank for his help with computer issues. I express my gratitude to Christine Riemann, Nicole Jennisen, and Conny Luther for their support at the Geological Institute.

I acknowledge Geosciences Institute of Kiel University, Birgit Mohr, Angela Trumpf, Claudia Müller, and Konabe Watanabe for their endless support.

Special thanks to all my colleagues; Nabel, Hanaa, Maike, Kim, Mirjam, Throni, Max, Jörg, Tabea, Christoph, Sebastian, Frank for the support and good memories.

To my mother, brothers, Nasution and Sutisna family, Alin, friends in Indonesia, Aachen, and Kiel which I cannot name one by one. I am blessed to have you all as my support system during good times and bad times.

Chapter 1

Introduction

1 Introduction

1.1 Study objectives

This thesis deals with reef platforms from the Kepulauan Seribu complex, Indonesia namely Panggang, Pramuka, and Semak Daun.

Cenozoic shallow marine tropical carbonates form major hydrocarbon reservoirs in various parts of the world. In Southeast Asia, Cenozoic carbonates are extensive, diverse, and often form hydrocarbon reservoirs in the subsurface (Wilson, 2002). Almost half the cumulative production and a sizeable proportion of the remaining oil and gas reserves in Indonesia are found in the Java Sea, offshore southeast Sumatra, and northwest Java. Reservoir quality and rock properties of carbonate reservoirs are often difficult to predict. Quantitative facies models from modern carbonate are essentials for the interpretation of their fossil counterparts. However, most modern analogue studies for carbonate systems come from subtropical latitudes. Southeast Asian equatorial carbonates are somewhat different from their subtropical counterparts and therefore should be re-examined as distinct depositional systems (Wilson, 2002, 2012; Park *et al.*, 2010).

The small, isolated carbonate platforms forming the islands of the Kepulauan Seribu complex provide useful modern analogue for buried carbonate systems in Indonesia (Park *et al.*, 1995; Wilson, 2002) and other similar Cenozoic carbonates from Southeast Asia and northern Australia (Rosleff-Soerensen *et al.*, 2016; Belde *et al.*, 2017). Sediment distribution patterns form the fundamental studies on sediment formation, redeposition, sediment dynamics and early diagenesis in modern reefs and carbonate platforms (Gischler, 2011; Gischler *et al.*, 2017). This research aims to use conventional field-based and satellite-based mapping to gain dimensional data about sediment distribution pattern. The combination of statistical satellite image analysis and sediment data was recently proposed as a technique for producing satellite derived facies maps for carbonate platforms (Kaczmarek *et al.*, 2010).

Key questions for this study are: What controls sedimentary and environmental facies of modern carbonate in Kepulauan Seribu? Does facies distribution in shallow water carbonate related to bathymetry?

During the last decade, the awareness has grown that carbonate systems in the humid equatorial zone have common characteristics that distinguishes them from carbonates in more arid regions (Tomascik *et al.*, 1997; Wilson & Vecsei, 2005). However, equatorial carbonates share some similarities with cool water systems. This can complicate the distinction between non-tropical and equatorial carbonates (Wilson & Vecsei, 2005). Wilson (2012) recommended the use of additional geochemical and isotopic proxies to identify warm temperatures and low salinities associated with equatorial carbonates in the rock record. A key region for the study of these humid equatorial carbonates is Southeast Asia, where the shallow shelfs are strongly affected by river runoff and/or upwelling (Tomascik *et al.*, 1997; Wilson, 2002). To investigate how far the mineralogy and stable isotope signature of shallow water (< 20m) equatorial carbonate from Kepulauan Seribu in the Java Sea are distinct from other carbonate systems, stable isotope ($\delta^{13}C$ and $\delta^{18}O$) analysis in combination with X-ray diffraction (XRD) and Scanning Electron Microscopy (SEM) were used.

An important question in this respect is: what are the mineralogic and isotopic fingerprints that characterized humid equatorial carbonates in Southeast Asia from other carbonates systems?

Only recently, microplastic pollution have been reported from coral reef systems all over the tropics including Indonesia. Exposure to microplastics have several negative impacts on coral health, such as bleaching, tissue necrosis or an impairment of the corals immune system. On the long run, microplastics therefore pose a threat to reef corals and their ability to act as framework builders in coral reef systems. Half of all plastics have a density greater than seawater (Morét-Ferguson *et al.*, 2010) and therefore eventually sinks to the seafloor, which is considered to be a major sink for global plastic (Van Cauwenberghe *et al.*, 2013; Woodall *et al.*, 2014). Integration of process based sedimentological knowledge with insights from modern sedimentary systems can provide crucial constraints on the transfer and distribution of microplastics to marine environments (Kane & Clare, 2019). This study investigates the distribution of microplastics in different environmental and sedimentary facies in a patch reef system from Kepulauan Seribu. Microplastics were concentrated from sediment using density floatation and characterized by stereomicroscopy, scanning electron microscopy, and micro Fourier transform infrared (µFT-IR) spectroscopy.

Key questions in this respect are: Which processes control microplastics transfer and distribution in reef platform environments? How does buoyant microplastic sink to the seafloor? What mechanism allows microplastics to be permanently buried in the reef sediment?

In summary, the main objectives of this thesis are to contribute towards a greater understanding of modern equatorial Southeast Asia carbonate systems (chapter 2), to investigate the mineralogical and isotopic signature of oligophotic equatorial carbonates (chapter 3), and to analyze the controlling processes for microplastic dispersion and accumulation in reefs sediments (chapter 4).

1.2 Structure of thesis

This thesis consists of five chapters. Chapter 1 gives a general introduction to the key study areas and the aims of the study. The following three chapters are written in publication format and the first one has been published in June 2018 in the international, peer-reviewed scientific journal."The Depositional Record" (Utami *et al.*, 2018). This chapter investigates the controls of sediment distribution patterns using conventional field-based and satellite-based mapping with the aid of multivariate statistical analysis. Chapter 3 has been accepted in November 2020 to the journal "International Journal of Earth Sciences" (Utami *et al*., accepted). This chapter shows that shallow water carbonates in Southeast Asia are different from their sub-tropical counterparts and can be distinguished according to their mineralogic and isotopic fingerprints. Chapter 4 has been submitted in October 2020 to the journal "Sedimentology" (Utami *et al*., subm). This chapter analyzes transport and accumulation behavior of microplastics particles in the reef platform environment. Chapter 5 summarizes chapters 2-4 and provides an outlook for future work.

1.3 Study Area: Kepulauan Seribu reef platforms

Kepulauan Seribu (The Thousand Islands) is located in the Java Sea, north of Jakarta Bay at 5°12’S to 6°02’S and 106°38’E to 106°28’E (Figure1-1A). Kepulauan Seribu consists of numerous coral reef islands ranging in size from a few meters across to length greater than one kilometer. From about 10 km off the northwest Java coastline, the island chain extends for about 50 km into the Java Sea (Figure1-1B). The focus of this research is the patch reef systems of Pramuka, Panggang, and Semak Daun which lies in the middle part of the reef platforms complex (Figure1-1C). Kepulauan Seribu is situated on the NNE-SSW structural high of the Seribu platform, which is separated from the Sunda Basin towards the west and Arjuna basin to the east by the active N-S oriented Seribu Fault system (Park *et al.*, 2010). The north - south elongation of the platform is largely controlled by the regional fault pattern that was established during the early Cenozoic and reactivated at various times since (Park *et al.*, 2010). The E-W oriented inter island channels that can be in places more than 50 m deep are the remains of a late Pleistocene drainage pattern that was later modified and truncated by river capture (Park *et al.*, 2010). Little is known about the internal architecture of the Seribu platform. Based on three shallow cores from two islands, Park *et al.* (1992, 2010) showed that modern reef growth initiated in the early Holocene. Vertical reef growth continued with a rate of 5–10 mm/year to around 4,500 years BP. This stage was followed by a slight late Holocene sea-level fall that led to lateral growth of the patch reef systems (Park *et al.*, 1992, 2010).

The patch reef system of Kepulauan Seribu is located on the shallow Sunda Shelf where it rises from a water depth of 30 - 50 meters to the sea surface. A deep and several kilometers wide, east - west oriented channel separates Pari Island to the south from most other islands to its north. It appears that this channel forms an important hydrologic barrier, channeling the sediment-laden coastal waters off Java and Kalimantan away from the reef (Tomascik *et al.*, 1997; Jordan, 1998). The reefal buildups on the platform vary in size and shape but most of them are elongated in a roughly east - west orientation. Each island and platform of Kepulauan Seribu is built up from the skeletal debris of coral reefs which rim the platform margins (Jordan, 1998). The steep reef front extends seaward from the reef crest to a depth of about 15 meters.

Well-developed reef facies occur down to a depth of about 16 - 18 m (Jordan, 1998). Reef framework builders at Kepulauan Seribu consist of a diverse fauna of Indo-Pacific corals and encrusting red algae. Below the base of continuous reef development, occurs a transition zone of small reef knolls or coralgal knobs that are surrounded by unconsolidated sediments. In water depths of about 24 meters, the seafloor becomes entirely sediment and begins to slope less steeply. Below the reef and near reef zone, in a depth from 27 to 88 meters occurs a foraminiferal molluscan packstone facies that is rich in terrigenous mud. The dominant bioclasts are benthic foraminifers, mollusc and coral fragments (Jordan, 1998). The sedimentation on the shelf further away from the direct influence of the reef system is dominated by siliciclastic mud.

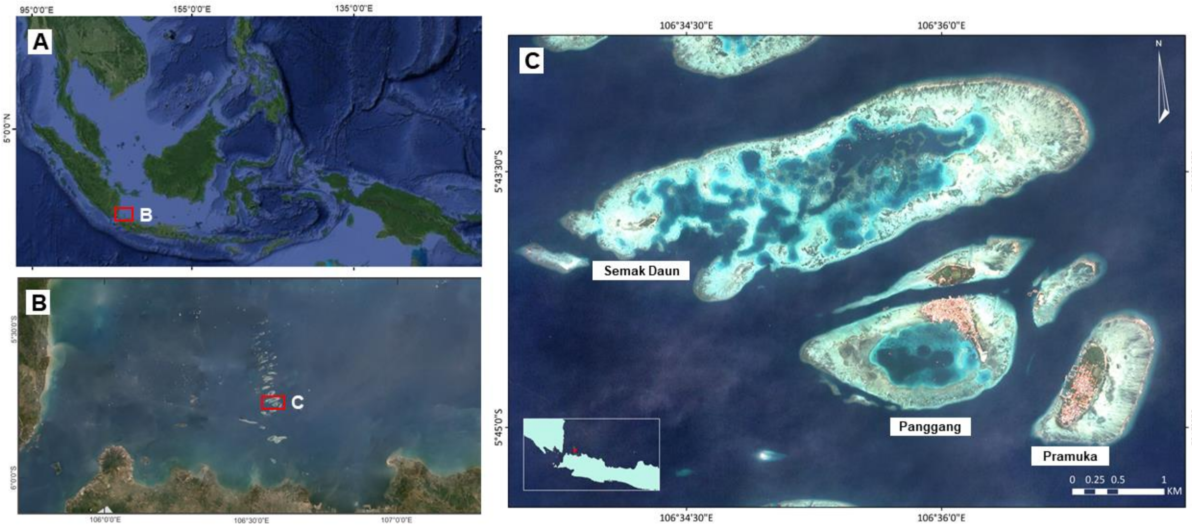

Figure 1-1. (A) Location map of Kepulauan Seribu in the Java Sea as the key study area (image from Google Earth). (B) Kepulauan Seribu complex that extends about 50 km into the Java Sea. The focus area of this study is situated in the middle part of the complex (image from Allen Coral Atlas. The Satellite Coral Reef Mosaic is *© 2019 Planet Labs and licensed CC BY_SA_NC 4.0).* (C) Sediment from Pramuka, Panggang, and Semak Daun reef platforms served as the basis of this study.

The controlling influence on modern reef growth and morphology in Kepulauan Seribu is believed to be the seasonal change in wind and current directions (Scrutton, 1976). The Java Sea is characterized by a monsoonal climate with a seasonal reversal between the West Monsoon (December – February), and the East Monsoon (April - October). The West Monsoon winds are known to be stronger than the East Monsoon winds, but less persistent (3 vs. 7 months). The East Monsoon winds therefore are the dominant factor for the net sediment transport (Poerbandono, 2016). The climate in Kepulauan Seribu is tropical with relative humidity of 80 to 90% (Tomascik *et al.*, 1997). The maximum sea surface temperature (SST) is observed in April (29.8°C) and minimum in January (28.6°C) (Cahyarini *et al.*, 2016). Surface salinity in the Java Sea (30-34‰) is well below normal open ocean levels, reaching as low as 22‰ in the vicinity of some of the larger river mouths. The low salinity of the Java Sea is due to heavy precipitation and intensive river runoff from Java and Kalimantan (Sofian &

Kozai, 2007). The water column of the shallow western Java Sea is well mixed and shows little temperature or salinity stratification (Hamzah *et al.*, 2020). The tidal range in Kepulauan Seribu is micro tidal, averaging about 52 cm with a range from 15 to 82 cm and a typical diurnal tidal cycle with one high and one low stand per day (Wyrtki, 1962). Generally, surface currents in Kepulauan Seribu show a maximum speed of 0.5 m/s (Farhan & Lim, 2011). Wave height in Kepulauan Seribu varies between 0.5 and 1 m during the east monsoon and between 2 and 3 m during the west monsoon, while mean wave speed is only 1 knot due to the wave absorption by the island chain (Sachoemar, 2008).

References

Baum, G., **Januar, H.I.**, **Ferse, S.C.A.** and **Kunzmann, A.** (2015) Local and Regional Impacts of Pollution on Coral Reefs along the Thousand Islands North of the Megacity Jakarta, Indonesia. *PLoS One*, **10**, e0138271.

Belde, J., **Back, S.**, **Bourget, J.** and **Reuning, L.** (2017) Oligocene and Miocene Carbonate Platform Development In the Browse Basin, Australian Northwest Shelf. *J. Sediment. Res.*, **87**, 795–816.

Cahyarini, S.Y., **Zinke, J.**, **Troelstra, S.**, **Suharsono**, **Aldrian, E.** and **Hoeksema, B.W.** (2016) Coral Sr/Ca-based sea surface temperature and air temperature variability from the inshore and offshore corals in the Seribu Islands, Indonesia. *Mar. Pollut. Bull.*, **110**, 694–700.

Farhan, A.R. and **Lim, S.** (2011) Resilience assessment on coastline changes and urban settlements: A case study in Seribu Islands, Indonesia. *Ocean Coast. Manag.*, **54**, 391–400.

Gischler, E. (2011) Sedimentary Facies of Bora Bora, Darwin's Type Barrier Reef (Society Islands, South Pacific): The Unexpected Occurrence of Non-Skeletal Grains. *J. Sediment. Res.*, **81**, 1–17.

Gischler, E., **Isaack, A.** and **Hudson, J.H.** (2017) Sediments of the Dry Tortugas, south Florida, USA: Facies distribution on a ramp-like isolated carbonate platform. *Sediment. Geol.*, **351**, 48–65.

Gischler, E. and **Lomando, A.J.** (1999) Recent sedimentary facies of isolated carbonate platforms, Belize-Yucatan system, Central America. *J. Sediment. Res.*, **69**, 747–763.

Hamzah, F., **Agustiadi, T.**, **Susanto, R.D.**, **Wei, Z.**, **Guo, L.**, **Cao, Z.** and **Dai, M.** (2020) Dynamics of the Carbonate System in the Western Indonesian Seas During the Southeast Monsoon. *J. Geophys. Res. Ocean.*, **125**, 1–18.

Jordan, C.F. (1998) The Sedimentology of Kepulauan Seribu: A Modern Patch Reef Complex in the West Java Sea, Indonesia. *Indones. Pet. Assoc.*, 1–81.

Kaczmarek, S.E., **Hicks, M.K.**, **Fullmer, S.M.**, **Steffen, K.L.** and **Bachtel, S.L.** (2010) Mapping facies distributions on modern carbonate platforms through integration of multispectral Landsat data, statistics-based unsupervised classifications, and surface sediment data. *Am. Assoc. Pet. Geol. Bull.*, **94**, 1581–1606.

Kane, I.A. and **Clare, M.A.** (2019) Dispersion, Accumulation, and the Ultimate Fate of Microplastics in Deep-Marine Environments: A Review and Future Directions.

Front. Earth Sci., **7**, 80.

Kowalski, N., **Reichardt, A.M.** and **Waniek, J.J.** (2016) Sinking rates of microplastics and potential implications of their alteration by physical, biological, and chemical factors. *Mar. Pollut. Bull.*, **109**, 310–319.

Morét-Ferguson, S., **Law, K.L.**, **Proskurowski, G.**, **Murphy, E.K.**, **Peacock, E.E.** and **Reddy, C.M.** (2010) The size, mass, and composition of plastic debris in the western North Atlantic Ocean. *Mar. Pollut. Bull.*, **60**, 1873–1878.

Morgan, W.A., **George, A.D.**, **Harris, P.M.**, **Kupecz, J.** and **Sarg, J.F.** (2010) Cenozoic carbonate systems of Australasia - Introduction and Perspective. In: *Cenozoic Carbonate Systems of Australasia*, *SEPM Special Publication 95*, 3–9.

Park, R.K., **Crevello, P.D.** and **Hantoro, W.** (2010) Equatorial Carbonate Depositional Systems of Indonesia. In: *Cenozoic carbonate systems of Australasia* (Ed. W.A. Morgan, A.D. George, P.M. Harris, J.A. Kupecz, and J.F. Sarg), *SEPM Special Publication 95*, Tulsa, Oklahoma, 41–77.

Park, R.K., **Matter, A.** and **Tonkin, P.C.** (1995) Porosity Evolution in the Batu Raja Carbonates of the Sunda Basin - Windows of Opportunity. *Indones. Pet. Assoc. 24th Annu. Conv. Proc.*, 163–184.

Park, R.K., **Siemers, C.T.** and **Brown, A.A.** (1992) Holocene carbonate sedimentation, Pulau Seribu, Java Sea—the third dimension. In: *Carbonate Rocks and Reservoirs of Indonesia, A Core Workshop. Indonesian Petroleum Association, Jakarta*, 2–1 – 2–15.

Poerbandono (2016) Wind characteristics and the associated risk of erosion in Seribu Islands patch reef complexes, Java Sea, Indonesia. In: *The 5th International Symposium on Earthhazard and Disaster Mitigation. AIP Conf. Proc.*, 1730, 080001.

Rosleff-Soerensen, B., **Reuning, L.**, **Back, S.** and **Kukla, P.** (2016) The response of a basin-scale Miocene barrier reef system to long-term, strong subsidence on a passive continental margin, Barcoo Sub-basin, Australian North West Shelf. *Basin Res.*, **28**, 103–123.

Sachoemar, S.I. (2008) Karakteristik lingkungan perairan kepulauan seribu. *J. Air Indones.*, **4**, 109–114.

Scrutton, M. (1976) Aspects Carbonate Sedimentation in Indonesia. In: *Indonesian Petroleum Association, Proceeding 5th Annual Convention*, 179–193.

Sofian, I. and **Kozai, K.** (2007) Literature review of the climatology of the Java Sea. *Kobe Univ. Repos. Kernel*, 133–138.

Tomascik, T., **Mah, A.J.**, **Nontji, A.** and **Moosa, M.K.** (1997) The Ecology of the Indonesia Seas Volume VIII Part II. *Oxford University*, 1231–1239 pp.

Utami, D.A., **Reuning, L.** and **Cahyarini, S.Y.** (2018) Satellite- and field-based facies mapping of isolated carbonate platforms from the Kepulauan Seribu Complex, Indonesia. *Depos. Rec.*, **4**, 255–273.

Van Cauwenberghe, L., **Vanreusel, A.**, **Mees, J.** and **Janssen, C.R.** (2013) Microplastic pollution in deep-sea sediments. *Environ. Pollut.*, **182**, 495–499.

Wilson, M.E.J. (2002) Cenozoic carbonates in Southeast Asia: Implications for equatorial carbonate development. *Sediment. Geol.*, **147**, 295–428.

Wilson, M.E.J. (2012) Equatorial carbonates: an earth systems approach. *Sedimentology*, **59**, 1–31.

Wilson, M.E.J. and **Vecsei, A.** (2005) The apparent paradox of abundant foramol facies in low latitudes: Their environmental significance and effect on platform development. *Earth-Science Rev.*, **69**, 133–168.

Woodall, L.C., **Sanchez-Vidal, A.**, **Canals, M.**, **Paterson, G.L.J.**, **Coppock, R.**,

Sleight, V., **Calafat, A.**, **Rogers, A.D.**, **Narayanaswamy, B.E.** and **Thompson, R.C.** (2014) The deep sea is a major sink for microplastic debris. *R. Soc. Open Sci.*, **1**, 140317.

Wyrtki, K. (1962) Physical Oceanography of the Southeast Asian Waters By Klaus Wyrtki NAGA Report Volume 2. Scientific Results of Marine Investigations of the South China Sea and the Gulf of Thailand, 1959–1961. S.I.O., La Jolla, Calif., 1961. *J. Mar. Biol. Assoc. United Kingdom*, **42**, 707.

Chapter 2

Controls on sedimentary pattern

2 Satellite and Field Based Facies Mapping of Isolated Carbonate Platforms from the Kepulauan Seribu Complex, Indonesia

Dwi Amanda Utami[1,2], Lars Reuning[1], Sri Yudawati Cahyarini[1,2]
[1]Energy and Mineral Resources Group, Geological Institute, RWTH Aachen University, Germany
[2]Geotechnology Research Center, Indonesia Institute of Sciences LIPI. Bandung, Indonesia.

Published by The Depositional Record

Abstract

Quantitative facies models from modern carbonate are essential for the interpretation of their fossil counterparts. The isolated carbonate platforms of the Kepulauan Seribu archipelago has many atoll-like islands with reef belts exposed to bidirectional monsoon winds. Statistical analysis based on texture and composition reveal that there are four sedimentary facies; coral grainstone, coral packstone/grainstone, coral-mollusc packstone, and mollusc wackestone. The occurrence of mollusc wackestone in the lagoon is controlled by water depth, while the sand apron and reef front do not show significant facies separation with water depth. The co-occurrence of these different facies in the same depth window is contrary to the common thought that changes in bathymetry should be reflected in facies changes. The studied reef systems therefore show aspects of random and ordered facies distribution with respect to water depth. A satellite derived environmental facies map generated by an image analysis algorithm indicates that environmental facies distribution is mainly controlled by water depth, density of sea grass cover and coral abundance. The sand apron can be subdivided into three environmental facies with no, sparse and dense sea grass cover. The deeper water zone can be separated into shallow and deep subtidal parts of lagoons and platform margins. In the lagoon, satellite derived environmental facies directly correlated with sedimentary facies. No direct correlation of environmental facies to sedimentary facies was possible in the sand apron due to the heterogeneity and complexity of the environment. However, the mean sediment grain size is significantly smaller in areas of the sand apron colonised by dense sea grass. This study aims to contribute towards a better understanding of modern equatorial Southeast Asian carbonate systems, delineate modern carbonate facies based on sediment texture and composition with the aid of multivariate statistical analysis combined with statistic-based satellite mapping, and give insights regarding the correlation between depositional facies and water depth.

Keywords Atoll, coral, equatorial carbonate, Holocene, modern carbonate, Monsoon.

2.1 Introduction

Cenozoic shallow marine tropical carbonates form major hydrocarbon reservoirs in various parts of the world. In Southeast Asia, Cenozoic carbonates are extensive, diverse, and often form hydrocarbon reservoirs in the subsurface (Wilson & Evans, 2002). Almost half the cumulative production and a sizeable proportion of the remaining oil and gas reserves in Indonesia are found in the Java Sea, offshore southeast Sumatra and northwest Java (Fig. 2-1). These fields are hosted by Miocene carbonates of the Baturaja and Parigi Formation (Burbury, 1977; Fainstein, 1987; Bukhari *et al*., 1992; Park *et al*., 1995). Reservoir quality and rock properties of these carbonate reservoirs are often difficult to predict. Most modern analogue studies for carbonate systems come from sub-tropical latitudes, such as the Florida Reef Tract (Ginsburg, 1956; Enos, 1974), Belize atoll and barrier reefs (Purdy & Gischler, 2003), Great Bahama Bank (Purdy 1963a, b; Reijmer *et al*., 2012), the Hawaiian chain (Gross *et al*., 1969), the Great Barrier Reef (Orme *et al*., 1978) and the South Pacific (Gischler, 2011). However, Southeast Asian equatorial carbonates are somewhat different from their subtropical counterparts and therefore should be re-examined as distinct depositional systems (Gischler & Lomando, 1999; Park *et al*., 2010; Wilson 2002, 2012). Carbonate systems in Southeast Asia form a broad variety of platform types such as land attached shelves, isolated platforms or localized and/or ephemeral carbonates (Tomascik *et al*., 1997; Wilson, 2002). Carbonate deposition is often dominated by bioclastic assemblages, few non-skeletal grains and a notable absence of coated grains (Lees & Buller, 1972; Scrutton, 1976a, b; Jordan *et al*., 1993; Wilson, 2002). The small, isolated carbonate platforms forming the islands of the Kepulauan Seribu Complex therefore provide a useful modern analogue for buried carbonate systems in Indonesia (Park *et al*., 1995; Wilson, 2002) and other similar Cenozoic carbonates from Southeast Asia and northern Australia (Morgan *et al*., 2010; Rosleff-Soerensen *et al*., 2012, 2016; Belde *et al*., 2017). Sediment distribution patterns form the fundamental studies on sediment formation, redeposition, sediment dynamics, and early diagenesis in modern reefs and carbonate platforms (Gischler, 2011; Gischler *et al*., 2017).

Studies of modern carbonate systems in Kepulauan Seribu typically focus on their biota and ecology (Umbgrove, 1947; Hoeksema, 1991; Rachello-Dolmen & Cleary, 2007; De Voogd & Cleary, 2008; Farhan & Lim, 2011; Toruan *et al*., 2013; Cleary *et al*., 2014; Cahyarini *et al*., 2016), with only a few focusing on carbonate sedimentology (Scrutton 1976a, b; Park *et al*., 1992; Jordan *et al*., 1993). Major carbonate facies zones in Kepulauan Seribu were mapped based on grab and dive samples by Scrutton (1976a, b) and Jordan *et al*. (1993). However, a modern statistically based facies analysis for the Kepulauan Seribu complex is still lacking.

Conventional field-based mapping studies of carbonate platforms have long been used to gain dimensional data about sediment distribution patterns, while the satellite-based studies have the advantage of being able to cover larger areas in a more timely and cost-efficient manner. Satellite-based remote sensing has been established as a beneficial examination tool and has been extensively applied within the earth sciences, including the mapping of coral reef biota and bottom sediments (Lyzenga, 1981; Gischler & Lomando 1999; Kaczmarek *et al*., 2010; Madden *et al*., 2013; Purkis *et al*., 2015). Modern carbonate platforms are ideal for satellite-based studies as they generally are only covered by shallow and relatively clear water, which facilitates accurate characterization of satellite data in marine environments. The combination of statistical satellite image analysis and sediment data was recently proposed as a quantitative technique for producing satellite derived facies maps for carbonate platforms (Kaczmarek *et al*., 2010).

This study follows this approach intending to (1) contribute towards a greater understanding of modern equatorial Southeast Asia carbonate systems, (2) compare modern carbonate facies with satellite derived environmental facies maps (3) test to what degree the carbonate facies distribution on small patch reef systems is related to water depth.

2.2 Study Area

Situated on the outer shelf margin of Sumatra in the Java Sea, Kepulauan Seribu (Thousand Islands) consists of numerous coral reef islands ranging in dimension from a few metres across to length greater than 7 km. The archipelago commencing about 25 km northwest of the Java coastline, extends for about 40 km into the Java Sea. Kepulauan Seribu sits on a NNE-SSW structural high, the Seribu platform (Fig. 2-1), which is separated from the Sunda Basin towards the west by the still active N-S oriented Seribu Fault (Park *et al*., 2010). The N-S orientation of the Seribu platform likely is also inherited from this structural grain (Park *et al*., 2010). The E-W oriented inter island channels that can be in places more than 50 m deep are the remains of a late Pleistocene drainage pattern that was later modified and truncated by river capture. In this respect, the preceding topography has played an important role in establishing the location and nature of Holocene reefal carbonate build-ups in Kepulauan Seribu (Park *et al*., 1992). Little is known about the internal architecture of the Seribu platform. Based on three shallow cores from two islands, Park *et al*. (1992, 2010) showed that modern reef growth initiated in the early Holocene. Vertical reef growth continued with a rate of 5-10 mm/year to around 4,500 years BP. This stage was followed by a slight late Holocene sea-level fall that led to lateral growth of the patch reef systems (Park *et al*., 1992, 2010).

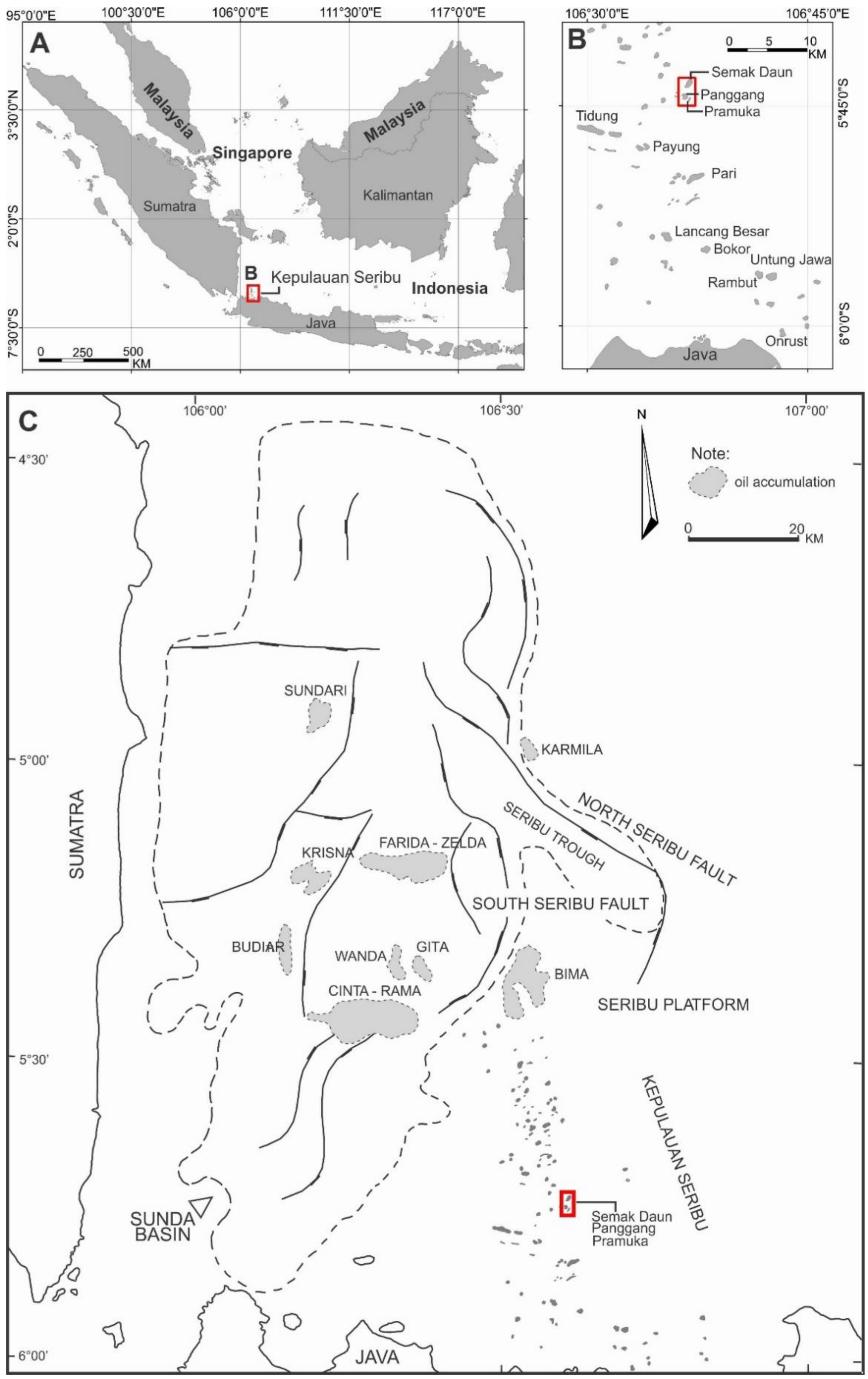

Figure 2-1. Study area as indicate in the red box (a) Kepulauan Seribu complex, Java Sea, Indonesia. (b) Location of Semak Daun, Panggang and Pramuka Island in the middle of Kepulauan Seribu complex. (c) Major structural features in the Sunda Basin and the Seribu Platform (after Fainstein, 1987).

The controlling influence on modern reef growth and morphology in Kepulauan Seribu is believed to be the seasonal change in wind and current directions (Scrutton, 1976a). The Java Sea is a relatively shallow sea with water depth generally between 40 and 50 m and only limited connection to the ocean. The Java Sea is characterized by the monsoonal wind with a seasonal reversal between the west monsoon (December – February), and the east monsoon (April – October). The east monsoon wind is two times more persistent than the west monsoon wind, but the west monsoon wind shows more extreme variations in wind strength (Poerbandono, 2016). The climate in Kepulauan Seribu is tropical with high air humidity of 80 mmHg, a mean temperature of 27°C and a seasonal cycle from 32.3°C to 21.6°C (Sachoemar, 2008). Salinity measurements in the west Java Sea indicate average values of 32‰ total dissolved salts, well below normal open ocean salinities. These relatively low salinities result from high seasonal rainfall and high runoff associated with the monsoonal climate. The tidal range in Kepulauan Seribu is micro tidal, averaging about 52 cm with a range from 15 to 82 cm and a typical diurnal tidal cycle with one high and one low stand per day (Wyrtki ,1962). Generally, surface currents in Kepulauan Seribu show a maximum speed of 0.5 m/s (Farhan & Lim, 2011). Wave height in Kepulauan Seribu varies between 0.5-1 m during the east monsoon and 2-3 m during the west monsoon, while mean wave speed is only 1 knot due to the wave absorption by the island chain (Sachoemar, 2008).

This study focuses on the patch reef systems of Panggang Island, Pramuka Island, and Semak Daun Island which are situated in the middle part of the Kepulauan Seribu chain (Fig. 2-1). Panggang Island is the island in Kepulauan Seribu with the highest population density and is separated from the less inhabited Pramuka Island by a shallow inter-reef channel. Panggang is an atoll-like reef with an approximate area of 3.2 km^2, and a central lagoon surrounded by reefs and its sand apron. From the reef flat, the water depth increases from about 1 m to about 20 m in the deepest part of the lagoon. Some of the reef on the reef crest will be exposed during low tide, showing various kinds of corals dominated by platy Acropora and foliated corals (Fig. 2-2). The sand apron on the eastern and western side of the lagoon is roughly two times wider compared to the sand apron on the northern and southern side (Fig. 2-3). Only one small inlet traverses the sand aprons allowing only very limited connection between the lagoon and the open sea. There are two small islands on the northeastern side of Panggang, preventing the reef system from direct wave exposure from the Java Sea. Pramuka is a fringing reef with an extensive reef flat on the eastern and northern part, while almost no reef flat exists on the western part (Fig. 2-3). The island itself lies on the southwestern part of the platform, emerging about 2 m above the sea surface. Most of the reef flat is covered by less than 1 m of water with no distinct reef crest observed. The reef slope on the western side reaches depths of approximately 20 m, while on the eastern side it falls off into much deeper water, reaching depths of about 40 m in the Java Sea. Semak Daun is a platform lagoon with an extensive reef flat surrounding a partially filled shallow lagoon with active coral growth in its center (Fig. 2-3). Similar to Panggang, the reef flat in Semak Daun is expanded broadly on the eastern and western side, leaving a narrow reef flat on the northern and southern side. Water exchange between the lagoon and the Java Sea is restricted to few inlets on its western side, while the eastern side of Semak Daun is directly exposed to the Java Sea.

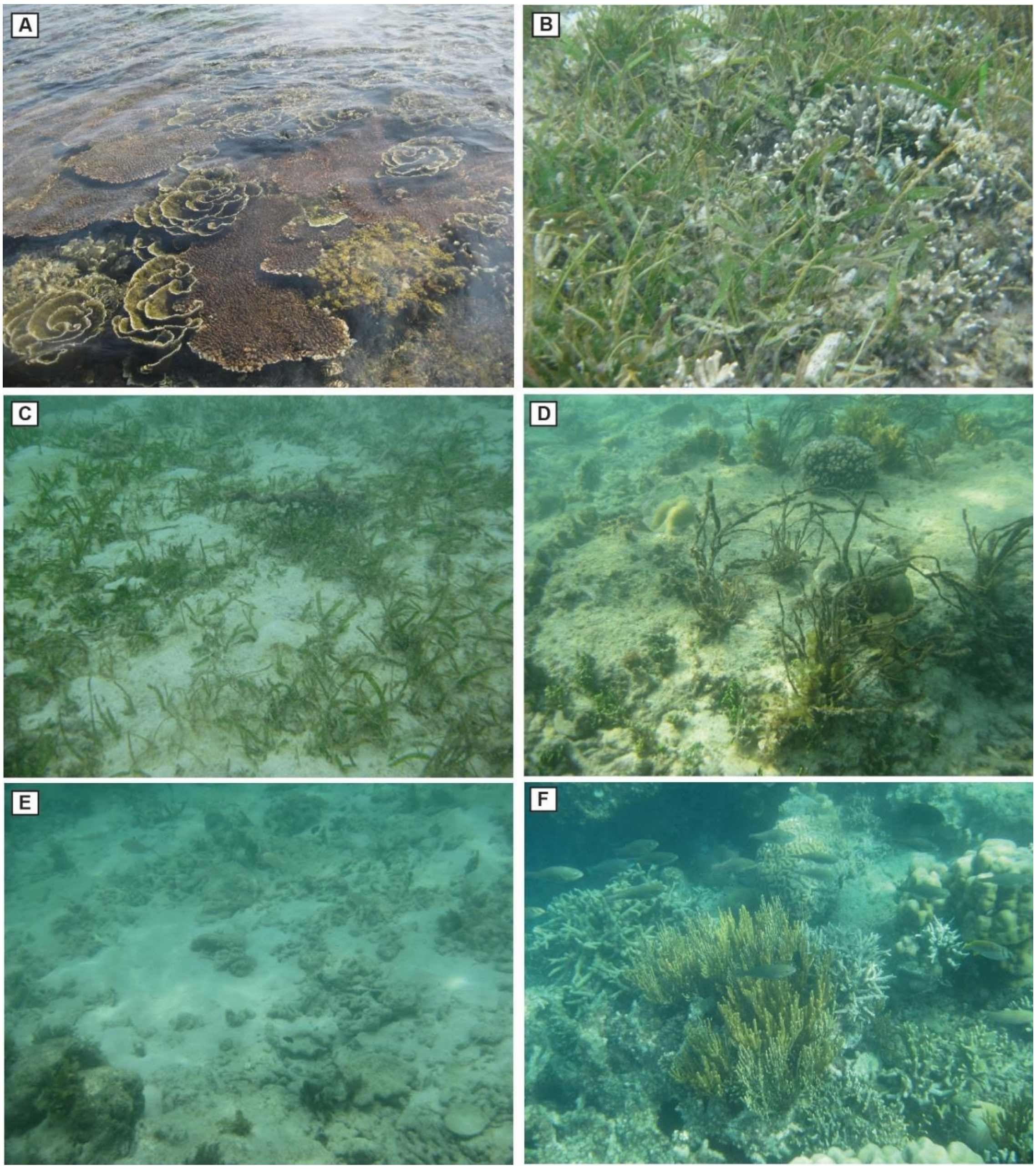

Figure 2-2. (a) Platy Acropora and foliaceous Montipora on the reef crest, south of Panggang lagoon, often exposed during low tide. (b) Sand apron with dense seagrass in Pramuka Island, individual corals often occur within the seagrass meadows. Underwater photograph of: (c) Sand apron with sparse short seagrass cover in Pramuka Island. (d) Sand apron with sparse seagrass, Halimeda, and small isolated coral heads in Panggang Island. (e) Sand apron without seagrass in Pramuka Island. (f) Coral framework on the reef front of Semak Daun Island.

2.3 Methods

A total of 102 surface sediment samples were collected from three islands in Kepulauan Seribu; Panggang (May 2015, 45 samples), Pramuka (May 2016, 32 samples), and Semak Daun (May 2016, 25 samples). In shallow water, sediments were collected by hand and water depth was measured using a marked stick. Sampling in the inner lagoon and at the reef slope was conducted by scuba diving and water depth was determined using the diving gear. Latitude and longitude of sampling locations were measured with a global positioning system (GPS) and plotted on SPOT-6/7 satellite imagery. In the laboratory, samples were washed in fresh water and dried using an oven set to 70°C for 7 hours. Dried samples were first sieved through a 125 µm sieve and a split of the coarse fraction was stored in a glass bottle for later point counting analysis. The remaining portion of the >125 µm fraction was sieved through 250 µm, 500 µm, 1 mm, and 2 mm sieves. All individual grain size fractions were weighed. Mean grain size and sorting were calculated using the software Gradistat (Blott & Pye, 2001). Sorting of samples was quantified as graphic standard deviation using the equation of Folk and Ward (1957). Values below 2 indicate moderate sorting, while values <4 and >4 indicate poor and very poor sorting, respectively. Point counting analysis was done on the split of the >125 µm fraction by counting 300 grains under a binocular microscope. Selected samples of the < 125 µm fraction were further analyzed using scanning electron microscopy in the SEM laboratory of FMIPA (Institut Teknologi Bandung) and the SEM/EDS laboratory of UPP Chevron-Prodi Geologi (Institut Teknologi Bandung). Correlation, cluster, and principle component analysis were conducted using the software package PAST (Hammer *et al*., 2001). Sediment samples were classified using a modified Dunham (1962) classification following the method outlined in Gischler *et al*. (2017) which proposed a threshold value of 50% matrix to separate mud supported from grain supported textures. Grainstone has 0-10%, packstone 10-50%, wackestone 50-90%, and mudstone 90-100% matrix. The <125 µm fraction was defined as matrix.

The relationship between water depth and facies diversity was explored using the Shannon evenness index (Shannon, 1948). Rankey (2004) employed the maximum entropy concept whereby divergence from a state of disorder is statistically assessed using the Shannon evenness index to examine facies diversity. Evenness (E) for each water depth is calculated following Purkis *et al*. (2015) as:

$$E = 1 - [(-\Sigma p_i \times \ ln p_i)/\ln(n)] \qquad (1)$$

whereby n is the number of facies and p is the proportion of each facies within a depth interval. Evenness (E) can reach values from zero to one, with values near one indicating that only one facies is present, meaning that the facies present can be predicted with confidence for a given water depth (Rankey, 2004; Purkis *et al*., 2015). Because the sample distribution is skewed towards shallow water-depth, the binning size of the depth intervals with water depth were increased following an exponential function ($f(x) = 2^x$), resulting in depth bins from 0-1 m, 1-3 m, 3-7 m, 7-15 m, etc.

A satellite-based facies map was produced by statistical analysis of the colour spectrum of high-resolution SPOT-6/7 satellite images to quantitatively discriminate between combined benthic sediment and biota types across the study area. This study applied the simplified workflow of Kaczmarek *et al*. (2010) with slight modifications to generate SPOT-6/7 derived environmental facies maps. The SPOT-6/7 satellite image was used in this study because the spatial high resolution (1.5 m) is expected to cover benthic diversity in the relatively small (± 24 km^2) study area. For this study, only the red, green, and blue bands were used due to low level returns from subsurface features within the panchromatic band which was deemed unsuitable for work below the ocean surface (Riegl *et al*, 2006), and due to almost no penetration potential of the infrared bands because of increasing absorption of the longer wavelength by water (Kaczmarek *et al*., 2010). Thus deeper water areas contain less data on which to classify (Kaczmarek *et al*., 2010). Because of this limitation, no environmental facies could be derived for some sampling points at the deeper part of the reef front.

Figure 2-3. Location and sorting of sediment samples.

SPOT standard products are delivered application ready, therefore there is no need for pan sharpened and orthorectified imagery in natural colours. Discrimination of bottom benthic sediments into distinct thematic classes was conducted using the spatial analysis tool “isocluster unsupervised classification” in ArcGIS. This method assessed each pixel in the satellite image by conducting a calculation based on a compilation of the spectral values of an individual band. Applying a large number of thematic classes in the unsupervised classification is critical for capturing the wide range of variability in sediment reflectance (Kaczmarek *et al*., 2010). In this study, 30 spectral classes were utilized to produce an environmental facies map, resulting in six distinct environmental facies groups which were subsequently validated with field observation.

2.4 Results

Texture

Most sediment samples are grain-supported (Tab. 2-1) and can be categorized as either grainstone (0% - 10% matrix) or packstone (10% - 50% matrix) in nearly equal abundance. Wackestone (50% - 90% matrix) is the only matrix-supported texture and forms only a small proportion of all sediment samples. In Panggang Island, the majority of sediment samples are grainstone, while packstones dominate in Pramuka and Semak Daun islands. Sorting is generally poor, but “very poorly sorted” samples also occur frequently (Fig. 2-3). Only one sample classified as “moderately sorted” was found on the eastern reef flat of Pramuka Island.

Sediment composition

Skeletal components, including fragments of corals and mollusc shells (Fig. 2-4) constitute most of the sediment in Kepulauan Seribu. Less abundant skeletal components are echinoderm spines, *Halimeda* flakes, crustose coralline algae, the red algae *Amphiroa* sp., foraminiferal tests, sponge needles, and tunicate spicule. The benthic foraminifera *Homotrema* sp. occurs pervasively, while *Calcarina* sp. is most abundant in sandy environments and *Amphystegina* sp. is most prolific at the reef slope. Non-skeletal grains generally are very rare, limited to only aggregates and peloids. Aggregates, usually ~ 3 mm in size, consist of bioclasts bound together by marine fibrous or microcrystalline cement. Peloids were sporadically found in the inner lagoon as opaque and cemented faecal pellets. The statistical analysis shows several statistically significant (p<0.05) and strong (r >0.6) correlations (Tab. 2-2). The fine fraction (<125 µm) content increases strongly with water depth (r=0.87), while the abundance of most bioclasts, and especially coral fragments, (r= -0.77) decreases. Other components, which encompass mainly unidentified grains and sponge spicules, show a moderate positive correlation (r= 0.36) to the fine fraction. The reason for this is likely the small grain-size of close to 125 µm for most of the unidentified grains.

Foraminifera abundance shows a negative correlation (r= -0.51) to the fine fraction indicating that most foraminifera seem to be adopted to sandy substrates.

Table 2-1. Sediment composition, texture and environmental facies for each sedimentary facies. Dunham texture: GST = grainstone, PST = packstone, WST = wackestone. Environmental facies: DSPL/PM = deeper subtidal part of lagoon/platform margin, SSPL/PM = shallower subtidal part of lagoon/platform margin, SRM/SC = subtidal reef margin/sparse coral, SAWDSG = sand apron with dense seagrass, SAWSSG = sand apron with sparse seagrass, SAWSG = sand apron without seagrass. *n* = number of samples.

Sedimentary Facies	n	Coral (%)	Red Algae (%)	*Halimeda* (%)	Mollusk (%)	Foraminifers (%)	Echinoderm (%)	Non Skeletal (%)	other (%)	Fines (%)	mean grainsize (µm)	sorting (µm)	Dunham			Environment					
													GST	PST	WST	DSPL/PM	SSPL/PM	SRM/SC	SAWDSG	SAWSSG	SAWSG
Coral Grainstone	22	59.5	2.9	3.9	16.6	6.8	3.2	0.3	0.2	6.5	620	3.32	77%	23%	-	-	-	6%	29%	29%	35%
Coral Packstone/Grainstone	50	49.0	2.5	5.5	24.5	5.8	3.3	0.2	0.8	8.3	573	3.56	66%	34%	-	-	-	5%	36%	48%	12%
Coral-Mollusk Packstone	18	37.2	3.0	2.5	21.2	4.8	4.6	0.4	3.0	23.3	293	5.89	-	100%	-	-	18%	27%	27%	27%	-
Mollusk Wackestone	12	12.8	0.5	0.3	17.9	1.5	3.4	0.7	7.1	55.9	99	6.26	-	33%	67%	73%	27%	-	-	-	-

Facies types

Principle component analysis shows three facies groupings that can be differentiated based on their grain-size and the relative importance of coral and mollusc fragments (Fig. 2-5). Relatively fine-grained sediments containing abundant molluscs form a broad group on the right side of the diagram. The central part of the diagram shows a group of samples which are very poorly sorted and contain corals besides molluscs as an important component. A large group of relatively coarse-grained samples on the right-hand side of the diagram is dominated by coral fragments. Using cluster analysis (Fig. 2-6) this group can be subdivided further into a grainstone (upper part) and a packstone/grainstone dominated facies. In summary, the combination of cluster and principal component analysis allows four facies to be distinguished: coral grainstone, coral packstone/grainstone, coral-mollusc packstone, and mollusc wackestone (Fig. 2-7, Tab. 2-1).

Coral grainstone

The coral grainstone facies is generally very poorly sorted and has the coarsest grain size (mean: 0.6 mm) of all facies in this area. The fine fraction content varies between 0%-15%, with a mean of 7% in packstones (20%) and grainstones (80%). Coral fragments are the most abundant components in this facies, on average reaching 60%. Molluscs are quite common and reach an average abundance of 17%, followed by foraminifera tests, which on average contribute 6%. Fragments of red algae, *Halimeda*, and echinoderms are also present in a limited amount of only 3-4% each. Non-skeletal

(0.3%) and other constituents (0.2%) are very rare. This facies occurs from the sand apron to the reef front in water depths of 0.3-2 m and sporadically at the deeper reef front from 15-20 m.

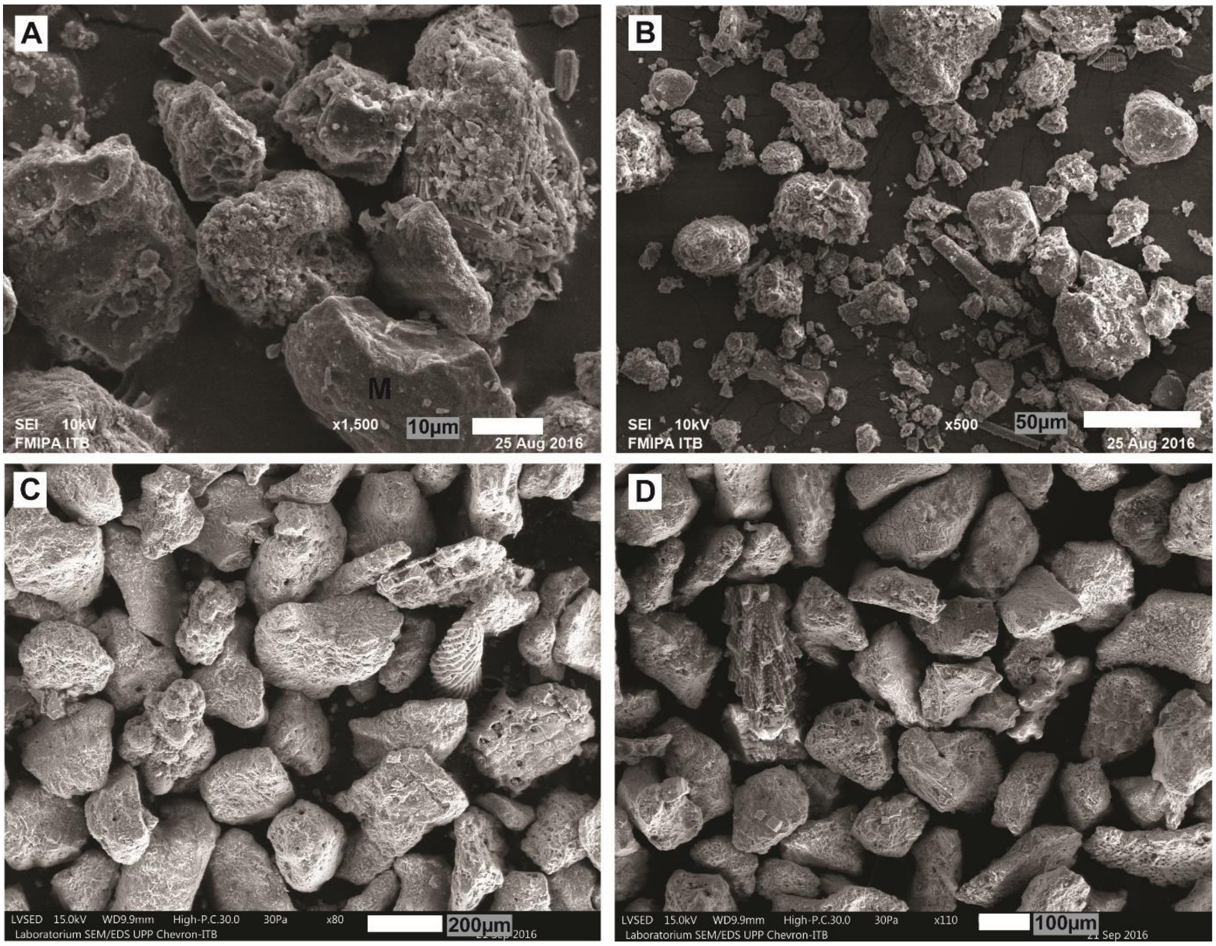

Figure 2-4. SEM images of fine fraction (<125 µm) from Panggang Island for samples: (a) MPG 4-1L located in the northwestern sand apron. (b) MPG 3-3A located in the lagoon. (c) MPG 2-4A located at the northern reef front. (d) MPG 3-1C located in the eastern sand apron. Bioclasts are the major sediment components.

Table 2-2. Correlation matrix: Significant ($p < 0.05$) correlations are marked bold. p-values in upper right part, r-values in lower left part.

	Coral	Red Algae	Halimeda	Mollusc	Foram	Echinoderm	Non Skeletal	other	Fines	water depth
Coral		0.02	0.01	0.74	<0.01	0.25	0.03	<0.01	<0.01	<0.01
Red Algae	**0.26**		0.85	0.02	<0.01	0.80	0.08	0.26	<0.01	0.04
Halimeda	**0.30**	0.02		0.35	<0.01	0.23	0.20	0.01	<0.01	<0.01
Mollusc	0.04	**-0.25**	0.10		0.11	0.80	0.76	0.27	0.01	<0.01
Foram	**0.31**	**0.41**	**0.44**	-0.17		0.68	0.45	0.03	<0.01	<0.01
Echinoderm	-0.13	0.03	-0.13	-0.03	0.05		0.06	0.98	0.95	0.50
Non Skeletal	**-0.24**	0.19	-0.14	0.03	-0.08	0.20		<0.01	0.88	0.84
other	**-0.56**	-0.12	**-0.28**	-0.12	**-0.24**	<0.01	**0.51**		<0.01	<0.01
Fines	**-0.87**	**-0.34**	**-0.48**	**-0.27**	**-0.51**	0.01	0.02	**0.36**		<0.01
water depth	**-0.77**	-0.23	**-0.45**	**-0.31**	**-0.34**	0.07	0.02	**0.33**	**0.87**	

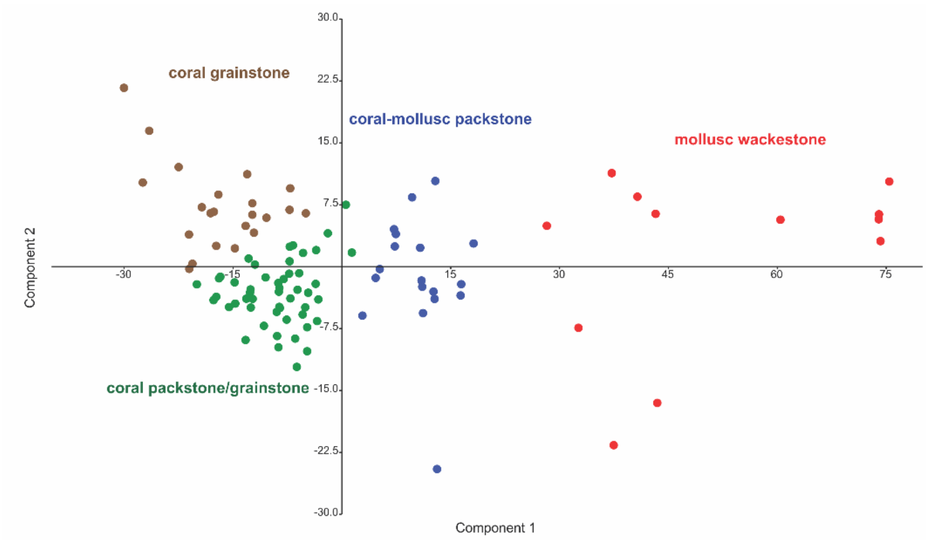

Figure 2-5. Principle component analysis using texture and composition data.

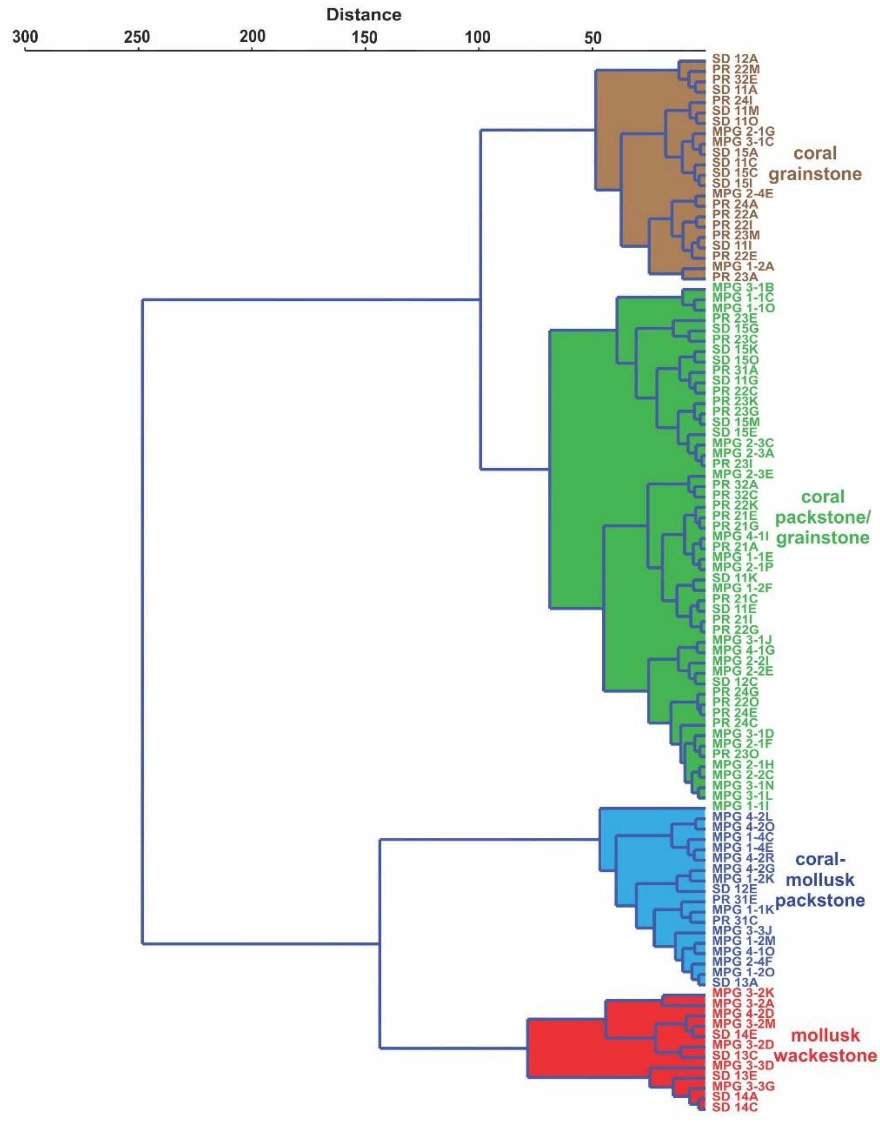

Figure 2-6. Tree diagram of a cluster analysis (Ward's method) based on texture and composition data.

Coral packstone/grainstone

Nearly 50% of all samples belong to the coral packstone/grainstone facies. It contains 0-21% fine fraction in grainstones (66%) and packstones (34%). Coral packstone/grainstones are characterized by a high amount of corals (49%) and mollusc fragments (25%), followed by a small number of foraminifera (6%), *Halimeda* (5%), echinoderms (3%), and red algae (2%). Non-skeletal grains occur only in trace amounts (0.5%). The mean grain size of this facies is 0.5 mm and the samples are dominantly poorly sorted. This facies can be found on the sand apron and reef front of Panggang, Pramuka, and Semak Daun Island in water depths between 0.3 m and 21 m (Fig. 2-7).

Coral-mollusc packstone

All samples in this group have 10%-50% matrix (mean:23%) and are classified as packstone. The amount of corals (37%) and molluscs (21%) is moderate, followed by foraminifera (5%), echinoderms (4%), red algae (3%), and *Halimeda* (2.5%). Non-skeletal grains are very rare (0.4%). The mean grain size of this facies is 0.3 mm and it can be classified as very poorly sorted. This facies occurs in water depths between 0.4 and18 m in the shallow part of lagoons, at parts of the reef front and sporadically on the sand apron of Panggang Island (Fig. 2-7).

Mollusc wackestone

This facies shows the highest fine fraction content with an average of almost 60%. The most common skeletal components in this facies are molluscs and corals. Foraminifera tests and echinoderm fragments contribute less than 2 and 4 %, respectively. *Halimeda*, red algae, and non-skeletal components are rare, contributing on average less than 1%. The mean grain size is ~ 0.1 mm and samples in this facies are generally very poorly sorted. This facies is found in water depths between 3 and 15 m at the reef slope and in the lagoons of Panggang and Semak Daun Island (Fig. 2-7).

Satellite derived environmental facies map

Six environmental facies (Fig. 2-8) have been derived by integrating SPOT-6/7 multispectral data, statistic based isocluster unsupervised classification, and ground-truthing with field observation. The sand apron can be subdivided into three facies with no, sparse and dense sea grass cover. One facies is formed by areas with active coral growth. The deeper water zone can be separated into a shallow and a deep subtidal part of lagoons and platform margins. Variation in reflectance can be attributed to benthic biota and water depth. In general, the environmental facies map (Fig. 2-8) indicates that the sand apron with sparse sea grass is the dominant environmental facies and the subtidal reef margin coral facies often occurs adjacent to the sand apron with dense sea grass cover. This might in part be due to the reflectance similarity of the chlorophyll-producing organisms which make coral reefs difficult to distinguish from loose sediments inhabited by sea grass (Luczkovich *et al*., 1993; Zainal *et al*., 1993; Kaczmarek *et al*., 2010). Field observations show that the natural complexity of benthic organism associations cannot be completely resolved by the satellite data. This is most apparent on the sand apron where usually small solitary coral lumps occur among algae and sea grass (Fig. 2-2). Cluster analysis has recognized four sedimentary facies whilst six environmental facies have been derived from the satellite data (Fig. 2-8, Tab. 2-1). In general, sedimentary facies do not correlate directly with environmental facies except for the mollusc wackestone facies that only occurs in lagoonal environments. In contrast, there is no close correspondence between the density of sea grass cover and sedimentary facies in the sand apron. Generally, the texture associated with the subtidal lagoon is wackestone, while packstone and grainstone textures dominate all environmental facies on the sand apron (Tab. 2-1).

2.5 Discussion

Distribution of sediment, carbonate components, and facies

Coral and mollusc are the most abundant sedimentary grains with minor contributions from *Halimeda*, red algae, foraminifera, and echinoderms (Tab. 2-1). Non-skeletal components occur only in trace amounts in the form of aggregates and faecal pellets (Tab. 2-1). In Panggang Island, coral fragments occur mainly at the reef front, where corals are actively growing (Fig. 2-8) and in the sand apron where the fragments are washed by waves and tides. In the lagoon, coral fragments are generally sparse (Fig. 2-9A), except in areas where corals are actively growing (Fig. 2-8). In Pramuka Island, coral fragments occur mostly in the sand apron near the island and reduce in numbers towards the outer sand apron and the reef front (Fig. 2-9B). A possible explanation for this trend indicated by satellite data (Fig. 2-8) and field observations (Fig. 2-2B and D) could be the local contribution from corals growing amongst the sea grass on the sand apron (Fig. 2-2B and D).

Mollusc debris occurs in all sedimentary and environmental facies zones and its distribution shows no clear pattern (Fig. 2-9C and D). This generally agrees with the notion of Scrutton (1976b) that molluscan debris is ubiquitous in the Seribu archipelago, a fact that distinguished the modern systems from their Neogene counterparts. Park *et al*. (2010) believe that the dominant easterly monsoon has formed a large bank consisiting of argillaceous foram – mollusc packstone along the western margin of the platform. However, field observation, sedimentary facies analysis (Fig. 2-7) and satellite derived environmental facies study (Fig. 2-8) shows no evidence to support this argument. Mollusc fragments are distributed relatively equally along the western and eastern part of the platform (Fig. 2-9C and D), suggesting the influence of bidirectional monsoon winds rather than an easterly domination.

Halimeda is generally a minor constituent (Fig. 2-9E and F) that occurs mainly in the sand apron and to a lesser degree on the reef front. It is virtually absent from the lagoon. This study agrees with the findings of Jordan *et al*. (1993) who reported that *Halimeda* is usually found in the reef flats and only locally concentrated at the reef front and contrary to the findings of Scrutton (1976b) who observed that *Halimeda* appears to be prolific on the reef flank (approximate depth 10 to 40 m). Nevertheless, the observations reported here cover only the shallow part of the reef flank (down to 22 m) and therefore does not rule out more abundant *Halimeda* growth below this depth.

Figure 2-7. Facies distribution based on sediment samples collected in this study as indicated by coloured dots.

Generally, the sedimentary facies of the studied patch reef systems is comparable to other equatorial carbonate systems from Indonesia. Madden *et al*. (2013) investigated foreshore/backshore and intertidal deposits of the Kaledupa-Hoga in Tukang Besi Archipelago offshore Southeast Sulawesi, Indonesia. They found a similar association of sand sized bioclasts dominated by coral and molluscs fragments and a general absence of fines and non-skeletal grains. They stress the role of waves and storms in the fragmentation and accumulation of these skeletal sands and coarse coral debris; a process also important in the monsoonal dominated system of Kepulauan Seribu. The shape of the mud sized sediment particles in the Seribu Archipelago also suggests that maceration and other physical processes play an important role in the breakdown of the skeletal components such as coral, mollusc, echinoderm, red algae, foraminifera (Fig. 2-4). Bioerosion, e.g. by the sponge *Cliona* seems to contribute to mud production (Fig. 2-4) but does not seem to play the dominant role suggested by Park *et al*. (2010). Clear evidence for other mud sources such as inorganic precipitation or bacterial induced precipitation as proposed by Scrutton (1976b) is lacking.

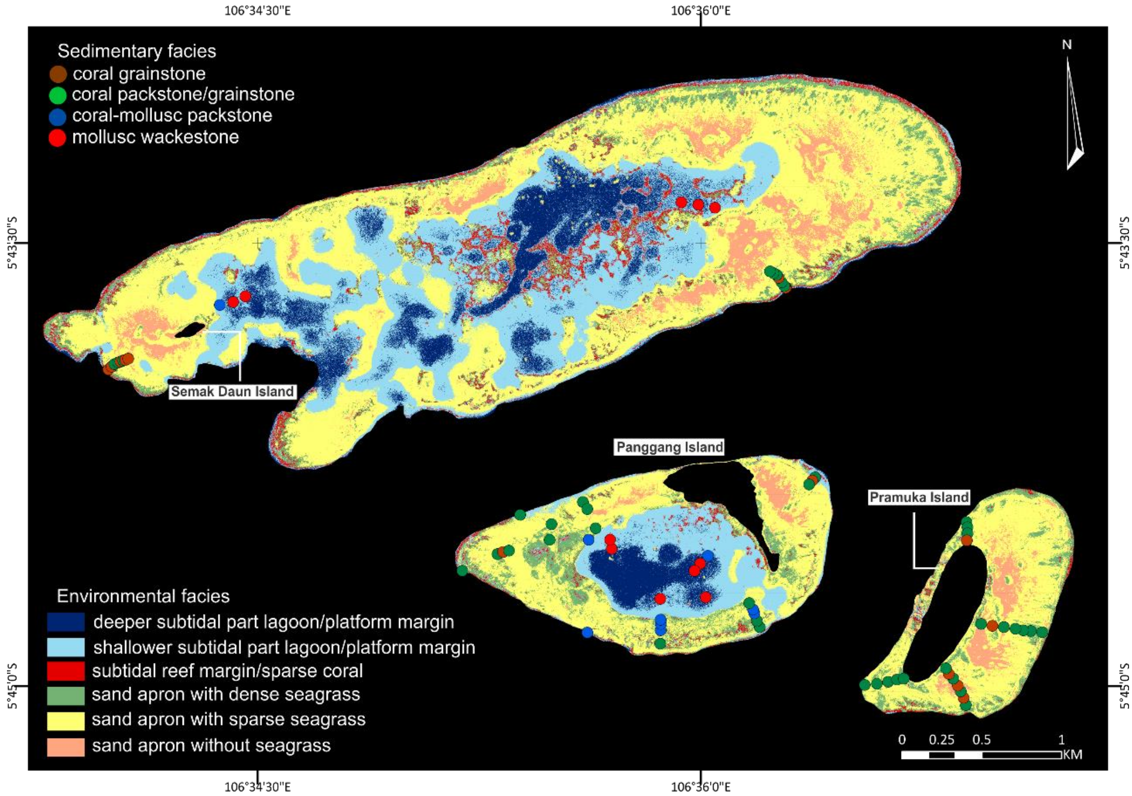

Figure 2-8. Satellite-derived environmental facies map generated by an image analysis algorithm for unsupervised classification. Sedimentary facies is shown for comparison as coloured dots. Ocean and land area have been masked. Classification results were subsequently validated with field observation.

The dominance of sand-sized grains is also apparent in Figure 2-10, that shows distinct trends in the distribution of the fine fraction (<125 µm) and mean grain size. At Panggang Island the fine fraction is concentrated in the center of the lagoon (Fig. 2-10A), which also corresponds to the finest mean grain size (Fig. 2-10C). The sand apron is characterized by coarser grained sediments and a low fine fraction content, whereas the reef front shows a generally finer mean grain size and an increase in the fine fraction content. In Pramuka Island, the coarser mean grain sizes and low fine fraction contents occur in the west-southwest sand apron and reef front which is exposed to waves and currents from the Java Sea (Fig. 2-10B). In contrast, the fine fraction and the finer mean grain sizes are concentrated in the east-northeast sand apron and reef front in more protected environments (Fig. 2-10D). This asymmetry in grain size distribution on Pramuka Island likely reflects the stronger wind force of the east monsoon compared to the west monsoon in the area. Poerbandono (2016) argued that this imbalance also results in a north – westward net drift of beach sediments. Another expression of the predominance of the eastern monsoon is likely the broader sand apron on the eastern side and the location of Pramuka Island on the more western side of the Seribu platform. In contrast, Panggang Island shows no pronounced morphological asymmetry in its east – west sand apron (Fig. 2-7) and grain size distribution, which likely results from its more sheltered position between the adjacent islands.

Correlation between water depth, sedimentary and environmental facies

There is no close correspondence between the environmental and sedimentary facies in the sand apron. This lack of congruency partly arises from the low fine fraction content on the wave and tide swept sand apron. A similar discrepancy between sedimentary texture and environmental facies has been described for other mud lean settings such as in the Holocene tidal carbonates from offshore Al Ruwais in Qatar (Purkis et al., 2017). Despite the absence of a direct correspondence between sedimentary and environmental facies in the sand apron, the satellite derived environmental facies map allow some predictions about the grain size distribution. This is apparent from the predominance of the coral grainstones and the lack of coral-mollusc packstones in the sand apron without seagrass (Tab. 2-1). Three different environmental facies can be distinguished on the sand apron, based on the density of sea grass cover (Fig. 2-8). Grain size differences in areas without and with sparse sea grass are statistically not significant, but areas with a dense sea grass cover are characterized by a significantly ($p<0.05$) finer sediment grain size compared to other areas on the sand apron (Fig. 2-11). The dense sea grass meadows effectively reduce current velocities and attenuate bed shear stress (Ward *et al*., 1984; Koch & Gust, 1999; Hansen & Reidenbach, 2012) thus resulting in a baffling effect which decreases sediment erosion and enhances particle deposition (Koch *et al*., 2006). Therefore, sediment in vegetated areas is usually finer and more organic rich compared to those in unvegetated areas (Kenworthy *et al*., 1982; Fonseca & Koehl, 2006). This baffling effect results in a slight increase in the fine fraction with denser sea grass cover and the generally finer grain sizes in the sand apron environment with dense sea grass cover (Fig. 2-11). An even clearer relationship between sedimentary facies and satellite derived environmental facies exists for the molluscs wackestone that occurs exclusively in the central lagoons of Panggang and Semak Daun (Tab. 2-1, Fig. 2-8). This correlation results likely from the strong control of water depth on the satellite derived map (Fig. 2-8) and the abundance of the fine fraction (Tab. 2-2). However, a distribution plot of the four sedimentary facies for the entire data set shows a large overlap of the four facies in water depth from 0 to 22 m. This results in a facies predictability of less than 40% and therefore an apparently low degree of ordering (Fig. 2-12A and B). If the data from the reef front is not considered, a high facies diversity is only observed in shallow waters less than 7 m in depth (Fig. 2-12C and D). On the other hand, a clear relationship between facies and water depth, and therefore a high predictability, can be observed for water depths below 7 m (Fig. 2-12C and D). The difference between the two scenarios basically results from the stronger wave and current exposure of the reef front compared to similar depths in the protected lagoon. This in part random or mosaic-like facies distribution is very different from the observation of Scrutton (1976b) who stated that the boundaries between major facies units are relatively sharp and also differs from the lithofacies maps of Jordan *et al*. (1993) which suggest broad, homogenous facies belts.

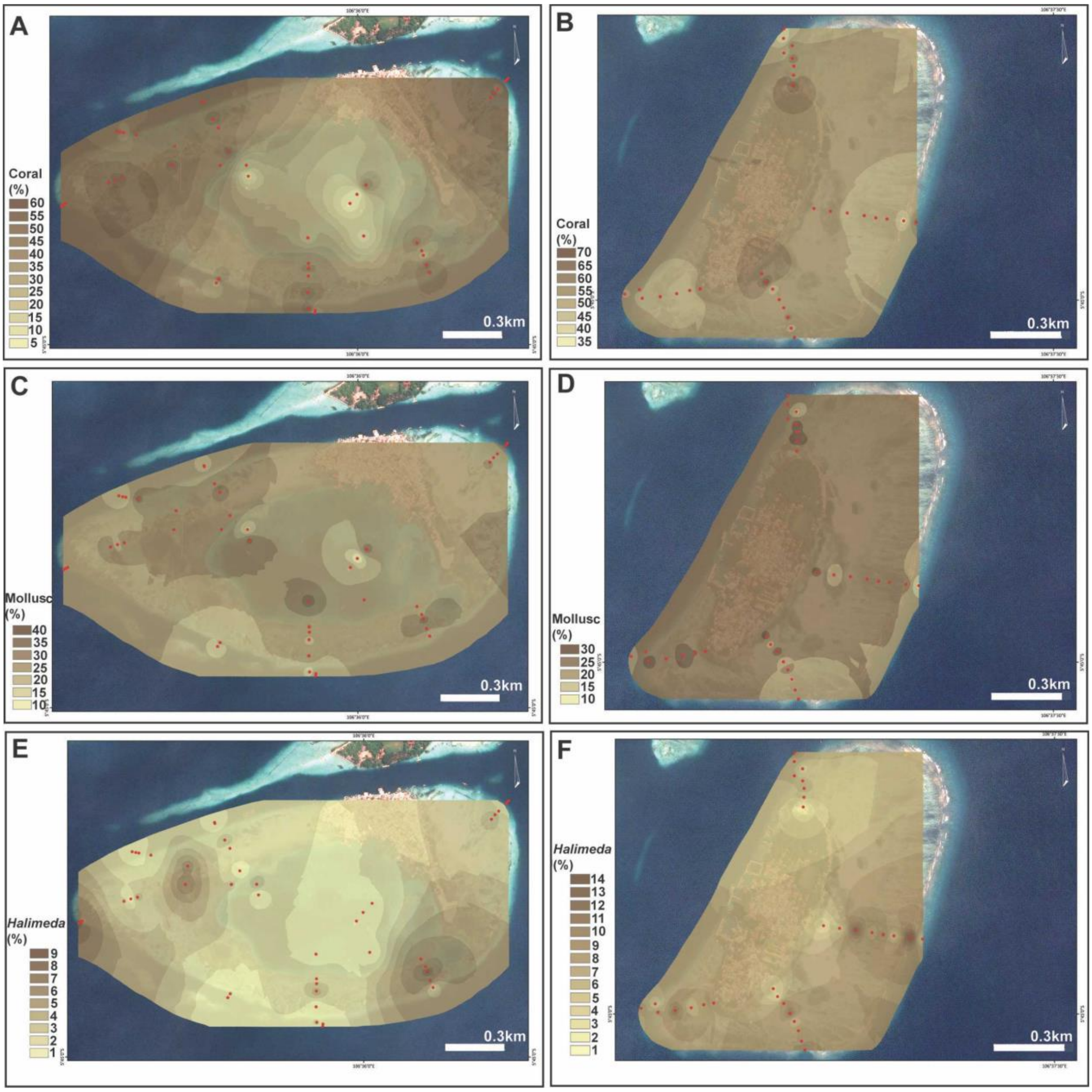

Figure 2-9. Distribution of coral fragments in (a) Panggang Island and (b) Pramuka Island. Distribution of mollusc fragments in (c) Panggang Island and (d) Pramuka Island. Distribution of Halimeda fragments in (e) Panggang Island and (f) Pramuka Island

Recent studies on carbonate sediment, especially in shallow water, have focused on whether facies distribution is related to bathymetry, questioning the long-held concept in carbonate geology that changes in water depth can be recognized through analysis of the lithofacies (Wilkinson *et al*., 1996; Rankey, 2002, 2004; Bosence, 2008; Purkis *et al*., 2015; Gischler *et al*., 2017). These authors briefly outline that the understanding of where and how carbonate sediments are produced and accumulated has evolved from the rather simple concept of direct productivity-depth relationships to the recognition that carbonate depositional environments are influenced to some degree by depth, and also by a complex suite of autogenic factors that lead to facies mosaics especially in shallow waters where sediments migrate and superimpose on each other over short distances as a result of subtle environmental changes. Purkis *et al*., (2015) showed that observations on the relationship between facies and water depth can be subdivided into three groups: indistinguishable from random (Wilkinson *et al*., 1996; Rankey, 2004; Purkis & Riegl, 2005; Purkis *et al*., 2015), deterministic order with respect to depth (Bosence, 2008; Maloof & Grotzinger, 2012), and incorporating aspects of both random and deterministic (Purkis & Vlaswinkel, 2012; Gischler *et al*., 2017). Study area scale and sampling density emerged to be a significant factor as well because large scale studies usually show a distinct relationship between facies and water depth whereas smaller areas and depth range do not seem to represent a clear cut relationship (Rankey 2004; Harris *et al* 2011; Purkis *et al*., 2015) and high resolution sediment maps are commonly more heterogeneous with facies mosaics instead of broad, homogenous facies belts (Kaczmarek *et al*., 2010; Purkis *et al*., 2012).

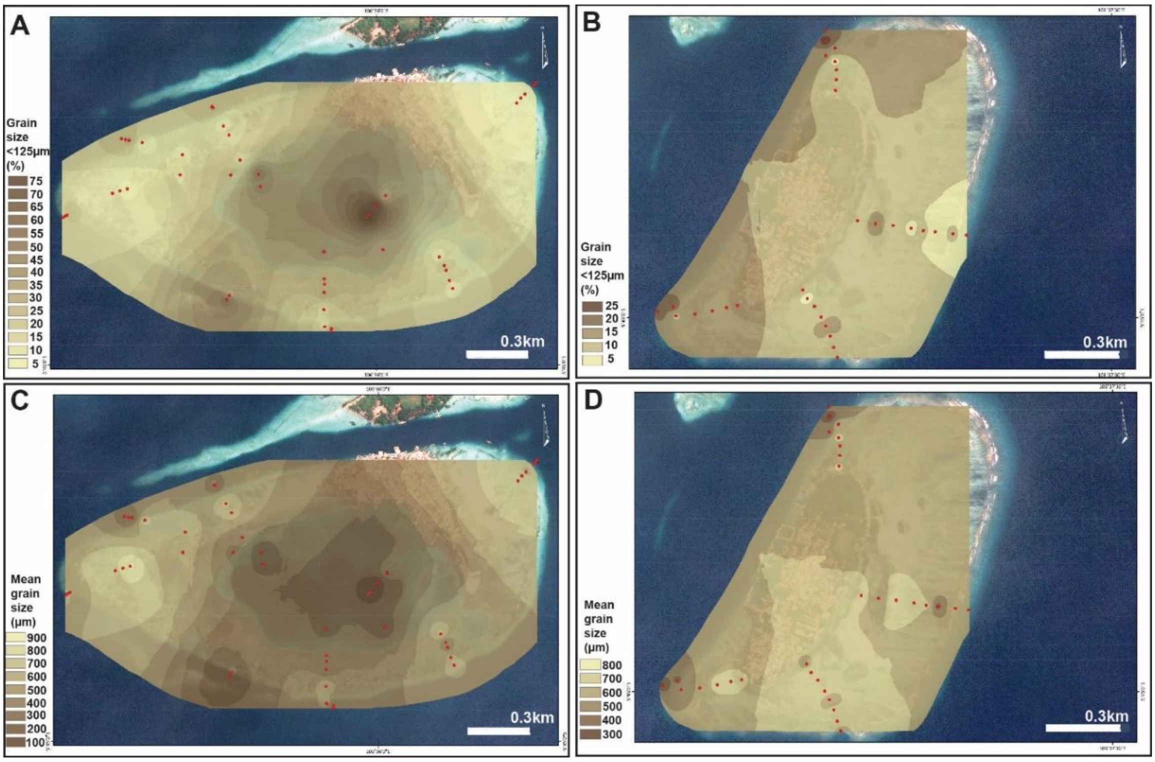

Figure 2-10. Distribution of the fine fraction (<125 µm) in (a) Panggang Island and (b) Pramuka Island. Mean grain-size distribution in (c) Panggang Island and (d) Pramuka Island.

The results obtained here for the relatively small patch reefs of the Seribu archipelago indicate elements of randomness but also deterministic ordering (Fig. 2-12). The lagoonal sediments in water depths of more than 7 m are distinct from the sand apron or reef front. The nearly complete lack of tidal inlets in the relatively wide sand aprons prevents flushing of fine sediments from the interior lagoon. This is in contrast to other studies where currents prevent deposition of fines in the relatively deep lagoons of atoll-like carbonate systems (Gischler, 2006; Betzler *et al*., 2015). Three factors were likely important for the formation of the continuous sand aprons. First, the late Holocene sea-level fall is thought to have led to widespread progradation of the sand aprons and partial infilling of the lagoons (Park *et al*. 2010). Second, bimodal monsoonal winds lead to a relatively symmetrical distribution of the sand aprons without pronounced lee effects. Third, the small size of the patch reefs of the Seribu archipelago leads to a high ratio between the length of the productive reef front and the area of the platform interior (Purdy & Gischler, 2005). The sediments that are produced by the reef and transported by monsoonal winds and currents to the sand apron therefore can fill in the available accommodation space rapidly. Sea-level fall, monsoonal climate and size therefore all contribute to the effective isolation of the lagoon and the development of a distinct facies.

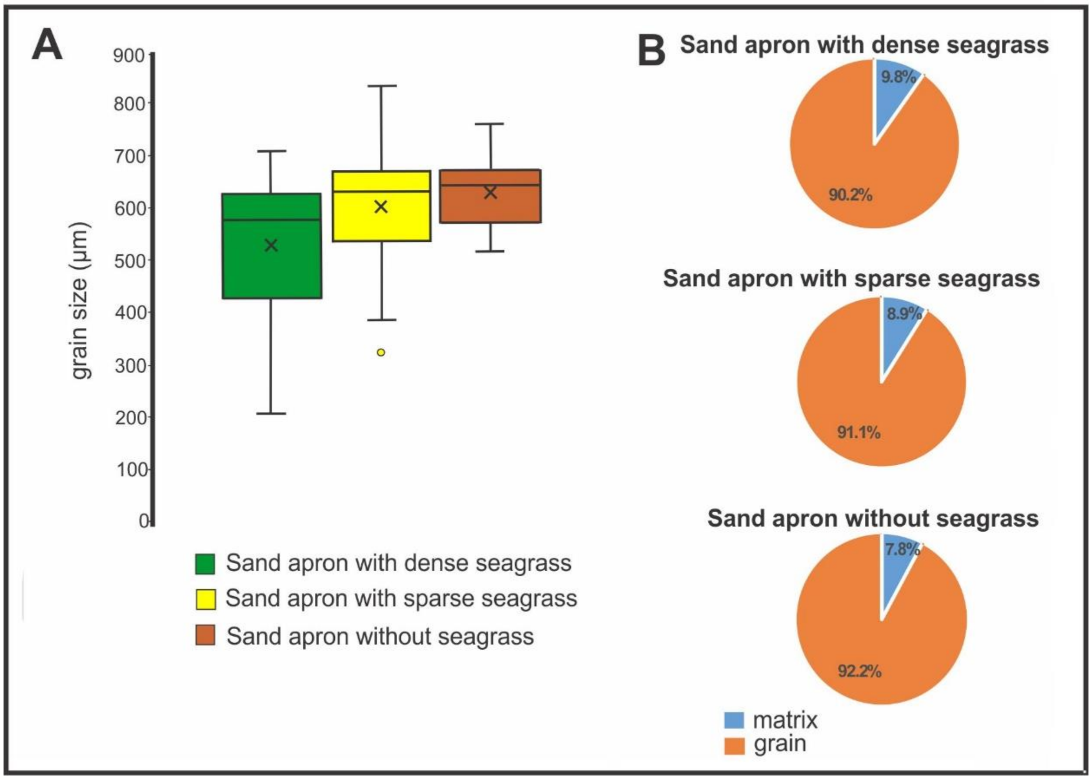

Figure 2-11. (a) Box plot and arithmetic mean (x) for the sediment grainsize distribution within different sand apron environments. (b) Abundance of coarse and fine fraction (<125 µm) within different sand apron environments.

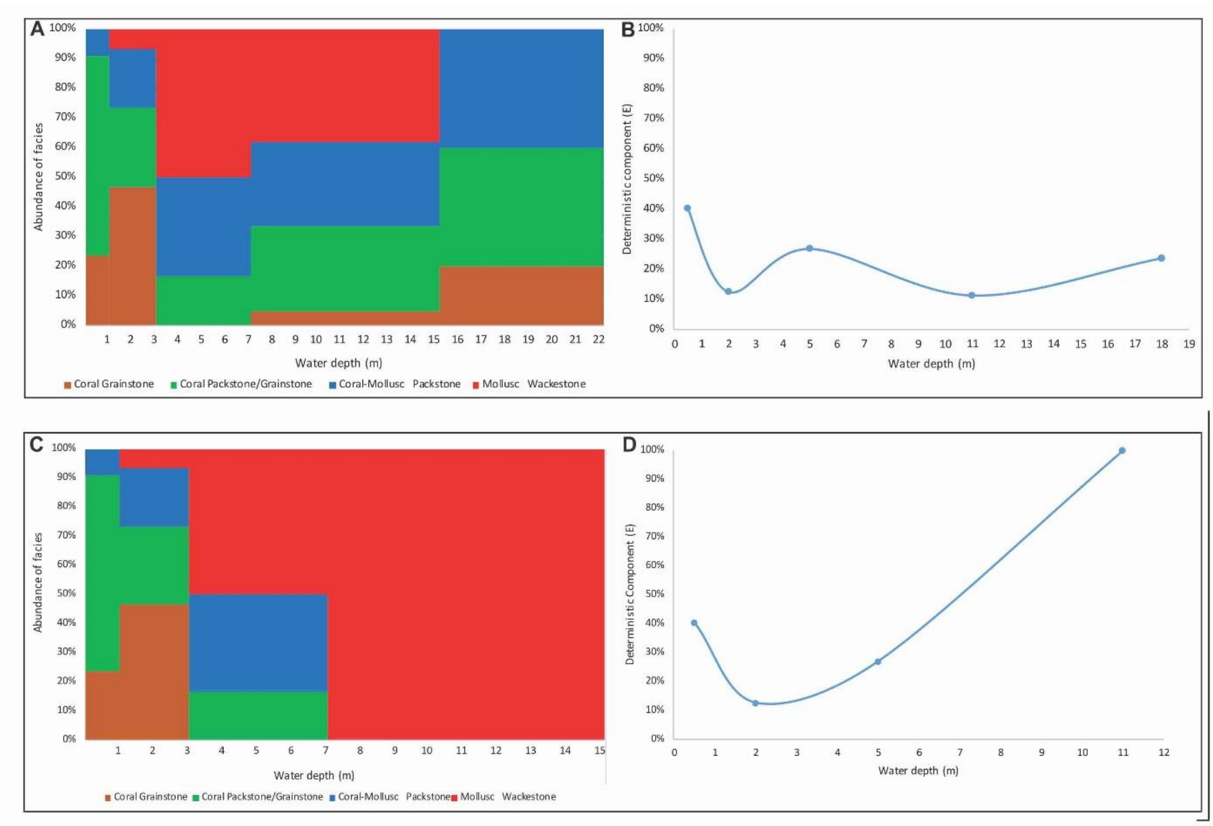

Figure 2-12. (a) The abundance of four delineated facies against water depth for the complete data set. (b) Shannon–Wiener evenness (E) of facies as related to water depth. (c) The abundance of four delineated facies against water depth excluding samples from the reef front and (d) Shannon–Wiener evenness (E) of facies as related to water depth.

2.6 Conclusion

Four sedimentary facies occur in isolated carbonate platforms of Kepulauan Seribu: coral grainstone, coral packstone/grainstone, coral-mollusc packstone, and mollusc wackestone. Six environmental facies could be distinguished using statistical satellite image analysis. These include the deeper lagoon/platform margin, shallower lagoon/platform margin and the subtidal reef margin/coral. The sand apron can be subdivided into three environmental facies based on the density of sea-grass cover: sand apron with dense sea grass, with sparse sea grass and without sea grass. The distribution of the environmental facies is mainly controlled by water depth, density of sea grass cover and coral abundance. Only one sedimentary facies (mollusc wackestone) can be directly correlated to satellite mapped environmental facies (lagoon). In contrast, there is no close correspondence between the density of sea grass cover and sedimentary facies due to the heterogeneity and complexity of the environment. Although no close correspondence was found between the sea grass cover and sedimentary facies, there is a clear influence of sea grass density on the grain size distribution. In areas of the sand apron with dense sea grass meadows, the grain size is significantly smaller compared to areas with sparse or no sea grass cover.

The mean grain-size and the abundance of coral fragments exerts a strong control on sedimentary facies. Both parameters are negatively correlated with water depth. However, sedimentary facies cannot be predicted based on water depth alone if the complete dataset is considered. This can be explained by the stronger wave exposure at the reef front compared to similar water depth in the lagoon. The analysis shows that the shallow carbonate depositional environment (< 7 m) is influenced by a complex suite of autogenic processes, resulting in an apparently random facies distribution. For water depths below 7 m, the sedimentary facies can be predicted reliably if the reef front samples are excluded from the analysis. This facies dependence on water depth is in contrast to several other facies studies from atoll structures that showed random facies distributions at similar water depth. This difference can be explained by a lack of tidal inlets at this study site, leading to homogeneously low energy conditions in the lagoon. The relatively closed nature of the lagoons is interpreted to result from a late Holocene sea-level fall, leading to progradation of the sand apron under high energy monsoonal conditions and a partial infilling of the accommodation space on these kilometre-scale carbonate platforms.

Acknowledgement

We would like to thank the anonymous reviewer and Sam Purkis for their constructive and detailed comments on our manuscript. We are grateful to Lembaga Pengelola Dana Pendidikan (LPDP) who awarded a scholarship to Dwi Amanda Utami Nasution (No: PRJ-4137/LPDP.3/2016), and to Geotechnology Research Center, Lembaga Ilmu Pengetahuan Indonesia (LIPI) for DIPA 079.01.2.017152/2015 Project no 3408.001.014.H who funded this field work. We thank Marfasran Hendrizan and Dudi Prayudi for their assistance in the field work. Philipp Binger is thanked for his assistance during sampling in the laboratory. The Authors thank Tubagus Solihuddin for his help in providing satellite imagary as well as Ilham Arisbaya for discussion during the making of the satellite-based map.

References

Belde, J., **Reuning, L.** and **Back, S.** (2017) Bottom currents and sediment waves on a shallow carbonate shelf, Northern Carnarvon Basin, Australia. *Cont. Shelf Res.*, **138**, 142–153.

Betzler, C., **Lindhorst, S.**, **Lüdmann, T.**, **Weiss, B.**, **Wunsch, M.** and **Braga, J.C.** (2015) The leaking bucket of a Maldives atoll: Implications for the understanding of carbonate platform drowning. *Mar. Geol.*, **366**, 16–33.

Blott, S.J. and **Pye, K.** (2001) Gradistat: A grain size distribution and statistics package for the analysis of unconsolidated sediments. *Earth Surf. Process. Landforms*, **26**, 1237–1248.

Bosence, D.W.J. (2008) Randomness or order in the occurrence and preservation of shallow-marine carbonate facies? Holocene, South Florida. *Palaeogeogr. Palaeoclimatol. Palaeoecol.*, **270**, 339–348.

Cahyarini, S.Y., **Zinke, J.**, **Troelstra, S.**, **Suharsono**, **Aldrian, E.** and **Hoeksema, B.W.** (2016) Coral Sr/Ca-based sea surface temperature and air temperature variability from the inshore and offshore corals in the Seribu Islands, Indonesia. *Mar. Pollut. Bull.*, **110**, 694–700.

Cleary, D.F.R., **Polónia, A.R.M.**, **Renema, W.**, **Hoeksema, B.W.**, **Wolstenholme, J.**, **Tuti, Y.** and **De Voogd, N.J.** (2014) Coral reefs next to a major conurbation: A study of temporal change (1985-2011) in Coral cover and composition in the reefs of Jakarta, Indonesia. *Mar. Ecol. Prog. Ser.*, **501**, 89–98.

De Voogd, N.J. and **Cleary, D.F.R.** (2008) An analysis of sponge diversity and distribution at three taxonomic levels in the Thousand Islands/Jakarta Bay reef complex, West-Java, Indonesia. *Mar. Ecol.*, **29**, 205–215.

Dunham, R.J. (1962) Classification of carbonate rocks according to deposition texture. *Am. Assoc. Pet. Geol.*, **1**, 108–121.

Fainstein, R. (1987) Exploration of the North Seribu Area, northwest Java Sea. In: *Indonesian Petroleum Association, Proceedings 16th annual convention Jakarta, 1987*, I, 191–214.

Farhan, A.R. and **Lim, S.** (2011) Resilience assessment on coastline changes and urban settlements: A case study in Seribu Islands, Indonesia. *Ocean Coast. Manag.*, **54**, 391–400.

Folk, R.L. and **Ward, W.C.** (1957) Brazos River bar [Texas]; a study in the significance of grain size parameters. J. Sediment. Res. 27:3–26.

Fonseca, M.S. and **Koehl, M.A.R.** (2006) Flow in seagrass canopies: The influence of patch width. *Estuar. Coast. Shelf Sci.*, **67**, 1–9.

Ginsburg, R.N. (1956) Environmental Relationships of Grain Size and Constituent Particles in Some South Florida Carbonate Sediments. *Am. Assoc. Pet. Geol. Bull.*, **40**, 2384–2427.

Gischler, E. (2011) Sedimentary Facies of Bora Bora, Darwin’s Type Barrier Reef (Society Islands, South Pacific): The Unexpected Occurrence of Non-Skeletal Grains. *J. Sediment. Res.*, **81**, 1–17.

Gischler, E. (2006) Sedimentation on Rasdhoo and Ari Atolls, Maldives, Indian ocean. *Facies*, **52**, 341–360.

Gischler, E., **Isaack, A.** and **Hudson, J.H.** (2017) Sediments of the Dry Tortugas, south Florida, USA: Facies distribution on a ramp-like isolated carbonate platform. *Sediment. Geol.*, **351**, 48–65.

Gischler, E. and **Lomando, A.J.** (1999) Recent sedimentary facies of isolated carbonate platforms, Belize-Yucatan system, Central America. *J. Sediment. Res.*, **69**, 747–763.

Gross, M.G., **Milliman, J.D.**, **Tracey Jr., J.I.** and **Ladd, H.S.** (1969) Marine geology of Kure and Midway atolls, Hawaii--a preliminary report. *Pacific Sci.*, **v. 23**, 17–25.

Hammer, Ø., **Harper, D.A.T.** and **Ryan, P.D.** (2001) PAST: Paleontological Statistics Software Package for Education and Data Analysis. *Palaeontol. Electron.*, **4(1)**, 1–9.

Hansen, J.C.R. and **Reidenbach, M.A.** (2012) Wave and tidally driven flows in eelgrass beds and their effect on sediment suspension. *Mar. Ecol. Prog. Ser.*, **448**, 271–287.

Harris, P.M., **Purkis, S.J.** and **Ellis, J.** (2011) Analyzing Spatial Patterns in Modern Carbonate Sand Bodies From Great Bahama Bank. *J. Sediment. Res.*, **81**, 185–

206.

Hoeksema, B.W. (1991) Control of bleaching in mushroom coral populations (Scleractinia: Fungiidae) in the Java Sea: stress tolerance and interference by life history strategy. *Mar. Ecol. Prog. Ser.*, **74**, 225–237.

Jordan, C.F., **Wharton, R.J.** and **Cook, R.E.** (1993) The sedimentology of Kepulauan Seribu: A modern patch reef complex in the west Java Sea, Indonesia. *Mod. Carbonates their Anc. Counterparts Indones. A Guid. to Interpret. Underst. Carbonate Reserv.*, 2.1-2.6.

Kaczmarek, S.E., **Hicks, M.K.**, **Fullmer, S.M.**, **Steffen, K.L.** and **Bachtel, S.L.** (2010) Mapping facies distributions on modern carbonate platforms through integration of multispectral Landsat data, statistics-based unsupervised classifications, and surface sediment data. *Am. Assoc. Pet. Geol. Bull.*, **94**, 1581–1606.

Kenworthy, W.., **Zieman, J.C.** and **Thayer, G.W.** (1982) Evidence for the influence of seagrasses on the benthic nitrogen cycle in a coastal plain estuary near Beaufort, North Carolina (USA). *Oecologia*, **54**, 152–158.

Koch, E.W. and **Gust, G.** (1999) Water flow in tise and wave dominated beds of the seagrass Thalassia testudinum. **184**, 63–72.

Koch, E.W., **Sanford, L.P.**, **Chen, S.**, **Shafer, D.J.** and **Smith, J.M.** (2006) Waves in Seagrass Systems : Review and Technical Recommendations Engineer Research and Development Center Waves in Seagrass Systems : Review and Technical Recommendations.

Lees, A. and **Buller, A.T.** (1972) Modern temperate-water and warm-water shelf carbonate sediments contrasted. Mar Geol. doi: 10.1016/0025-3227(72)90011-4

Luczkovich, J.J., **Wagner, T.W.** and **Stoffle, R.W.** (1993) Discrimintation of Coral Reefs, Seagrass Meadows, and Sand Bottom Types from Space: A Dominican Republic Case Study. Photogramm. Eng. Remote Sens. 59:385–389.

Lyzenga, D.R. (1981) Remote sensing of bottom reflectance and water attenuation parameters in shallow water using aircraft and landsat data. *Int. J. Remote Sens.*, **2**, 71–82.

Madden, R.H.C., **Wilson, M.E.J.** and **O'Shea, M.** (2013) Modern fringing reef carbonates from equatorial SE Asia: An integrated environmental, sediment and satellite characterisation study. *Mar. Geol.*, **344**, 163–185.

Maloof, A.C. and **Grotzinger, J.P.** (2012) The Holocene shallowing-upward parasequence of north-west Andros Island, Bahamas. *Sedimentology*, **59**, 1375–1407.

Morgan, W.A., **George, A.D.**, **Harris, P.M.**, **Kupecz, J.** and **Sarg, J.F.** (2010) Cenozoic carbonate systems of Australasia - Introduction and Perspective. In: *Cenozoic Carbonate Systems of Australasia*, *SEPM Special Publication 95*, 3–9.

Orme, G.R., **Flood, P.G.** and **Sargent, G.E.G.** (1978) Sedimentation Trends in the Lee of Outer (Ribbon) Reefs, Northern Region of the Great Barrier Reef Province. *Philos. Trans. R. Soc. London. Ser. A, Math. Phys. Sci.*, **291**, 85–99.

Park, R.K., **Matter, A.** and **Tonkin, P.C.** (1995) Porosity Evolution in the Batu Raja Carbonates of the Sunda Basin - Windows of Opportunity. *Indones. Pet. Assoc. 24th Annu. Conv. Proc.*, 163–184.

Park, R.K., **Siemers, C.T.** and **Brown, A.A.** (1992) Holocene carbonate sedimentation, Pulau Seribu, Java Sea—the third dimension. In: *Carbonate Rocks and Reservoirs of Indonesia, A Core Workshop. Indonesian Petroleum Association, Jakarta*, 2–1 – 2–15.

Poerbandono (2016) Wind characteristics and the associated risk of erosion in Seribu Islands patch reef complexes, Java Sea, Indonesia. In: *The 5th International*

Symposium on Earthhazard and Disaster Mitigation. AIP Conf. Proc., 1730, 080001.

Purdy, E.G. (1963a) Recent Calcium Carbonate Facies of the Great Bahama Bank. 1. Petrography and Reaction Groups. *J. Geol.*, **71**, 334–355.

Purdy, E.G. (1963b) Recent Calcium Carbonate Facies of the Great Bahama Bank. 2. Sedimentary Facies. *J. Geol.*, **71**, 472–497.

Purdy, E.G. and **Gischler, E.** (2003) The Belize margin revisited: 1. Holocene marine facies. *Int. J. Earth Sci.*, **92**, 532–551.

Purkis, S.J., **Harris, P.M.** and **Ellis, J.** (2012) Patterns of Sedimentation In the Contemporary Red Sea As An Analog for Ancient Carbonates In Rift Settings. *J. Sediment. Res.*, **82**, 859–870.

Purkis, S.J. and **Riegl, B.M.** (2005) Spatial and temporal dynamics of Arabian Gulf coral assemblages quantified from remote-sensing and in situ monitoring data. Mar. Ecol. Prog. Ser. 287:99–113.

Purkis, S.J., **Rowlands, G.P.** and **Kerr, J.M.** (2015) Unravelling the influence of water depth and wave energy on the facies diversity of shelf carbonates. *Sedimentology*, **62**, 541–565.

Purkis, S.J. and **Vlaswinkel, B.** (2012) Visualizing lateral anisotropy in modern carbonates. *Am. Assoc. Pet. Geol. Bull.*, **96**, 1665–1685.

Rachello-Dolmen, P.G. and **Cleary, D.F.R.** (2007) Relating coral species traits to environmental conditions in the Jakarta Bay/Pulau Seribu reef system, Indonesia. *Estuar. Coast. Shelf Sci.*, **73**, 816–826.

Rankey, E.C. (2004) On the Interpretation of Shallow Shelf Carbonate Facies and Habitats: How Much Does Water Depth Matter? *J. Sediment. Res.*, **74**, 2–6.

Rankey, E.C. (2002) Spatial Patterns of Sediment Accumulation on a Holocene Carbonate Tidal Flat, Northwest Andros Island, Bahamas. *J. Sediment. Res.*, **72**, 591–601.

Reijmer, J.J.G., **Bauch, T.** and **Schäfer, P.** (2012) Carbonate facies patterns in surface sediments of upwelling and non-upwelling shelf environments (Panama, East Pacific). *Sedimentology*, **59**, 32–56.

Riegl Laser Measurement Systems (2006) Riegl Vz-400. *http://www.riegl.com/uploads/tx_pxpriegldownloads/10_DataSheet_VZ-400_2014-09-19.pdf*, 3–6.

Rosleff-Soerensen, B., **Reuning, L.**, **Back, S.** and **Kukla, P.** (2012) Seismic geomorphology and growth architecture of a Miocene barrier reef, Browse Basin, NW-Australia. *Mar. Pet. Geol.*, **29**, 233–254.

Rosleff-Soerensen, B., **Reuning, L.**, **Back, S.** and **Kukla, P.** (2016) The response of a basin-scale Miocene barrier reef system to long-term, strong subsidence on a passive continental margin, Barcoo Sub-basin, Australian North West Shelf. *Basin Res.*, **28**, 103–123.

Sachoemar, S.I. (2008) Karakteristik lingkungan perairan kepulauan seribu. *J. Air Indones.*, **4**, 109–114.

Scrutton, M. (1976a) Aspects Carbonate Sedimentation in Indonesia. In: *Indonesian Petroleum Association, Proceeding 5th Annual Convention*, 179–193.

Scrutton, M. (1976b) Modern Reefs in the West Java Sea. In: *Indonesian Petroleum Association, Proceeding 5th Annual Convention*, 14–36.

Shannon, C.E. (1948) A Mathematical Theory of Communication. *Bell Syst. Tech. J.*, **27**, 379–423.

Toruan, L.N.L., **Soedharma, D.** and **Dewi, K.T.** (2013) Komposisi Dan Distribusi Foraminifera Bentik Di Ekosistem Terumbu Karang Pada Kepulauan Seribu. *J.*

Ilmu dan Teknol. Kelaut. Trop., **5**, 1–16.

Umbgrove, J.H.F. (1947) Coral Reefs of the East Indies. *Bull. Geogr. Sociaty Am.*, **58**, 729–778.

Ward, L., **Kemp, W.** and **Boynton, W.** (1984) The influence of water depth and submerged vascular plants on suspended particulates in a shallow estuarine embayment. *Mar. Geol.*, **59**, 85–103.

Wilkinson, B.H., **Diedrich, N.W.** and **Drummond, C.N.** (1996) Facies successions in peritidal carbonate sequences. J. Sediment. Res. 66:1065–1078.

Wilson, M.E.J. (2002) Cenozoic carbonates in Southeast Asia: Implications for equatorial carbonate development. *Sediment. Geol.*, **147**, 295–428.

Wilson, M.E.J. (2012) Equatorial carbonates: an earth systems approach. *Sedimentology*, **59**, 1–31.

Wilson, M.E.J. and **Evans, M.J.** (2002) Sedimentology and diagenesis of Tertiary carbonates on the Mangkalihat Peninsula, Borneo: Implications for subsurface reservoir quality. *Mar. Pet. Geol.*, **19**, 873–900.

Wyrtki, K. (1962) Physical Oceanography of the Southeast Asian Waters By Klaus Wyrtki NAGA Report Volume 2. Scientific Results of Marine Investigations of the South China Sea and the Gulf of Thailand, 1959–1961. S.I.O., La Jolla, Calif., 1961. *J. Mar. Biol. Assoc. United Kingdom*, **42**, 707.

Zainal, A.J.M., **Dalby, D.H.** and **Robinson, I.S.** (1993) Monitoring Marine Ecological Changes On The East-Coast Of Bahrain With Landsat Tm. *Photogramm. Eng. Remote Sensing*, **59**, 415–421.

Chapter 3

The Fingerprints of Humid Equatorial Carbonates

3 The mineralogic and isotopic fingerprint of equatorial carbonates: Kepulauan Seribu, Indonesia

Dwi Amanda Utami[1,2,3], Lars Reuning[2], Maximillian Hallenberger[1], Sri Yudawati Cahyarini[3]
[1]Geological Institute, Energy and Mineral Resources Group, RWTH Aachen University, Aachen, Germany
[2]Institute of Geosciences, Kiel University, Kiel, Germany
[3]Geotechnology Research Center, Indonesian Institute of Sciences, Bandung, Indonesia

Accepted in International Journal of Earth Sciences

Abstract

Kepulauan Seribu is an isolated patch reef complex situated in the Java Sea (Indonesia) and is a typical example for a humid, equatorial carbonate system. We investigate the mineralogical and isotopic fingerprint of Panggang, one of the reef platforms of Kepulauan Seribu, to evaluate differences to other carbonate systems, using isotope in combination with XRD and SEM analysis. A characteristic property of shallow water (<20 m) sediments from Kepulauan Seribu is their increased LMC content (~ 10%) derived from some genera of rotaliid foraminifers and bivalves. The relative abundance of these faunal elements in shallow waters might be related to at least temporary turbid conditions caused by sediment laden river runoff. This influence is also evidenced by the presence of low amounts of siliciclastic minerals below the regional wave base. Kepulauan Seribu carbonates are characterized by very low $\delta^{13}C$ and $\delta^{18}O$ values. This is related to the isotopically depleted riverine input. The $\delta^{13}C_{DIC}$ in riverine water is reduced by the contribution of ^{12}C from riverside mangroves. Deep atmospheric convection and intensive rains contribute ^{18}O depleted freshwater in the river catchments, finally reducing salinity in the Java Sea. The depleted $\delta^{13}C$ signature in carbonates is further enhanced by the lack of green algae and inorganic carbonates and abundance of coral debris. Low $\delta^{18}O$ values in carbonates are favored by the high water-temperatures in the equatorial setting. Since equatorial carbonates in SE Asia, including the Java Sea, are typically influenced by high turbidity and/or river runoff, the observed distinctively low isotope values likely are characteristic for equatorial carbonate systems in the region.

Keywords: patch reefs, oxygen isotopes, carbon isotopes, SE Asia, humid equatorial climate, maritime continent

3.1 Introduction

During the last decade the awareness has grown that carbonate systems in the humid equatorial zone have common characteristics that distinguishes them from carbonates in more arid regions (Tomascik *et al.*, 1997; Wilson, 2008). Features of these equatorial carbonates include the common occurrence of photozoan assemblages adapted to oligophotic (low light) conditions, common elements of the Heterozoan Association and mixed carbonate/clastic deposits. Humid equatorial carbonates are also characterized by a lack of coated grains, aggregates, chemically precipitated mud and the absence of associated evaporites (Wilson, 2002). They typically occur in a zone between 15/20°N and 15/20°S in areas with warm (> 22°C) surface waters and heavy precipitation (> 1500 mm per annum; Wilson, 2012). Due to the increased precipitation, carbonate deposition takes place in shelfal waters of normal to reduced salinity and high clastic influx. River runoff and upwelling cause increased nutrient concentrations in surface waters, which in turn lead to a shallow position of the photic zone.

A key region for the study of these humid equatorial carbonates is SE Asia, where the shallow shelfs are strongly affected by river runoff and/or upwelling (Tomascik *et al.*, 1997; Wilson, 2002). The diversity of environments and habitats renders SE Asia an ideal natural laboratory to investigate the variability of equatorial carbonate processes and deposits (Tomascik *et al.*, 1997; Wilson, 2002, 2008). Sediment discharge from each of the four largest SE Asian islands varies from *ca* 300 to 1650 million tons/year (Milliman *et al.*, 1999), leading to high turbidity and nutrient concentration in surface waters. Depth of abundant coral growth in SE Asian reefs is therefore limited to approximately 20 to 30 m and is considered among the shallowest in the world (Schlager, 1992; Wilson, 2008). This shallow photic zone corresponds with low light penetration in an oligo-mesotropic region characterized by nutrient input from river runoff, upwelling and plankton blooms (Wilson, 2008). Due to these environmental conditions, SE Asian carbonates can be considered as typical equatorial carbonate systems.

The low salinity in the semi-enclosed seas of SE Asia also lead to a relatively low aragonite supersaturation compared to more arid regions such as the tropical, western Atlantic (TWA). The development of Cenozoic carbonate systems in SE Asia is thought to be strongly influenced by regional changes in nutrient input and precipitation (Wilson, 2008). Late Oligocene carbonates from SE Asia were often characterised by calcitic dominated assemblages. This was likely promoted by the decreased aragonite supersaturation of the low salinity waters in the semi enclosed seas of SE Asia (Wilson, 2012). An increase of river runoff and associated decrease in aragonite supersaturation is also held responsible for a shelf wide switch from inorganic aragonite to bioclastic calcite dominated sedimentation on the tropical NW Shelf of Australia during the early Holocene (Hallenberger *et al.*, 2019; Ishiwa *et al.*, 2019); a process which seems to have occurred repeatedly during the Pleistocene (Gallagher *et al.*, 2018). Studies of modern carbonate systems from northern Australia and SE

Asia suggest that faunal assemblages from the oligophotic zone are relatively calcite rich (Wilson & Vecsei, 2005; Wilson, 2012). Generally, this change from coral dominated euphotic to foramol dominated oligophotic zones takes place in a water depth of around 20 m, but locally can be as shallow as 6 m in turbid coastal water (Wilson & Vecsei, 2005).

Equatorial carbonates share some similarities with cool water systems including the abundance of calcitic components and heterozoan elements. In some case this can complicate the distinction between non-tropical and equatorial carbonates (Wilson & Vecsei, 2005). Wilson (2012) therefore recommended the use of additional geochemical and isotopic proxies to identify warm temperatures and low salinities associated with regional equatorial carbonates in the rock record. However, stable isotope studies from modern SE Asia that could be used as a template for comparison with fossil counterparts are still missing. It is also unclear if the predominance of calcitic bioclasts, that is apparent in the oligophotic zone of many carbonate systems in SE Asia is visible in the mineralogy of the coral dominated shallow water area. In this study, we investigate how far the mineralogy and stable isotope signature of shallow water (< 20m) equatorial carbonate from Kepulauan Seribu in the Java Sea is distinct from other carbonate systems. Stable isotope ($\delta^{13}C$ and $\delta^{18}O$) analysis in combination with X-ray diffraction (XRD) and Scanning Electron Microscopy (SEM) is used to provide a fingerprint for equatorial carbonates from SE Asia. This data might be used as a template for comparison with carbonates in the rock record.

3.2 Study area

Situated in the Java Sea, Kepulauan Seribu (The Thousand Islands) consists of numerous coral reef islands ranging in size from a few meters across to length greater than one kilometer. From about 10 km off the northwest Java coastline, the island chain extends for about 50 km into the Java Sea. Kepulauan Seribu is situated on the NNE-SSW structural high of the Seribu platform, which is separated from the Sunda Basin towards the west and Arjuna basin to the east by the active N-S oriented Seribu Fault system (Scrutton, 1976a). The north - south elongation of the platform is largely controlled by the regional fault pattern that was established during the early Cenozoic and reactivated at various times since (Park *et al.*, 2010). The patch reef system of Kepulauan Seribu is located on the shallow Sunda Shelf where it rises from a water depth of 30 - 50 meters to the sea surface. A deep and several kilometers wide, east - west oriented channel separates Pari Island to the south from most other islands to its north (Fig. 3-1). It appears that this channel forms an important hydrologic barrier, channeling the sediment-laden coastal waters off Java and Kalimantan away from the reef (Tomascik *et al.*, 1997; Jordan, 1998). The reefal buildups on the platform vary in size and shape but most of them are elongated in a roughly east - west orientation. This pronounced orientation is inherited from the Pleistocene drainage pattern which was abandoned and truncated by river capture prior to the Holocene transgression

(Park *et al.*, 2010). The islands of Kepulauan Seribu are considered to be located in a relatively sheltered position protected from severe storms and ocean swells due to the fact that it is surrounded by major landmasses such as Sumatra, Java and Kalimantan (Fig. 3-1).

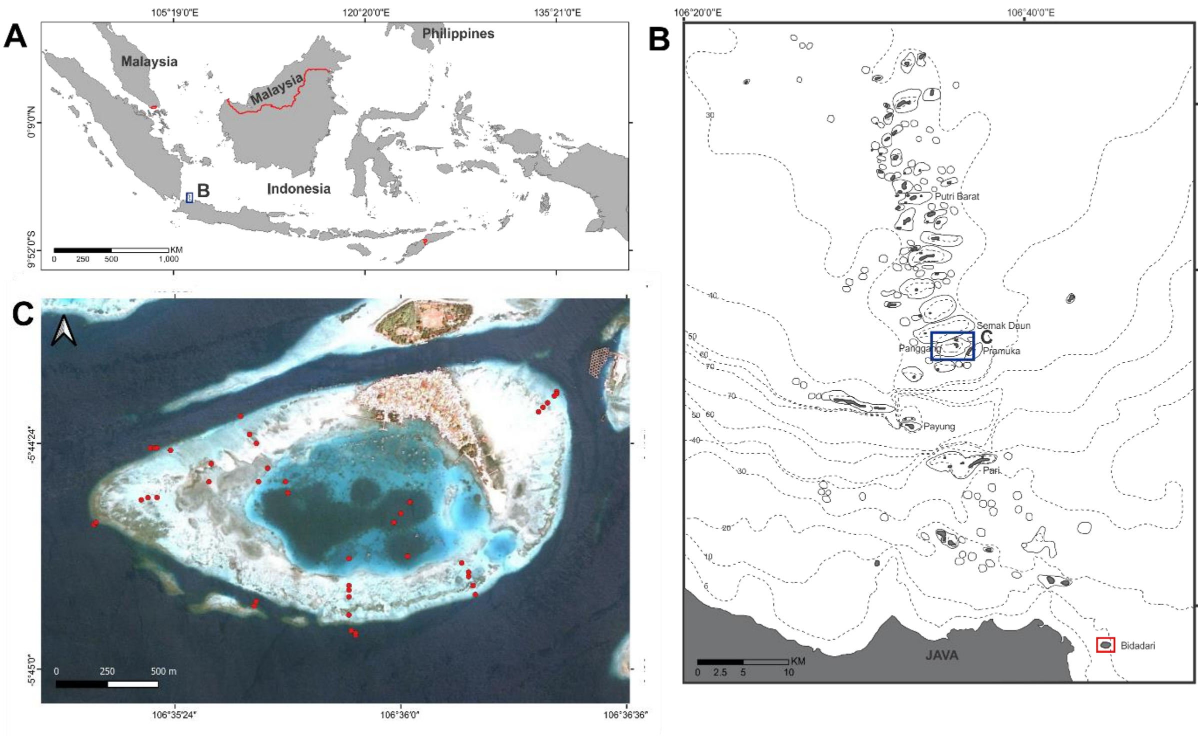

Figure 3.1. (A). Map of Indonesia, surrounding countries, and the study area (blue box). (B). Bathymetry in the vicinity of Kepulauan Seribu (basemap from National Bathymetry, Indonesia Geospatial Information Agency. Available on http://tides.big.go.id/DEMNAS/). Location of Panggang is indicated by the blue box, and Bidadari is indicated by the red box. (C). Satellite image showing Panggang reef platform. Sampling spots are indicated as red dots (satellite image from Google Earth).

The controlling influence on modern reef growth and morphology in Kepulauan Seribu is believed to be the seasonal change in wind and current directions (Scrutton, 1976a). The Java Sea is characterized by a monsoonal climate with a seasonal reversal between the West Monsoon (December – February), and the East Monsoon (April - October). The West Monsoon winds are known to be stronger than the East Monsoon winds, but less persistent (3 vs. 7 months). The East Monsoon winds therefore are the dominant factor for the net sediment transport (Poerbandono, 2016). The climate in Kepulauan Seribu is tropical with relative humidity of 80 to 90% (Tomascik *et al.*, 1997). The maximum sea surface temperature (SST) is observed in April (29.8°C) and minimum in January (28.6°C) (Cahyarini *et al.*, 2016). Surface salinity in the Java Sea (30-34‰) is well below normal open ocean levels, reaching as low as 22‰ in the vicinity of some of the larger river mouths. The low salinity of the Java Sea is due to heavy precipitation and intensive river runoff from Java and Kalimantan (Sofian &

Kozai, 2007). The water column of the shallow western Java Sea is well mixed and shows little temperature or salinity stratification (Hamzah *et al.*, 2020).

Water along Kepulauan Seribu is highly eutrophic (Baum *et al.*, 2015). Seasonal variability of Chlorophyll-α distribution in the Java Sea is influenced by monsoon, through water exchange with adjacent seas and nutrient supply from river discharge (Koropitan & Ikeda, 2016). In the eastern Java Sea episodic upwelling leads to phytoplankton blooms during the East Monsoon (Koropitan & Ikeda, 2016). The role of riverine nutrient input during the West Monsoon (rainy season) is limited to coastal regions (Koropitan & Ikeda, 2016). The reefs in Kepulauan Seribu are directly influenced by intense anthropogenic pressure from local as well as regional sources (Baum *et al.*, 2015). Polluted water masses from the Greater Jakarta Area are considered to affect reefs in nearshore areas close to river mouths around Jakarta Bay, while localized effects of anthropogenic stressors are more important for reef in the central and northern reefs of Kepulauan Seribu (Damar *et al.*, 2012; Farhan & Lim, 2012; Baum *et al.*, 2015).

Each island and platform of Kepulauan Seribu is built up from the skeletal debris of coral reefs which rim the platform margins (Jordan, 1998). The steep reef front extends seaward from the reef crest to a depth of about 15 meters. Well-developed reef facies occur down to a depth of about 16 - 18 meters (Jordan, 1998), whereas reef development is restricted to an even shallower depth of 3 - 10 m around 40 km towards the south in Jakarta Bay (Baum *et al.*, 2015). Reef framework builders at Kepulauan Seribu consist of a diverse fauna of Indo-Pacific corals and encrusting red algae. Below the base of continuous reef development, occurs a transition zone of small reef knolls or coralgal knobs that are surrounded by unconsolidated sediments. In water depths of about 24 meters, the seafloor becomes entirely sediment and begins to slope less steeply. Below the reef and near reef zone, in a depth from 27 to 88 meters occurs a foraminiferal molluscan packstone facies that is rich in terrigenous mud. The dominant bioclasts are benthic foraminifers, mollusc and coral fragments (Jordan, 1998). The sedimentation on the shelf further away from the direct influence of the reef system is dominated by siliciclastic mud.

Statistical analysis based on texture and composition reveal four sedimentary facies in the shallow waters (< 20m) of the Kepulauan Seribu: coral grainstone, coral packstone/grainstone, coral-mollusc packstone and mollusc wackestone (Utami *et al.*, 2018). The occurrence of mollusc wackestone in the lagoon is controlled by water depth, while the sand apron and reef front do not show significant facies separation with water depth. Environmental facies maps were derived from remote sensing data (Utami *et al.*, 2018): The sand apron can be subdivided into three facies with either no, sparse, or dense seagrass cover. One facies is further characterized by active coral growth. The deeper water zone can be separated into a shallow and a deep subtidal part of lagoons and platform margins. Distribution is therefore mainly controlled by water depth, density of seagrass cover and coral abundance (Utami *et al.*, 2018). The satellite derived environmental facies correlated only in the lagoon directly with sedimentary facies. No direct correlation of environmental facies to sedimentary facies exists in the sand apron due to the heterogeneity and complexity of the environment (Utami *et al.*, 2018).

Carbonate sediments from the shallow water (< 20m) zone of the Panggang reef platform, Kepulauan Seribu serve as the basis of this study (Fig. 3-1). Panggang is an atoll-like reef with an approximate area of 3.2 km^2 with a central lagoon surrounded by reef and sand apron facies. From the reef flat, the water depth increases from about 1 m to about 20 m in the deepest part of the lagoon. The sand apron on the eastern and western side of the lagoon is roughly two times wider compared to the sand apron on the northern and southern side. Only one small inlet traverses the sand aprons allowing very limited connection between the lagoon and the open sea. Panggang Island has the highest population density in Kepulauan Seribu, with more than 1000 people per km^2.

3.3 Methods

A total of 45 surface sediment samples were collected from Panggang reef platform, Kepulauan Seribu. In shallow water, sediments were collected by hand and water depth was measured using a marked stick. Sampling in the lagoon and at the reef slope was conducted by scuba diving and water depth was determined using the diving gear. In the laboratory, samples were washed in fresh water and dried using an oven set to 70°C for 7 hr. Dried samples were first sieved through a 125 µm sieve and split of the coarse fraction was stored in a glass bottle for later point counting analysis. The remaining portion of the >125 µm fraction was sieved through 250 µm, 500 µm, 1 mm, and 2 mm sieves. All individual grainsize fractions were weighed. Mean grainsize and sorting were calculated using the software Gradistat (Blott & Pye, 2001). Point counting analysis was done on the split of the >125 µm fraction by counting 300 grains under a binocular microscope. The results of these analyses were reported previously in Utami et al. (2018). Here we present data on the mineralogy, texture and isotopic composition of the same sample set.

Mineralogy was analyzed using a Bruker D8 X-ray diffractometer equipped with a Cu-anode, a secondary graphite monochromator and a scintillation counter. Forty-five bulk surface sediment samples covering all sedimentary facies (Utami *et al.*, 2018) were oven-dried, ground and mounted on sample holders. Additionally, the mineralogy of the < 125µm fraction from five of these samples and five individual bivalve shells was measured separately. All selected bivalve shells were clean and devoid of incrustations or epibenthos. All measurements were conducted over an angle field of 48° (16° - 64°) with a step size of 0.02° per five seconds. Identification and quantification of different mineral phases was achieved by standard Rietveld refinement using the software Profex (ver. 3.14.0). Standard analytical error is ± 2%. A total of 20 weight percent of corundum was added to each sample as an internal standard. This standard was systematically overestimated during Rietveld refinement (avg. 4%), which was attributed to the occurrence of amorphous silica in the form of sponge needles. The $MgCO_3$ content of calcite (in mol %) was determined using the shift in the position of the d(104) peak (Lumsden, 1979). The standard error is ± 0.15% on the mean composition.

Measurements of $\delta^{13}C$ and $\delta^{18}O$ values on 15 bulk and five fine fraction samples were made with a Finnigan MAT 253 mass spectrometer connected to a Kiel IV carbonate preparation device at the Leibniz Laboratory, Kiel University. Additionally, nine individual benthic foraminifers (*Calcarina*, *Amphistegina* and *Sorites*) and five individual bivalve shells were measured separately. Bivalve shells were ground to powder before measurement. All *Calcarina* and *Amphistegina*, as well as one individual *Sorites* were split into two aliquots and measured as subsamples. Standard external error is better than ± 0.05‰ for $\delta^{13}C$ and ± 0.08‰ for $\delta^{18}O$ (standards NBS 19 and 20). $\delta^{13}C$ and $\delta^{18}O$ values are reported in ‰ versus the Vienna PeeDee belemnite (V-PDB). A core of 68 cm length was drilled in September 2005 from a massive *Porites* coral in the Kepulauan Seribu complex, inshore of Bidadari Island at site 6°01'55''S, 106°44'47''E (Fig. 3-1) from 3 m water depth (Cahyarini *et al.*, 2016). $\delta^{13}C$ and $\delta^{18}O$ values were measured at the Stable Isotope Laboratory, Vrije University, Amsterdam. For the analysis, the samples were reacted with 100% H_3PO_4 at 75°C in a Kiel Device connected to a Finnigan MAT 252 mass spectrometer. Standard external error is ± 0.05‰ for $\delta^{13}C$ and ± 0.08‰ for $\delta^{18}O$ (standards NBS 19 and GICS).

A total of 16 selected samples of the < 125µm fraction were further analysed using scanning electron microscopy in the SEM laboratory of FMIPA (Institut Teknologi Bandung) and the SEM/EDS laboratory of UPP Chevron-Prodi Geologi (Institut Teknologi Bandung). Satellite images were acquired from Google Earth (http://www.google.com/earth). The inverse distance weighting tool of QGIS (ver. 3.14.1-Pi) was used to interpolate data between the sampling points for the generation of maps. All statistical analyses were performs using PAST (Hammer *et al.*, 2001). The Levene´s test was used to check if homogeneity of variances was met. The non-parametric Mann-Whitney *U* test was used for pairwise comparisons of median values. The non-parametric Kruskal-Wallis test for independent samples was used to examine the medians of $\delta^{13}C$ and $\delta^{18}O$ values in different sedimentary facies. The significance level for all analysis was set at 95%.

3.4 Results

Mineralogy

Sediments in Kepulauan Seribu are mostly composed of biogenic grains, most notably corals and molluscs, with minor components including benthic foraminifers, echinoderms, red algae and the green alga *Halimeda.* Non-skeletal grains are very rare and restricted to faecal pellets and aggregates cemented by red algae or serpulids (Tab. 3-1) (Scrutton, 1976b; Utami *et al.*, 2018). SEM investigation confirms that the fine fraction of sediments in Kepulauan Seribu is largely a product of skeletal breakdown (Fig. 3-2). X-ray diffraction results confirm that surface sediment on the Panggang reef platform in the central part of Kepulauan Seribu are composed mainly of carbonate minerals with small percentages of siliciclastic minerals. Aragonite is the dominant mineral and its contribution varies between 72 and 88%, with a mean of 82% (Tab. 1, Fig. 3-3). High magnesium calcite (HMC) and low magnesium calcite (LMC) contents are fairly equal throughout the island, for HMC the value ranges from 5 to 16% with a mean of 8%, for LMC the value varies between 5 and 17% with a mean of 9% (Fig. 3-4). Quartz composes only a minor fraction of the total bulk sample, with a maximum of 3% and a mean of 1%. From 45 bulk samples tested, three samples show smectite contents between 2% and 9%.

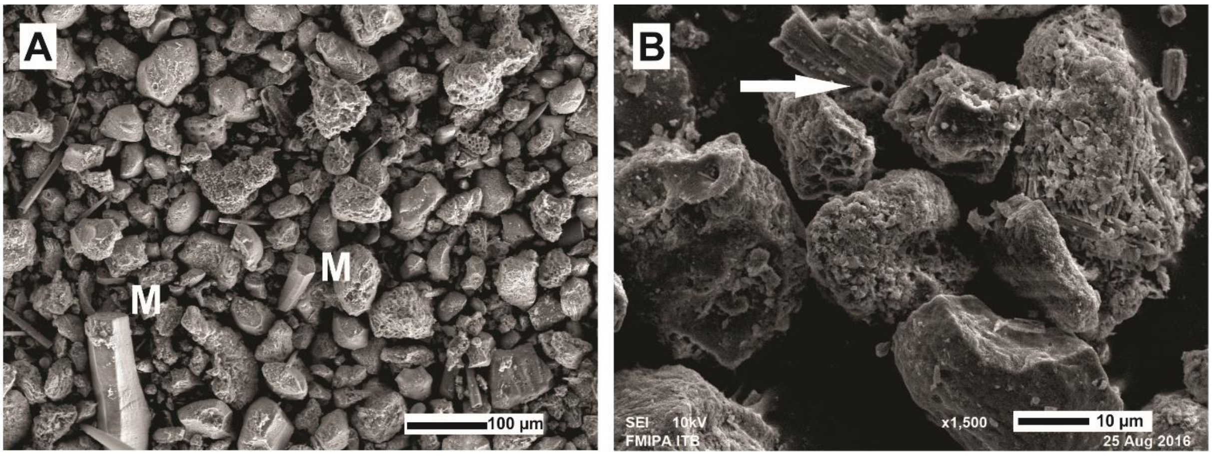

Figure 3-2. SEM images of the fine fraction: A. Sample MPG 11P from the southern reef flat. Sediment constituents are mostly bioclasts formed by skeletal breakdown including calcitic (LMC) prisms from bivalve shells (M). B. Sample MPG 41L from the northwestern reef flat. Arrow points at open microboring.

Throughout all sedimentary facies (Utami *et al.*, 2018), the mineralogical composition varies only slightly (Tab. 3-1, Fig. 3-3). The HMC content is very similar in all facies, with an average value of 8.5%. The $MgCO_3$ content in HMC varies between 13% and 14.2% in mollusc wackestone and coral grainstone facies, respectively. The content of LMC is equal or higher compared to HMC in all facies. The highest aragonite (82%) and lowest LMC content (9%) is found in the coral packstone/grainstone facies. The mollusc wackestone facies shows the lowest aragonite (77%) and highest LMC (11%)

content. The highest siliciclastic content is present in the mollusc wackestone facies (quartz: 2%, smectite: 2%).

Table 3-1. Average values of grain types and bulk mineralogy for each sedimentary facies (%). Grain types are reported as % of > 125µm fraction, fines (< 125µm) as % of total sediment. Abbreviation: C G = Coral Grainstone, C P/G = Coral Packstone/Grainstone, C-M P = Coral-Mollusc Packstone, M W = Mollusc Wackestone, *Hal* = *Halimeda*, Foram = foraminifers, Echi = echinoderm, N-S = non-skeletal, ARA = aragonite, HMC = high magnesium calcite, LMC = low magnesium calcite, Qz = quartz, Sm = smectite, Mg (%) = mole % $MgCO_3$ in Mg-Calcite.

Facies	Coral	Red Algae	*Hal*	Mollusc	Foram	Echi	N-S	other	Fines	ARA	HMC	LMC	Qz	Sm	Mg %
C G	58.8	5.5	1.7	19.5	8	4.2	1.1	1.1	6.2	80	9	10	1	0	14.2
C P/G	53.7	3.4	3.5	28.2	4.9	3.9	0.3	2.2	7	82	8	9	1	0	14.2
C-M P	48.1	3.8	2.5	28.1	5.6	6.1	0.7	5	23.4	81	9	9	1	trace	13.8
M W	24	1.3	0.8	40.7	3.6	5.7	2.4	21.5	51.5	77	8	11	2	2	13

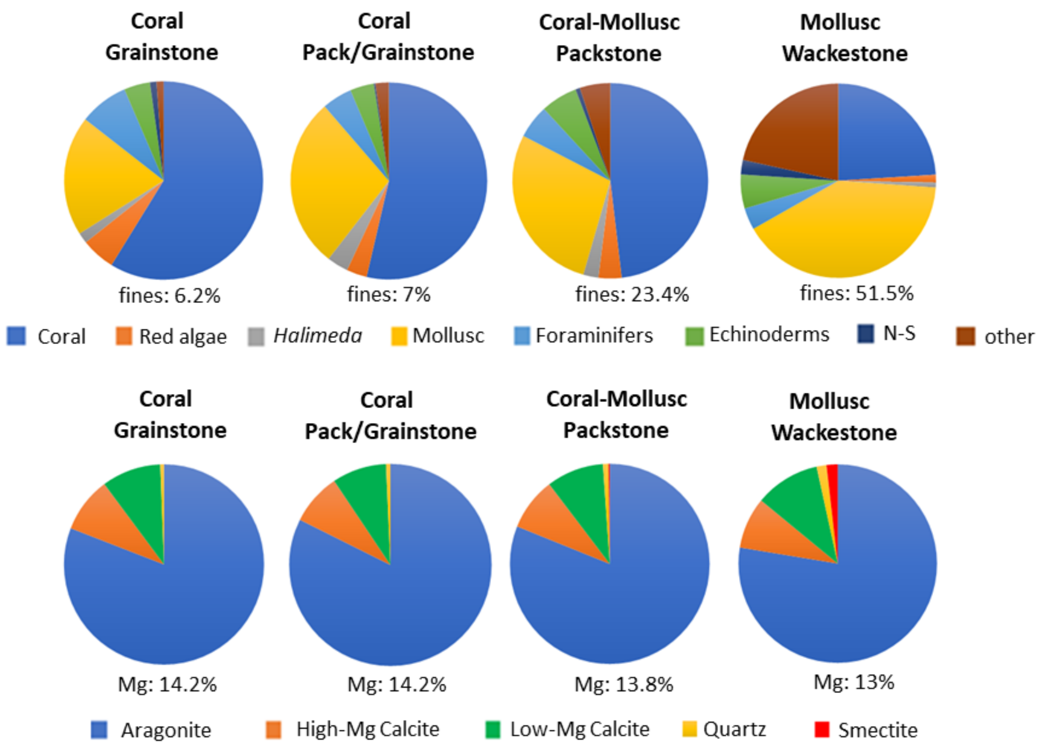

Figure 3-3. Composition and mineralogy of each sedimentary facies in % of > 125µm fraction as indicated in table 1. Mg: mole % $MgCO_3$ in Mg-Calcite.

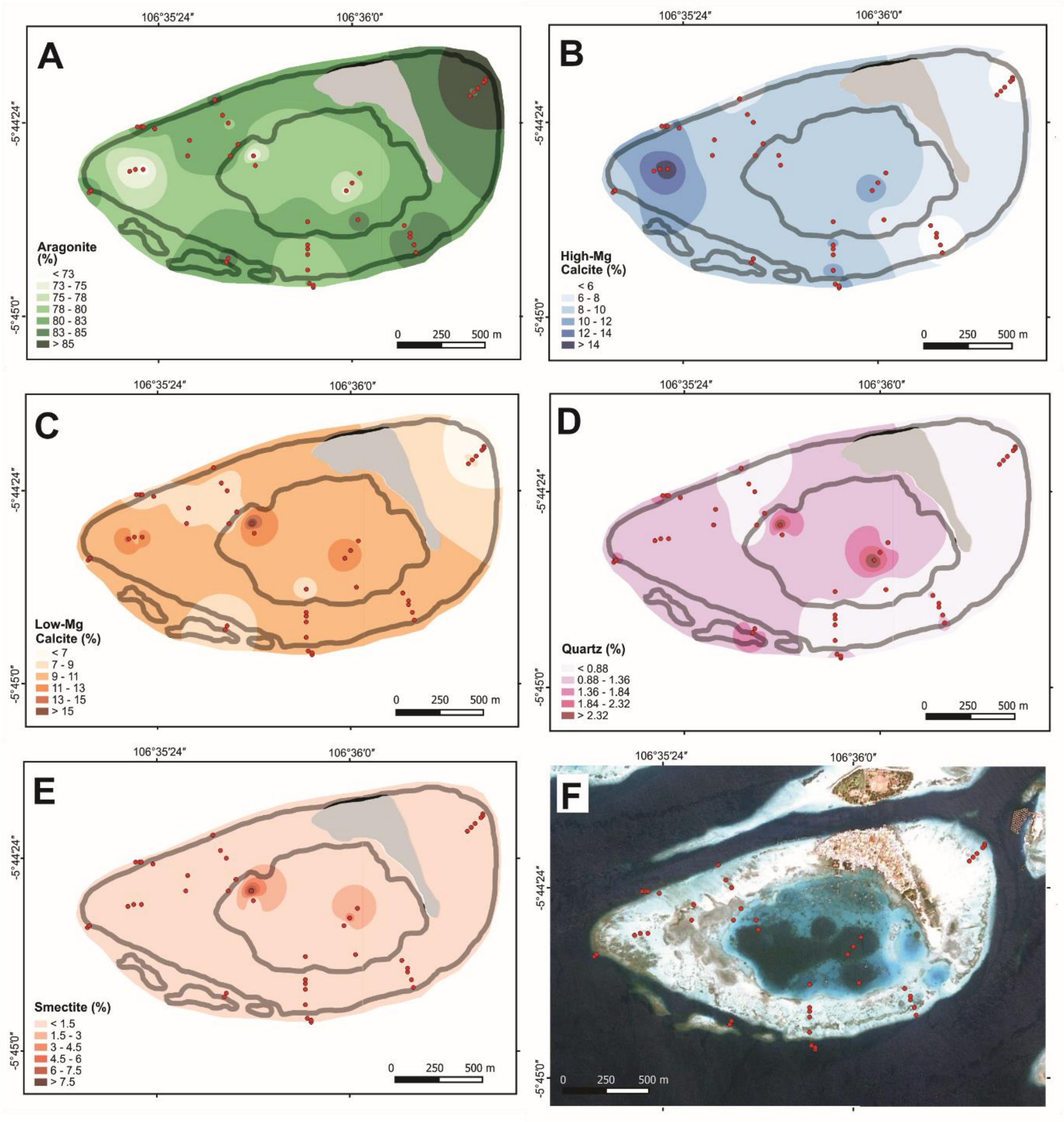

Figure 3-4. Carbonate mineral distribution (normalized to only carbonate mineral phases) on the Panggang reef platform from 45 bulk sediment samples for A. Aragonite. B. High-Mg Calcite. C. Low-Mg Calcite. Non-carbonate mineral distribution on Panggang reef platform from 45 bulk sediment samples for D. Quartz. E. Smectite. F. Satellite image of Panggang reef platform and sampling spots.

In addition, the mineralogy of the fine fraction (< 125µm) was measures for five samples (Tab. 3-2 and Fig. 3-5). Compared to their respective bulk samples, the fine fraction shows a ~1% higher quartz and significantly higher (9%) smectite content. If only the carbonate composition is considered, on average the fine fraction shows lower aragonite (bulk: 79%, < 125µm: 73%), higher HMC (bulk: 10%, < 125µm: 14%) and nearly equal LMC (bulk: 10%, < 125µm: 11%) contents. XRD analysis confirmed that all of the five individual bivalve shells are bimineralic, containing predominantly aragonite (90%) and LMC (10%) as a subordinate phase.

Table 3-2. Mineralogy (%) of five fine fraction (< 125µm) samples, along with their respective bulk sample mineralogy. Carbonate* is mineralogy normalized to only carbonate mineral phases. Abbreviations: Sed facies = sedimentary facies; C-M P = coral-mollusc packstone, M W = mollusc wackestone, ARA = aragonite, HMC = high magnesium calcite, LMC = low magnesium calcite, Qz = quartz, Sm = smectite, Mg (%) = mole % $MgCO_3$ in Mg-calcite.

Sample		MPG 14C	MPG 32D	MPG 33D	MPG 33G	MPG 42L	Mean
Sedimentary facies		C-M P	M W	M W	M W	C-M P	
< 125 µm		24%	40%	71%	75%	18%	
Carbonate* bulk mineralogy	ARA	79	83	77	75	81	79
	HMC	11	8	11	12	9	10
	LMC	9	8	11	13	9	10
	Mg (%)	13.0	14.0	11.7	12.7	14.0	13.1
Carbonate* <125 µm	ARA	74	76	73	71	74	73
	HMC	14	13	14	15	13	14
	LMC	12	9	13	12	10	11
	Mg (%)	15.3	11.7	14.0	13.3	14.0	13.7
Bulk mineralogy	ARA	78	83	73	72	79	77
	HMC	11	8	10	11	9	10
	LMC	9	8	11	13	9	10
	Qz	1	1	2	3	2	2
	Sm	0	0	4	0	0	1
<125 µm	ARA	66	62	64	64	62	64
	HMC	13	11	13	13	11	12
	LMC	11	8	12	11	8	10
	Qz	4	4	3	2	4	3
	Sm	7	14	9	8	11	10

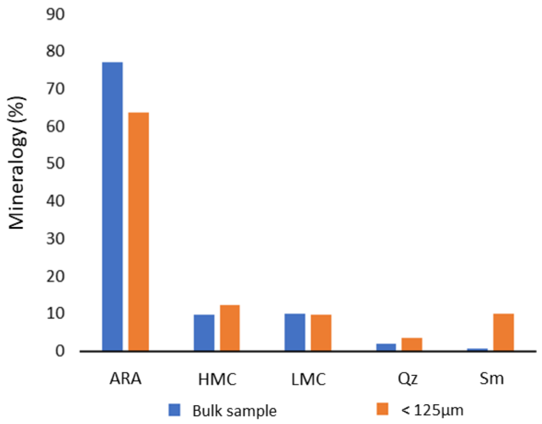

Figure 3-5. Average mineralogy (%) of five fine fraction (< 125µm) samples, along with their respective bulk sample mineralogy as indicated in table 2.

Stable isotopes of carbonates

Carbon isotope values ($\delta^{13}C$) range from -1.3 to 0.9 ‰ and oxygen isotopes ($\delta^{18}O$) from -3.4 to -4.9 ‰ for bulk sediment (Fig. 3-6). The fine fraction (< 125µm) samples did not show a systematic offset in their isotope values with respect to their bulk samples (Fig. 3-6). Coral abundance is negatively correlated with bulk sediment $\delta^{13}C$ (r = -0.52; p = 0.04) and $\delta^{18}O$ (r = -0.79; p < 0.01; Tab. 3-3), while mollusc abundance shows a positive correlation with $\delta^{13}C$ (r = 0.58; p = 0.02) and $\delta^{18}O$ (r = 0.79; p < 0.01). A negative correlation is also apparent for the relationship between the abundance of aragonite and $\delta^{18}O$ (r = -0.7; p = < 0.01). Aragonite and $\delta^{13}C$ also show a weak negative correlation (r = -0.43, p = 0.11). Coral isotope values from Bidadari (Fig. 3-6) are centered around -3 ‰ $\delta^{13}C$ and -6 ‰ $\delta^{18}O$ and lower compared to the bulk samples. Isotope values from bivalves and benthic foraminifers are generally higher compared to the bulk samples but partly overlap with samples from the mollusk wackestone facies (Fig. 3-6). Carbon and oxygen isotope values of bulk sediment from Kepulauan Seribu show more positive value in the inner lagoon and more negative value in the reef front (Fig. 3-7).

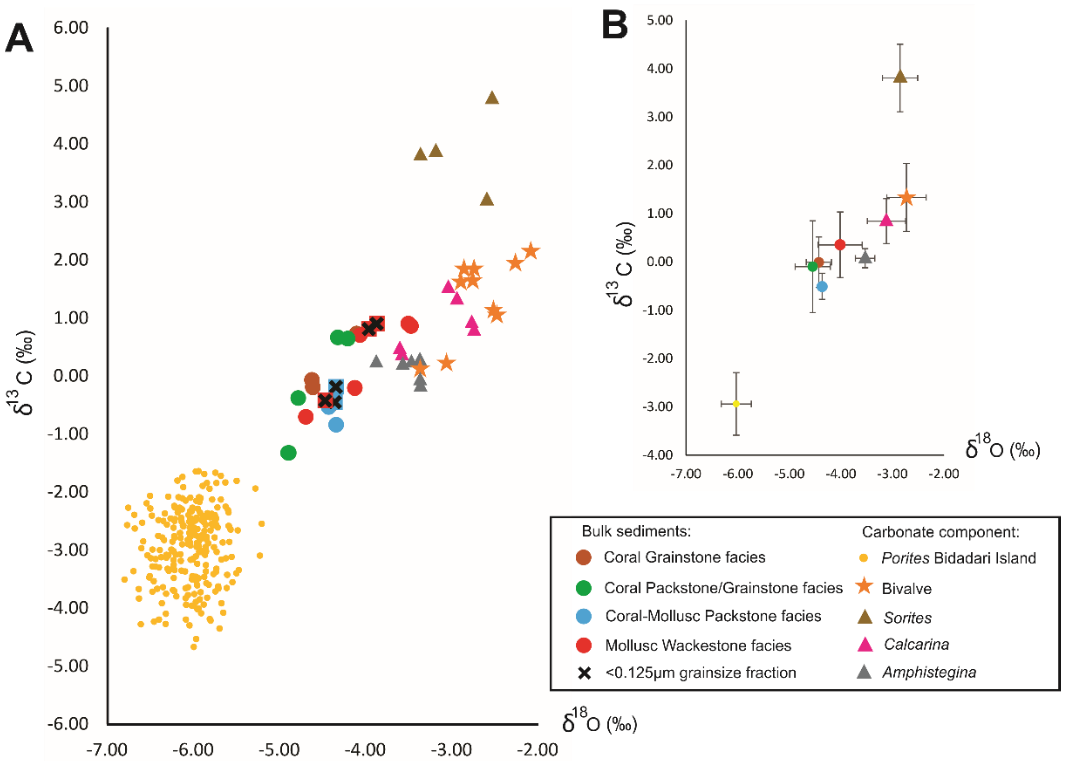

Figure 3-6. $\delta^{13}C$ - $\delta^{18}O$ plot. (A). Sedimentary facies show considerable overlap in their isotopic composition. Also shown is the isotopic composition of bivalves and benthic foraminifers (rotaliids and miliolids) from the Panggang reef platform and a *Porites* coral from Bidadari Island, Kepulauan Seribu. All bivalves, *Calcarina*, *Amphistegina*,

and one individual *Sorites* sample were split into two aliquots and measured as subsample. (B). Average values and standard deviation of measured isotopic composition for all facies and biota.

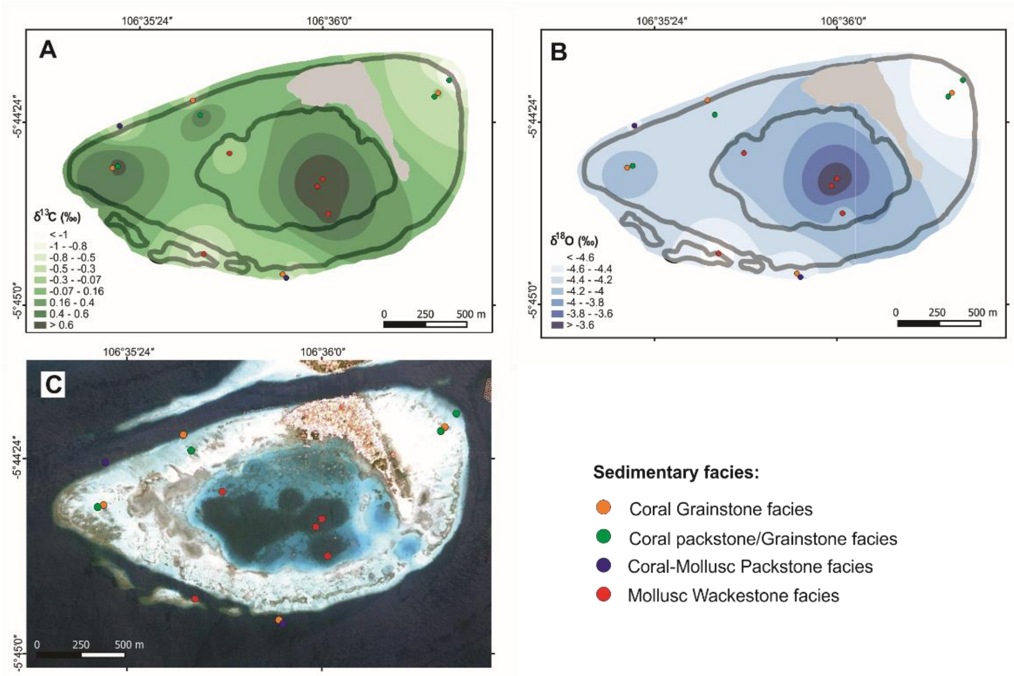

Figure 3-7. Spatial composition map of carbon and oxygen isotopes of sediments on the Panggang reef platform. (A). $\delta^{13}C$ (‰) of 15 bulk sediment samples. (B). $\delta^{18}O$ (‰) of 15 bulk sediment samples. (C). Satellite image of Panggang reef platform and sampling spots.

Table 3-3. Correlation matrix: Significant correlations ($p < 0.05$) are marked in bold. *p*-values in upper right part of table, *r*-values in lower left part. The basis for the correlation of grain types is the relative abundance in the > 125µm fraction. The correlation to fines is calculated based on the contribution of matrix (< 125µm) to the total sediment. Only the mineralogy and isotopic composition of the bulk values were used for the correlation. The correlation between isotope data and other parameters are based on a lower number of analyses (n=15) compared to point counting data and mineralogical composition (n=45). Abbreviation: R. Algae = red algae, *Hal* = *Halimeda*, Foram = foraminifers, Echi = echinoderm, ARA = aragonite, HMC = high magnesium calcite, LMC = low magnesium calcite, Qz = quartz, Sm = smectite.

	Coral	R Algae	Hal	Mollusc	Foram	Echi	Fines	ARA	HMC	LMC	Qz	Sm	water depth	$\delta^{13}C$	$\delta^{18}O$
Coral		0.051	0.34	<0.01	0.15	0.32	<0.01	0.06	0.86	0.03	0.04	0.1	0.66	0.049	<0.01
R Algae	0.29		0.98	<0.01	<0.01	0.19	0.06	0.45	0.78	0.88	0.3	0.36	0.42	0.1	0.22
Hal	0.14	-0		0.15	0.19	0.1	0.05	0.6	0.08	0.47	0.34	0.62	0.25	0.84	0.46
Mollusc	**-0.93**	**-0.54**	-0.22		<0.01	0.55	<0.01	0.1	0.66	0.09	0.08	0.18	0.92	0.02	<0.01
Foram	0.22	**0.58**	-0.2	**-0.48**		<0.01	0.02	0.29	0.98	0.22	0.31	0.27	0.61	0.02	<0.01
Echi	-0.15	0.2	-0.25	-0.09	**0.49**		0.13	0.89	0.53	0.55	0.4	0.72	0.11	0.02	0.16
Fines	**-0.74**	-0.28	-0.29	**0.74**	**-0.33**	0.23		<0.01	0.55	0.01	<0.01	<0.01	0.23	0.26	<0.01
ARA	0.28	-0.12	0.08	-0.25	0.16	0.02	**-0.47**		<0.01	<0.01	<0.01	<0.01	0.53	0.11	<0.01
HMC	-0.03	0.04	-0.26	0.07	0	-0.1	0.09	**-0.7**		0.09	0.22	0.95	0.19	0.03	0.04
LMC	**-0.32**	0.02	0.11	0.26	-0.18	0.09	**0.41**	**-0.8**	0.26		<0.01	<0.01	0.18	0.14	0.01
Qz	**-0.31**	0.16	-0.14	0.26	-0.16	0.13	**0.57**	**-0.6**	0.19	**0.5**		<0.01	0.01	0.95	0.08
Sm	-0.25	0.14	0.08	0.2	-0.17	-0.1	**0.46**	**-0.6**	0.01	**0.44**	**0.49**		0.73	0.78	0.2
water depth	-0.07	0.12	-0.17	0.02	0.08	0.24	0.18	0.1	-0.2	-0.2	**0.37**	0.05		0.06	0.65
$\delta^{13}C$	**-0.52**	-0.44	-0.06	**0.58**	**-0.6**	**-0.6**	0.31	-0.4	**0.55**	0.4	0.02	0.08	-0.49		<0.01
$\delta^{18}O$	**-0.79**	-0.34	-0.21	**0.79**	**-0.75**	-0.4	**0.71**	**-0.7**	**0.54**	**0.63**	0.47	0.35	-0.13	**0.78**	

3.5 Discussion

I. Spatial and compositional pattern in mineralogy

The dominant mineral phase in Panggang is aragonite (Tab. 3-1). Its concentration varies little between facies (Tab. 3-1, Fig. 3-3), with slightly increased values close to areas with dense coral cover on the reef front (Fig. 3-4). The aragonitic red algae genera *Galaxaura* and *Liagora* also thrive on the Kepulauan Seribu reef slope (Atmadja, 1977), likely also contributing to the high aragonite concentrations. HMC and LMC occur in fairly similar amounts in all facies (Tab. 3-1, Fig. 3-3), with slightly increased values of LMC in the mollusc wackestone facies of the inner lagoon and some isolated points on the western reef flat (Fig. 3-4). Corals as the main aragonite producers are less abundant in this area, while less light dependent carbonate producers such as molluscs and echinoderms are more common (Tab. 3-1). The highest LMC content is found in the mollusc wackestone facies (Tab. 3-1), which is known to dominate in the inner lagoon where coral grainstone and coral packstone/grainstone facies are absent (Utami *et al.*, 2018). High LMC content in the inner lagoon is likely due to the contribution from molluscs, the most important component in the mollusc wackestone facies (Tab. 3-1). Bivalves with calcitic or mixed aragonite-calcite shells in Kepulauan Seribu belong to the families Ostreidae (LMC), Pectinidae (LMC + ARA) and Pinnidae (LMC + ARA) (van der Meij et al. 2009; Ueda 2020). Five individual bivalve shells were measured using XRD. All of them have a mixed aragonite-calcite shell containing on average 90% aragonite and 10% LMC.

Locally, LMC is also abundant in the reef flat (Fig. 3-4), likely due to contributions from bivalves and larger benthic foraminifers (e.g. *Amphistegina* and *Elphidium*, Tab. 3-4) (Blackmon & Todd, 1959) which are abundant in the coral grainstone facies (Tab. 3-1). SEM analysis shows that calcareous nannoplankton, as a potential LMC source, is near absent in the sediment.

No clear correlation exists between HMC and individual biogenic grain types (Tab. 3-3). This is caused by the varied contribution of several different biota to the overall HMC content to the sediment. Red algae, such as *Amphiroa* that are typically associated with sea grass in Kepulauan Seribu (Atmadja 1977), contribute HMC to the coral grainstone facies on the reef flat (Tab. 3-1). Echinoderms are more important in the deeper water coral-mollusc packstone facies and mollusc wackestone facies (Tab. 3-1) compared to other facies. Increased HMC contents in the inner lagoon (Fig. 3-4) can therefore be interpreted as a higher contribution from echinoderms. Mg-content is generally higher in coralline algae compared to other organisms with HMC skeleton (Chave, 1954). This is consistent with the observation that the lowest Mg contents in HMC are found in the mollusc wackestone facies where coralline algae are rare (Tab. 3-1, Fig. 3-3).

Table 3-4. Faunal elements in Kepulauan Seribu (Atmadja 1977; Renema 2008; van der Meij et al. 2009; Park et al. 2010; Ueda 2020) and their mineralogy.

	Red Algae (Genus)	Brown Algae (Genus)	Green Algae (Genus)	Bivalve (Family)	Benthic Foraminifers (Genus)
Aragonite	*Liagora* *Galaxaura*	*Padina*	*Halimeda*	All other families	
HMC	*Amphiroa* *Goniolithon* *Jania* *Lithothamnion*				*Amphisorus* *Borelis* *Calcarina* *Dendritina* *Heterostegina* *Laevipeneroplis* *Monalysidium* *Operculina* *Parasorites* *Peneroplis* *Sorites*
LMC				Pectinidae (+ARA) Ostreidae Pinnidae (+ARA)	*Amphistegina* *Elphidium*

The mineralogy of five fine fraction (< 125µm) subsamples from the coral-mollusc packstone and mollusc wackestone facies were analyzed using XRD. The aragonite content in these fine fraction subsamples is 6% lower compared to their respective bulk samples (Tab. 2). In contrast, their HMC content is increased by 4% (Tab. 2). It has been proposed that fish can produce significant amounts of HMC mud (Salter *et al.*, 2012). Most of the important (> 5% abundance) fish families in the area of Kepulauan Seribu (Madduppa, 2013) produce Mg-rich amorphous calcium carbonate. This carbonate phase commonly dissolves within hours and therefore is unlikely to be preserved as sediment (Salter *et al.*, 2017). Only one family (Apogonidae) produces mud sized HMC ellipsoids with Mg-content of around 30 - 45% (Salter *et al.*, 2018). However, the typical crystal morphologies have not been observed during SEM investigations in our samples. It is therefore unlikely that fish derived Mg-calcite contributes significantly to the increased HMC values in the fine fraction. In contrast, SEM investigations confirm that the fine fraction is largely a product of skeletal breakdown (Fig. 3-2). Carbonate components that occur only in the mud to fine sand size (< 125µm) fraction, such as tunicate spiculae and needles from Padina thalli, are exclusively aragonitic. Laboratory studies suggest that abrasion rates of corals are much slower compared to dominant HMC components such as coralline algae and echinoderms (Milliman *et al.*, 1974). Increased HMC content in the fine fraction (Tab. 3-2) therefore could be related to preferential breakdown of HMC components. However, it remains unclear in how far these laboratory results can be applied to natural settings. Quantitative data on the composition of different grains size fractions from isolated carbonate platforms of Belize were presented by Gischler and Zingeler (2002). Our calculations based on this data indicate that coral fragments are actually increased in abundance relative to echinoderm and red algae fragments in the fine (< 125 µm) fraction as compared to the larger grain size fraction. This is opposite to what would be expected by the laboratory results on mechanical abrasion (Milliman *et al.*, 1974), possibly indicating that other processes such as bioerosion are more important in reef settings. The preferential abrasion of HMC components therefore seems not to be the reason for the increased HMC content in the fine fraction. A known source of mud sized HMC are red algae growing on sea grass (Land, 1970; Perry *et al.*, 2019). Patches of sea grasses are common on the Seribu islands and are associated with reduced grain sizes in the sediment, likely due to their baffling effect (Utami *et al.*, 2018). They also might contribute to the increased HMC contents in the fine fraction. However, a comparison of the mineralogical composition between locations with dense and sparse sea grass cover on the sand apron of Panggang does not show a significant difference with respect to HMC content (Mann-Whitney *U* test, $p = 0.91$). Due to the abundance of sea grass, our dataset does not include samples from locations without sea grass.

Alternatively, micritization in northern Belize increases the HMC content of skeletal grains, which later are preferentially abraded and contribute to carbonate muds. Cementation in microbioerosion traces is an important mechanism for micritization (Reid & Macintyre, 2000). High-Mg calcite cement has been observed, besides other mineral phases, in endolithic microborings in corals (Schroeder, 1972). Bioerosion and/or micritization are ubiquitous in reefs affected by terrestrial runoff or upwelling in SE Asia (Tomascik *et al.*, 1997; Madden & Wilson, 2012; Wilson, 2012) including the Seribu Islands (Fig. 3-2) (Park *et al.*, 1992, 2010). Both processes are most intense at the outer surface of carbonate grains. The higher surface to volume ratio of smaller grains could therefore lead to stronger alteration of its mineralogy compared to larger grains. Micritization and bioerosion could therefore have contributed to the increased HMC content in the fine fraction of Panggang (Tab. 3-2).

Small amounts of siliciclastic minerals are found in Kepulauan Seribu (Tab. 3-1). Quartz content increases with water depth (Tab. 3-3), in the inner lagoon and reef front. Quartz and smectite are strongly concentrated in the fine fraction (Tab. 3-2), indicating that quartz grains will settle from suspension in low energy environments but are easily winnowed by waves and currents in high energy environments. Smectite occurs only in > 6m water depth within the inner lagoon (Fig. 3-4), where it likely settles below the wave base. The fact that siliciclastic minerals are found in almost all samples (Fig. 3-4) shows that Panggang is influenced by terrestrial runoff (Fig. 3-1). A possible source for the siliciclastics could be Sumatra, since Kepulauan Seribu is relatively isolated from a direct influence from Java and Kalimantan by the regional current system (Tomascik *et al.*, 1997; Jordan, 1998). Partially due to this siliciclastic influence, the depth of abundant coral growth in Kepulauan Seribu (0 - 18 m, Jordan 1998) is typical for equatorial carbonates in SE Asia, but very shallow compared to other regions (0 - 100 m) with clearer water and lower nutrient input (Wilson, 2008).

II. Spatial patterns in stable isotope composition of sediment

Delineating facies based on their $\delta^{13}C$ and $\delta^{18}O$ values is not possible due to a lack of a significance difference between carbonate facies (Kruskal Wallis test, $p = 0.17$ and $p = 0.15$ respectively). However, the average stable isotope values of the coral grainstone facies ($\delta^{13}C = 0.0$, $\delta^{18}O = -4.4$) is lower compared to the mollusc wackestone facies ($\delta^{13}C = 0.4$, $\delta^{18}O = -4.0$), suggesting some facies control (Fig. 3-6). Coral abundance shows a significantly negative correlation to $\delta^{13}C$ and $\delta^{18}O$ values (Tab. 3-3). This results from a strong kinetic control on isotope fractionation in corals (McConnaughey, 2003). Coral skeletons therefore show a depletion of heavy isotopes and consequently a strong offset from equilibrium values towards more negative isotope ratios (Fig. 3-6). Corals exert a strong influence on the bulk isotope composition, since they are the predominant skeletal material and major aragonite producer (Fig. 3-6). Marine mollusc shells, as the second most important sedimentary component (Tab. 3-3), do not show kinetic effects in their isotopic composition (McConnaughey & Gillikin, 2008). Their $\delta^{18}O$ values are often close to equilibrium values (Grossman & Ku, 1986) and therefore more positive compared to corals (Fig. 3-6) (Aharon, 1991). Carbon isotope signatures in molluscs are complex, with near equilibrium values e.g. in giant clams (Aharon, 1991) but often several ‰ lighter due to metabolic carbon contribution (McConnaughey & Gillikin, 2008). In reefal carbonates, molluscs are typically less depleted in ^{13}C compared to cooccurring corals (Fig. 3-6) (González & Lohmann, 1985). This results in a positive (negative) correlation (Tab. 3-3) between oxygen and carbon isotopes and molluscs (corals). Higher stable isotope values in the inner lagoon and sand apron of Panggang (Fig. 3-7) result from the increased abundance of molluscs in mollusc wackestone and coral packstone/grainstone facies (Tab. 3-1) and coincides with the overall lowest aragonite value (Fig. 3-4). The most negative $\delta^{13}C$ and $\delta^{18}O$ values occur at the reef front in coral grainstone and coral packstone/grainstone facies where coral cover is densest (Fig. 3-7). However, the compositional differences between individual facies types (Tab. 3-1) are not strong enough to result in separate isotope fields for each facies (Fig. 3-6).

The most important group of purely calcitic components are benthic foraminifers. Many shallow water benthic foraminifers from reefal environments precipitate their skeleton close to oxygen isotope equilibrium (+/- 1‰) (Saraswati *et al.*, 2004; Maeda *et al.*, 2017), although slightly stronger depletion of ^{18}O was observed as well (Wefer & Berger, 1991). Carbon isotopes typically are lighter compared to equilibrium values with common ^{13}C depletion on the order of 1 - 3‰ for most miliolids and 2 - 5‰ for rotaliids (Wefer *et al.*, 1981; Saraswati *et al.*, 2004). This is consistent with lower $\delta^{13}C$ values in rotaliids (*Calcarina*, *Amphistegina*) compared to miliolids (*Sorites*) in the study area (Fig. 3-6). Benthic foraminifers from reefal environments therefore are characterized by generally more positive stable isotope values compared to cooccurring corals (Fig. 3-6), but can show partial overlap in their $\delta^{13}C$ ranges (González & Lohmann, 1985; Gischler *et al.*, 2012), especially if rotaliids are abundant. The observed negative correlation between aragonite content and stable isotope values (Tab. 3-3) likely results from this isotopic difference between corals and benthic foraminifers as the main aragonite and calcite producers, respectively. The fact that some molluscs contribute calcite to the sediment likely enhances this effect.

The positive correlation between stable isotopes and fines is a spurious relationship (Tab. 3-3), resulting from the strong positive (negative) correlation with molluscs (corals). This is supported by the observation that the fine fraction samples show no consistent isotopic difference to the bulk samples (Tab. 3-3). This similarity indicates that the fine fraction is genetically related to the coarse fraction and is formed by skeletal breakdown.

III. Comparison with other carbonate systems

To facilitate the comparison of mineralogical and stable isotope signatures between humid equatorial, arid (sub)tropical, and temperate carbonate systems we have grouped them geographically (Fig. 3-8 and 3-10). Carbonates from each geographical group share common characteristics and are deposited under similar environmental conditions (Fig. 3-9, Tab. 3-5). Carbonate systems from the tropical western Atlantic

(TWA) and Persian Gulf represent mostly (sub)tropical carbonates (sensu Wilson 2002; Wilson 2012) characterized by at least seasonally arid conditions. These carbonates often contain facies with non-skeletal grains and are deposited in normal marine to hypersaline waters (Tab. 3-5). Exceptions are Florida Bay and Belize, which are characterized by riverine input leading to strong gradients in salinity ranging from brackish to hypersaline and absence or low abundance of non-skeletal grains. The carbonates from the Indo-Pacific Warm Pool (IPWP) (Fig. 3-8 to 3-10, Tab. 3-5) are deposited on isolated carbonate platforms under the highest average temperatures (>28°C) and high seasonal precipitation, but outside the direct influence of river runoff. Non-skeletal grains are uncommon. High latitude systems (Fig. 3-8 to 3-10, Tab. 3-5) are typical temperate water Heterozoan carbonates (Wilson, 2012).

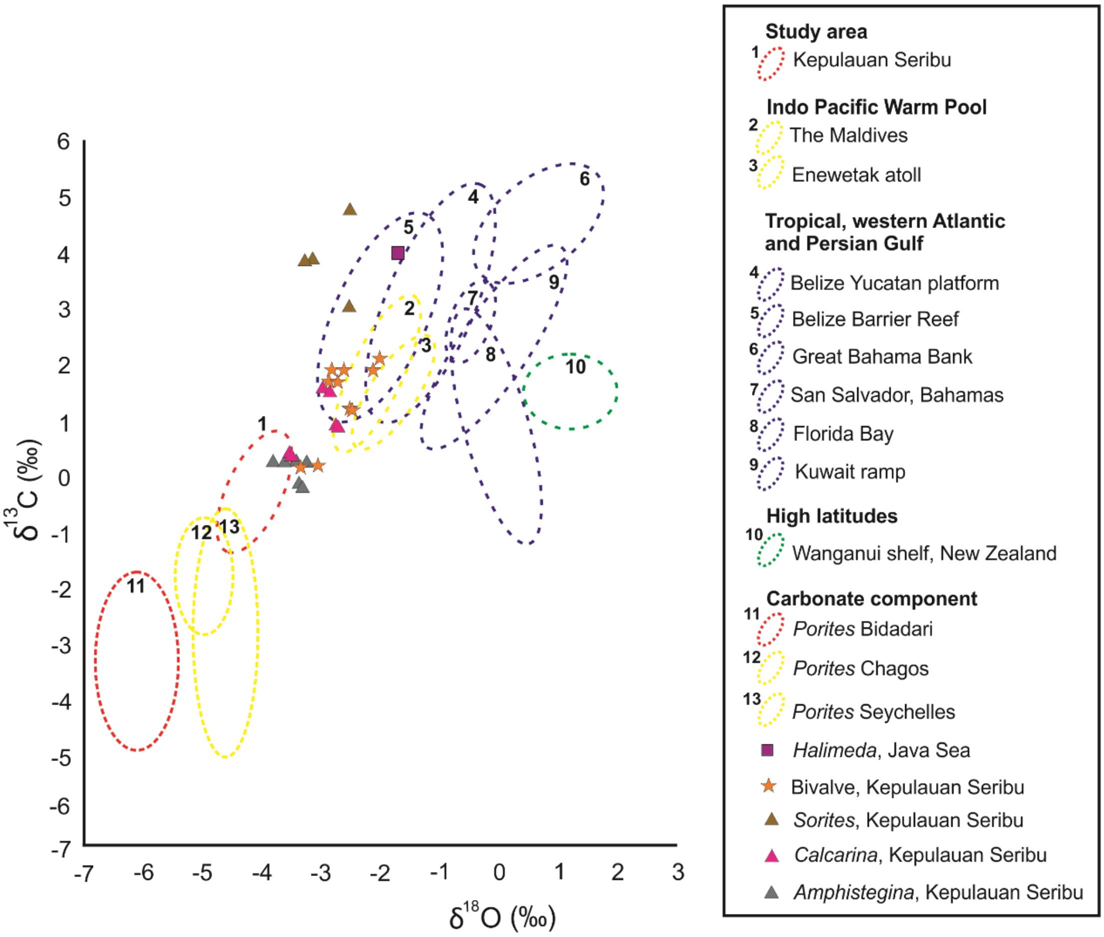

Figure 3-8. Cross-plot of $\delta^{13}C$ - $\delta^{18}O$ ranges of sediments from Panggang reef platform, Kepulauan Seribu. Also shown are stable isotope ranges of sediments from the Indo-Pacific Warm Pool (IPWP): Maldives (Gischler, 2006), Enewetak Atoll (Weber & Schmalz, 1968); Tropical, western Atlantic (TWA) and Persian Gulf: Belize Yucatan platform and Belize Barrier Reef (Gischler & Lomando, 1999; Gischler *et al.*, 2012), Great Bahama Bank (Swart *et al.*, 2009), San Salvador Island, Bahamas (Husinec *et al.*, 2019), Florida Bay (Swart *et al.*, 1989; Andrews, 1991), Kuwait ramp (Gischler & Lomando, 2005), and an example from high latitudes; Wanganui shelf, New Zealand (Gillespie & Nelson, 1997). For comparison the isotopes ranges of faunal elements are shown: *Porites* coral from Bidadari Island, Kepulauan Seribu (Cahyarini et al. 2016),

Porites corals from Seychelles and Chagos (Pfeiffer *et al.*, 2004; Pfeiffer & Dullo, 2006), *Halimeda* bioherm, eastern Java Sea (Aharon, 1991), bivalves and benthic foraminifers from Panggang reef platform. Location of Bidadari Island is shown in figure 3-1.

The $\delta^{13}C$ signature of carbonates from Kepulauan Seribu is considerably more negative compared to most other platform and reef systems (Fig. 3-8). The carbon isotopic composition of marine carbonates is mainly influenced by the $\delta^{13}C$ of the dissolved inorganic carbon (DIC) in water (Smith & Kroopnick, 1981), the mineralogy (Rubinson & Clayton, 1969; Romanek *et al.*, 1992) and so called "vital effects" in carbonate secreting organisms (e.g. kinetic and metabolic effects) (McConnaughey, 2003; McConnaughey & Gillikin, 2008). Because of these vital effects skeletal carbonates are typically depleted in $\delta^{13}C$ compared to inorganically precipitated carbonates from the same environment (Swart *et al.*, 2009; Gischler *et al.*, 2012). Non-skeletal grains and inorganically precipitated muds are much more common in modern platforms and reefs from the tropical, western Atlantic (TWA) and Persian Gulf compared to carbonate systems from the Indo-Pacific Warm Pool or New Zealand (Tab. 3-5) (Milliman *et al.*, 1974; Gischler, 2011; Gallagher *et al.*, 2018). Most carbonates from the TWA and Persian Gulf therefore show broader $\delta^{13}C$ ranges encompassing more positive $\delta^{13}C$ values (Fig. 3-8).

Due to mineralogical effects, inorganic aragonite is enriched in $\delta^{13}C$ by about 1.8 ‰ compared to coprecipitated calcite (Rubinson & Clayton, 1969; Romanek *et al.*, 1992). This mineralogical effect should favor a positive correlation between aragonite content and $\delta^{13}C$. However, the actual relation depends on the source and therefore isotopic signature of the aragonite. Aragonitic non-skeletal grains and green algae (Fig. 3-8) are characterized by more positive $\delta^{13}C$ values compared to most calcitic skeletal grains, resulting in a positive correlation between both parameters (Swart *et al.*, 2009; Gischler *et al.*, 2012). Corals on the other hand are more depleted in $\delta^{13}C$ compared to most calcite secreting organisms (Fig. 3-6), which explains the negative correlation between aragonite and $\delta^{13}C$ in the coral dominated Kepulauan Seribu (Tab. 3-3) and the lower $\delta^{13}C$ compared to the relatively calcite rich cool water carbonates (Fig. 3-8). However, the $\delta^{13}C$ signature of carbonate from Kepulauan Seribu is also more negative compared to most other coral dominated reef facies from the IPWP (Fig. 3-8).

Carbon isotope data from a *Porites* coral from Bidadari Island (Fig. 3-1) in the Java Sea, is on average more depleted compared to *Porites* corals from the Seychelles and Chagos both of which are located within the IPWP (Fig. 3-8) (Pfeiffer *et al.*, 2004; Pfeiffer & Dullo, 2006; Cahyarini *et al.*, 2016). It is unlikely that this difference is solely due to kinetic related offsets, since all three coral colonies show similar growth rates (Pfeiffer *et al.*, 2004; Pfeiffer & Dullo, 2006; Cahyarini *et al.*, 2016). More negative $\delta^{13}C$ values of the *Porites* colony from Bidadari Island are more likely due to the influence of river run off. Corals have the potential to record land-ocean carbon transfer because they draw on dissolved inorganic carbon (DIC) for calcification. The $\delta^{13}C$ of DIC in coastal water is influenced by the $\delta^{13}C$ signature from adjacent rivers (Moyer & Grottoli, 2011). Bidadari Island is located in the Java Sea (Fig. 3-1) and in close proximity to three major rivers in the Greater Jakarta Area (Farhan & Lim, 2012). Estuaries in SE Asia show low $\delta^{13}C_{DIC}$ values due to the contribution of ^{12}C from riverside mangroves (Miyajima *et al.*, 2009). The low $\delta^{13}C$ of the coral skeleton in Kepulauan Seribu therefore likely reflects the enrichment in ^{12}C of ambient seawater due to the input of riverine DIC to the Java Sea.

To a somewhat lesser extent, light intensity (photosynthesis) also has been shown to influence the value of skeletal $\delta^{13}C$ in corals (Moyer & Grottoli, 2011). Corals are usually depleted in ^{13}C relative to ambient seawater as a result of kinetic and metabolic fractionation (Swart, 1983; McConnaughey, 1989; Allison *et al.*, 1996; Grottoli & Wellington, 1999). Environmental variables that influence coral metabolism should therefore also affect $\delta^{13}C$ levels in coral skeletons (Grottoli, 2002). Under low light conditions photosynthesis decreases and metabolic fractionation increases with the consequence of decreased skeletal $\delta^{13}C$ (Grottoli, 2002). Sediment input from rivers into the Java Sea potentially enhances turbidity in the semi enclosed basin, leading to a reduction of light intensity and photosynthesis thus resulting in reduced skeletal $\delta^{13}C$ values. This would be consistent with the relatively shallow depth of reef growth (Jordan, 1998) and the presence of siliciclastic minerals in sediment samples below the wave base (Fig. 3-4) in the study area. Turbidity can also be produced by algae blooms caused by increased nutrient input either through river water or untreated sewage from populated islands (Baum *et al.*, 2015). Additionally, higher nutrient availability could influence the $\delta^{13}C$ of coral skeletons by an increase in the heterotrophic feeding rate or an increase in the photosynthesis rate related to higher zooxanthellate concentrations (Grottoli, 2002). However, these processes have opposing effect on the $\delta^{13}C$ of coral skeletons. The net effect therefore will depend on the relative magnitudes of these various influences but is expected to be small (Heikoop *et al.*, 2000).

The largest single anthropogenic influence on the isotope signature of recent corals likely is caused by the input of anthropogenic CO_2 to the global surface ocean. The accelerated admixture of fossil fuel derived CO_2 leads to a shift towards lower $\delta^{13}C$ values in atmospheric CO_2, the so called Suess effect (Keeling, 1979). This Suess effect is often recorded in declining coral skeleton $\delta^{13}C$ values over the 20th century (Swart *et al.*, 2010). Linsley et al. (2019) showed that the Suess effect can shift skeletal $\delta^{13}C$ in corals by more than 1 ‰ since the 1950s. The carbon isotope composition of corals in Fig. 3-8, which are largely derived from the 20th century, is therefore likely depleted relative to bulk sediments or sedimentary grains of mixed and/or unknown age.

Florida Bay is the only location that shows a nearly complete overlap but broader total range in $\delta^{13}C$ values compared to the sediments from Kepulauan Seribu (Fig. 3-8). In contrast to many other areas in the TWA, non-skeletal grains and inorganic mud are lacking in Florida Bay (Tab. 3-5). Average $\delta^{13}C_{DIC}$ of surface waters in Florida Bay is lowest in areas influenced by isotopically depleted river runoff from the Everglades, while the $\delta^{13}C$ variability in other areas is controlled by remineralization of marine organic matter (Swart & Price, 2002). Similar to Kepulauan Seribu, the lowest values in $\delta^{13}C$ of carbonates deposited in Florida Bay seem to be a result of isotopically depleted river runoff and a lack of inorganic carbonate precipitation.

Since the pioneering work by Urey (1947), the $\delta^{18}O$ values of carbonate minerals are known to be controlled by temperature of formation. Other controlling factors are the $\delta^{18}O$ value ($\delta^{18}O_w$) of the precipitating fluid (Urey, 1947; Epstein & Mayeda, 1953), mineralogy (Tarutani *et al.*, 1969), and “vital effects” in carbonate secreting organisms (McConnaughey, 2003). The slope of the $\delta^{18}O$/temperature relationship in carbonates is commonly assumed to be in the range from -0.2 to -0.25 ‰/°C (Grossman & Ku, 1986; Bemis *et al.*, 1998), resulting in a decrease of 0.8 to 1 ‰ $\delta^{18}O$ for a four degree increase in temperature.

Carbonates from Kepulauan Seribu are characterized by much lower $\delta^{18}O$ values compared to other carbonate systems (Fig. 3-8). This can be explained by the combined effect of high sea surface temperatures and low $\delta^{18}O_w$ in the Java Sea (Fig. 3-9). Modelling results confirm that for carbonates precipitated in equilibrium with seawater, SE Asia is globally the region with the most negative $\delta^{18}O$ signature (Fig. 3-9C). Within the IPWP the differences in temperature are small (Fig. 3-9A), but $\delta^{18}O$ water is significantly reduced in SE Asia compared to e.g. the central equatorial Indian Ocean or Pacific (Fig. 3-9B).

Table 3-5. Location and basic environmental and sedimentological data for carbonate systems used for comparison in Figs. 3-8 and 3-10. (*N/A = average and standard deviation data not available).

Location		**SST (°C)**	**SSS (‰)**	**$\delta^{13}C$ (‰)**	**$\delta^{18}O$ (‰)**	**non-skeletal grains**	**Source**
Panggang, Kepulauan Seribu	5° 44'S, 106° 36'E	28 - 30	30 - 34	0.02 ± 0.7	-4.27 ± 0.4	very rare	this study
Rasdhoo & Ari atoll, Maldives	3° 37' - 4° 17'N, 72° 54' - 72° 58'E	28 - 30	34.4 - 35.4	1.56 ± 0.58	-2.06 ± 0.83	very rare	(Gischler, 2006)
Enewetak	11° 25'N, 162° 20'E	28 - 32	34 - 35	1.75 ± 0.55	-1.90 ± 0.42	none	(Weber & Schmalz, 1968)
Honduras, Carribean oceanic barrier reef	16° 23'N, 86° 25'W	29 - 31	36 - 37	N/A	N/A	peloids common, ooids rare	(Schmitt & Gischler, 2017)
Belize Barrier Reef	16° 30 - 18N, 88°W	24 - 27	30 - 35	N/A	N/A	rare	(Gischler *et al.*, 2013)
Belize-Yucatan Platform (Glovers, Lighthouse, Turneffe)	16° 44' - 17° 18' N, 87° 32' - 87° 48' W	21.7 - 31.8	34.2 - 42.5	N/A	N/A	rare to moderate	(Gischler *et al.*, 2012)
Belize northern shelf	17° 45' - 18°N, 88°W	25.5 - 28.5	30 - 34	N/A	N/A	rare	(Gischler *et al.*, 2013)
Belize southern shelf	16° - 17°N, 88°W			N/A	N/A		(Weber & Schmalz, 1968)
Great Bahama Bank	23° - 26°N, 77° 30' - 79° 30'W	18.5 - 28.5	36 - 46	4.8 ± 0.3	0.4 ± 0.4	abundant	(Reijmer *et al.*, 2009; Swart *et al.*, 2009)
San Salvador Island, Bahamas	24° 05'N, 74° 26'W	24 - 30	35	2.2	-0.9	moderate to abundant	(Husinec *et al.*, 2019)
Florida Bay	25° 01'N, 80° 34'W	15 - 40	10 - 40	N/A	N/A	none	(Ginsburg, 1956; Swart *et al.*, 1989; Andrews, 1991)
Kuwait ramp	28° 30' - 29° 15'N, 18° 15' - 18° 45'E	13 - 32	38.5 - 42.5	N/A	N/A	abundant	(Gischler & Lomando, 2005)
Spencer Gulf, South Australia	33° - 35°S, 136° - 138°E	10 - 28	36 - 47	N/A	N/A	none	(O'Connell & James, 2015)
Lacepede Shelf (LS) and Great Australian Bight (GAB), Southern Australia	LS: 35° 30' - 38°S, 137° - 140°E, GAB: 33° 15 - 35°S, 124° - 134°E	LS: <14 - 20 GAB: 17 - 22	35.9 - 36.4	N/A	N/A	none	(O'Connell & James, 2015)
Wanganui Shelf, New Zealand	40°S, 175°E	ca. 15	34 - 35	N/A	N/A	none	(Gillespie & Nelson, 1997)

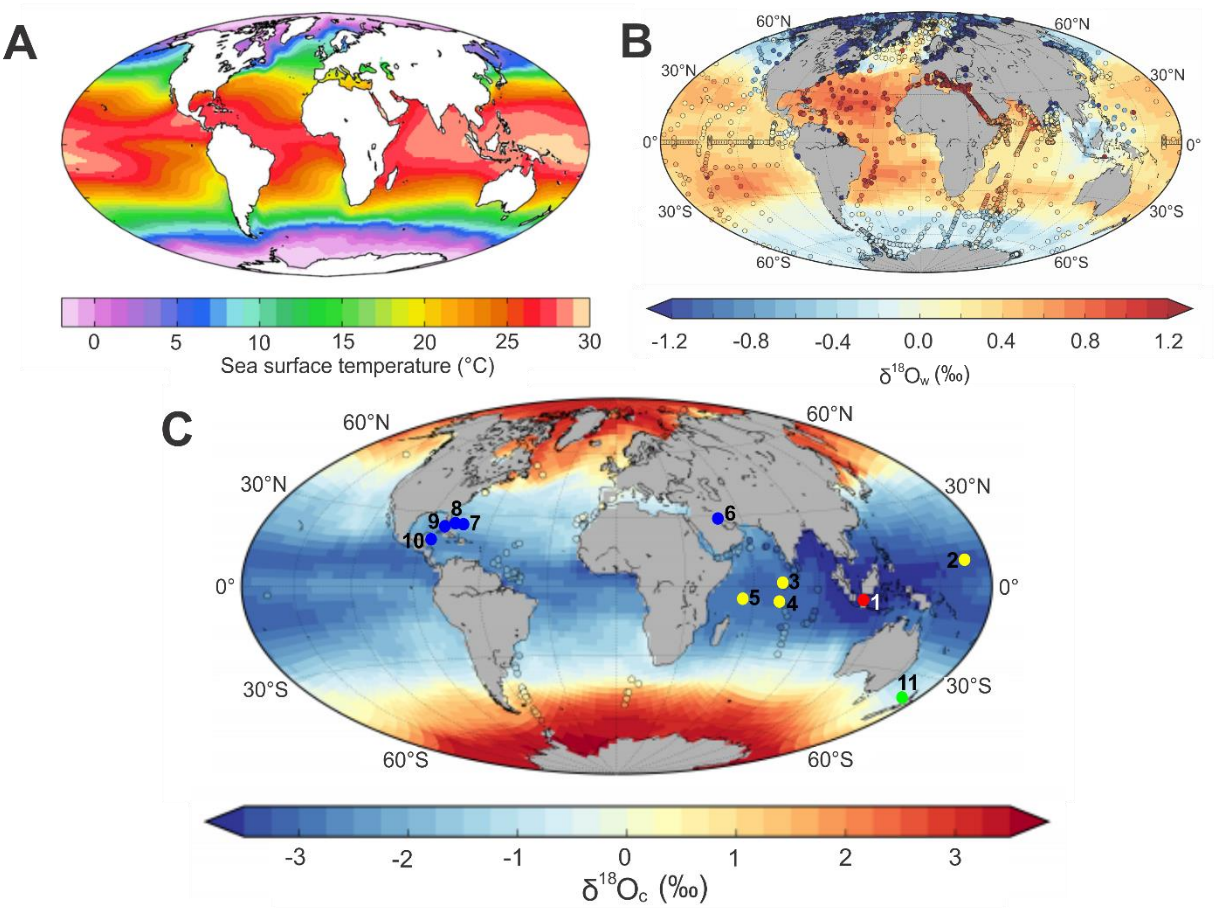

Figure 3-9. Main controlling factors for oxygen isotope composition of carbonate minerals are temperature and $\delta^{18}O$ of water (A). Annual mean sea surface temperature (World Ocean Atlas 2009; http://www. nodc.noaa.gov/OC5/WOA09/pr_woa09.html). (B). Global annual mean surface (upper 50m) $\delta^{18}O_w$ distribution simulated by a general circulation model (MITgcm) in comparison to the observational isotope data (colored symbols – Schmidt et al., 1990) for the global ocean (Völpel *et al.*, 2017). (C). Distribution of modelled annual mean sea surface (upper 50 m) $\delta^{18}O$ in calcite ($\delta^{18}O_c$) compared to $\delta^{18}O_c$ values measured on planktonic foraminifers from plankton tows (Völpel *et al.*, 2017). Location of carbonate sites: 1. Study area in Kepulauan Seribu, 2. Enewetak, 3. The Maldives, 4. Chagos, 5. Seychelles, 6. Kuwait ramp, 7. San Salvador, Bahamas, 8. Great Bahama Bank, 9. Florida Bay, 10. Belize, 11. Wanganui shelf, New Zealand.

Differences in hydrology are reflected in the lower $\delta^{18}O$ values of a *Porites* coral from Kepulauan Seribu compared to those from the Seychelles and Chagos (Fig. 3-8). The difference of more than 1 ‰ in $\delta^{18}O$ is more than can be explained by intercolony offsets (Sayani *et al.*, 2019) or the temperature difference of ~1°C between the Java Sea and the other two sites. Most of the difference therefore can be attributed to the contrasting $\delta^{18}O$ seawater values, which based on the difference in salinity should be around 0.9 – 1.1 ‰/$\delta^{18}O$ assuming a slope of 0.22 ‰ for the salinity/ $\delta^{18}O$ relationship (Fairbanks *et al.*, 1997). The lower $\delta^{18}O$ seawater values in the Java Sea result from heavy precipitation and increased runoff, and are also influenced by the $\delta^{18}O_w$ of the precipitation itself via the so called “amount effect” (Rozanski *et al.*, 1993; Lau & Yang, 2003).

Facies also could influence the $\delta^{18}O$ signature of bulk sediments due to differences in the “vital effects” of carbonate producing organisms (McConnaughey, 2003; McConnaughey & Gillikin, 2008) and mineralogy (Tarutani *et al.*, 1969). However, the different $\delta^{18}O$ values for individual grain types to a large extent seem to average out for bulk samples (Gischler *et al.*, 2012). This results in relatively large overlaps between facies in most atolls, barrier reefs and platforms (Gischler *et al.*, 2012), showing that the influence of facies in these settings is limited.

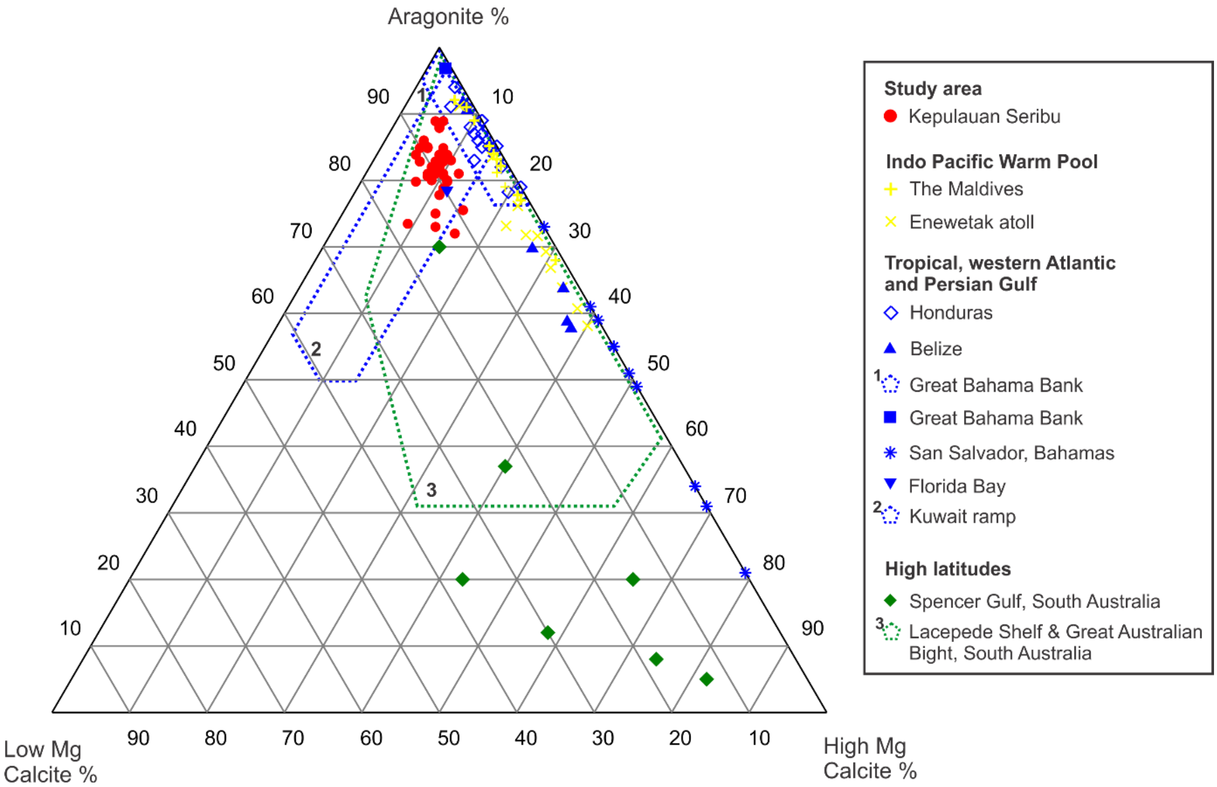

Figure 3-10. Mineralogical composition of bulk surface sediment from Panggang reef platform, Kepulauan Seribu (normalize to only carbonate mineral phases). Carbonate mineralogy of Holocene bulk surface sediment from the Maldives (Gischler, 2006), Enewetak Atoll (Weber & Schmalz, 1968), Honduras, Caribbean oceanic barrier reef (Schmitt & Gischler, 2017), Belize (Weber & Schmalz, 1968; Gischler *et al.*, 2012, 2013), Great Bahama Bank (Purdy, 1963; Reijmer *et al.*, 2009), San Salvador, Bahamas (Husinec *et al.*, 2019), Florida Bay (Ginsburg, 1956), Kuwait ramp (Gischler & Lomando, 2005), Spencer Gulf, South Australia (O’Connell & James, 2015), Lacepede Shelf and Great Australian Bight, South Australia (James *et al.*, 2005) are shown for comparison. All sample are from shallow water (< 20m) except sample from South Australia.

The carbonate mineralogy of shallow water (< 20m) bulk sediments in the tropics and subtropics (IPWP, TWA) is predominantly composed of aragonite and HMC, with LMC usually present in low quantities < 10% (Fig. 3-10) (Ginsburg, 1956; Purdy, 1963; Weber & Schmalz, 1968; Gischler, 2006; Reijmer *et al.*, 2009; Gischler *et al.*, 2013; Schmitt & Gischler, 2017; Husinec *et al.*, 2019). The only exception is the Kuwait ramp system that shows LMC contents of up to ~40% (Gischler & Lomando, 2005). In reef atoll and platform systems higher LMC content > 10% are usually spatially restricted and related to local dominance of rotaliid foraminifers, such as *Amphistegina* (Weber & Woodhead, 1972), contribution from calcite precipitated in meteoric waters (Swart & Kramer, 1997) or from microbial activity (Pusey, 1975; Purdy & Gischler, 2003). Otherwise, higher LMC (7 to 14%) contents generally occur only in deeper water between 20 and 70m, mainly contributed from planktonic foraminifers, coccoliths and molluscs (Weber & Schmalz, 1968; Gischler, 2006). Aragonite also dominates the mineralogy of the study area in Kepulauan Seribu but HMC and LMC occur in nearly equal proportions. The main mineralogical difference to other reefal systems in the IPWP is the occurrence of clastic mineral phases (Tab. 3-1) and a higher LMC content (~10%) in the shallow water sediment (Fig. 3-10).

Opposed to open ocean settings, the semi enclosed Java Sea is influenced by river runoff. Terrestrial sediments reaching Kepulauan Seribu (Tab. 3-1) most likely are derived from Sumatran rivers, since oceanic currents isolate Kepulauan Seribu from sediment input from Java and Kalimantan (Tomascik *et al.*, 1997; Jordan, 1998). The suspended particulate matter promotes oligophotic conditions in relatively shallow water. Wilson and Vecsei (2005) argued that oligophotic conditions in water depth below 20 m are typical for humid equatorial carbonate systems in SE Asia and would favor the deposition of e.g. relatively calcite-rich foramol facies. Foramol facies in Kepulauan Seribu dominates in water depth below 27 m (Jordan, 1998). In water depth < 20m, rotaliid foraminifers contribute to LMC (Tab. 3-4) but their abundance is not high enough to explain the generally increased LMC content. Another important source of LMC in Kepulauan Seribu seems to be mixed aragonite-calcite bivalve shells. More mineralogical analysis from humid equatorial settings are needed to test if the increased LMC content observed in Kepulauan Seribu is a common feature of shallow water (< 20m) reef systems in humid, equatorial settings.

Fine fraction sediment from the Panggang reef platform is showing a higher HMC compared to the bulk fraction, likely related to micritization and bioerosion. Higher HMC contents in the fine fraction are also found in Belize, the potential source is micritization of skeletal grains to Mg-calcite (Weber & Schmalz, 1968). Micritization of skeletal grains is also an important diagenetic process in other shallow marine carbonate platforms, e.g. The Bahamas where the grains are altered to aragonite (Purdy, 1963; Bathurst, 1966; Kendall & Skipwith, 1969; Trumbull, 1988). Preferential alteration of the carbonate grains into high-Mg calcite is potentially controlled by lower aragonite supersaturation in water off Kepulauan Seribu. Fresh water influx from rivers promotes low salinities in the semi-enclosed seas of SE Asia, leading to relatively low aragonite supersaturation compared to more arid regions as the tropical, western Atlantic (Park *et al.*, 2010). Seawater Mg:Ca ratios are another important control on carbonate mineralogy, with lower Mg:Ca favouring calcite precipitation at a given temperature (Morse *et al.*, 1997). A recent compilation of Mg:Ca ratios in seawater shows that values are not spatially constant but influenced by river waters with low Mg:Ca values (Lebrato *et al.*, 2020). No seawater data is available for the semi-enclosed seas of SE Asia, but the high riverine input could potentially also reduce the Mg:Ca ratios in the Java Sea. Depending on the magnitude of this effect, the reduced Mg:Ca ratios could facilitate the precipitation of calcite in the study area.

The mineralogical composition in the shallow water (< 20m), photozoan dominated carbonates from Kepulauan Seribu overlaps with the most aragonite rich part of the cool water carbonate field (Fig. 3-10). However, based on the dominance of reefal material, the sediments can be clearly differentiated from heterozoan dominated cool water carbonates. This might be more difficult for the foramol facies that dominates at the toe of slope and below (Jordan, 1998). Wilson (2012) pointed out that oligophotic, humid equatorial carbonates share many similarities with cool water carbonates. However, a marked difference is that HMC components in Panggang have much higher Mg-contents (11.7 – 14 mole% $MgCO_3$), compared to 4 – 12 mole% $MgCO_3$ in carbonate sediment of e.g. South Australia (James *et al.*, 2005; O'Connell & James, 2015). This difference can be best explained by the different water temperature between both regions. The $MgCO_3$ content in HMC of calcareous marine organism is strongly influenced by the water temperature, with an increase in Mg-content related to higher temperatures (Chave, 1954). However, this difference in Mg-content will not be helpful in the distinction of ancient carbonates since HMC is losing Mg from the crystal lattice relatively early during diagenesis (Brachert & Dullo, 2000).

3.6 Conclusion

The reef platforms of Kepulauan Seribu represent the shallow water, photozoan-dominated part of a humid equatorial carbonate system. The mineralogical and/or isotopic characteristic of their surface sediments are distinct from most other carbonate systems and likely are representative for many SE Asian reef systems affected by river runoff.

Biogenic debris from corals and molluscs are the most important grain types. Minor components include benthic foraminifers, echinoderms, red algae and the green alga *Halimeda,* while non-skeletal grains are very rare. Aragonite is the dominant mineral phase, mainly contributed from corals and to a lesser degree by molluscs. LMC and HMC occur in fairly similar amounts in all facies. Bivalves (calcitic and bimineralic) and some rotaliid foraminifers (e.g. *Amphistegina* and *Elphidium*) contribute LMC. Most red algae (e.g. *Amphiroa*), echinoderms, and benthic foraminifers (e.g. *Calcarina* and *Operculina*) are important sources for HMC. An increased HMC content in the fine fraction could be related to preferential breakdown of HMC components, possibly from red algae growing on sea grass. Alternatively, micritization and bioerosion could contribute to increased HMC. Small amounts of siliciclastic minerals (quartz and smectite) are preferentially deposited in deeper waters below the wave base. This shows that despite its relatively isolated position, Kepulauan Seribu is affected by sediment laden river runoff.

The main mineralogical difference between carbonates from Kepulauan Seribu and most other reefal systems in the tropic western Atlantic and Indo Pacific Warm Pool area, is the widespread presence of > 10% LMC content in the shallow water sediment. The LMC is contributed by organisms that are not or less light dependent (bivalves and some rotaliid foraminifers) and therefore can thrive under oligophotic conditions. The suspended particulate matter from terrestrial runoff likely limits the depth of the euphotic zone. This is reflected in the deposition of foramol facies below a depth of ~28m (Jordan, 1998), but seems to already affect the sediments in the upper 20m. Compared to similar foramol facies from higher latitudes, the Mg-content in HMC components from Kepulauan Seribu is much higher due to the different water temperature between both regions.

The $\delta^{13}C$ signature of carbonates from Kepulauan Seribu is considerably more negative compared to nearly all other platform and reef systems. This is likely due to the combination of low $\delta^{13}C_{DIC}$ in surface waters and the lack of green algal grains and inorganically precipitated carbonates. The $\delta^{13}C$ in surface waters likely is reduced by ^{12}C-enriched input of DIC to river water from riverside mangroves. Corals as the predominant skeletal material and major aragonite producer also excerpt an influence on the bulk isotope composition, resulting in depletion of heavy isotopes values due to kinetic “vital effects”. Low light intensity due to turbid water in the semi enclosed basin of the Java Sea potentially hampers photosynthesis, which further reduces skeletal $\delta^{13}C$ values in corals due to metabolic effects. The Suess effect, which is caused by the combustion of fossil fuel, leads to a decline of skeletal $\delta^{13}C$ over the 20th century in corals. This signal might not be recorded to its full extend in the bulk sediment yet, which represents a grain mixture of different ages.

Carbonates from Kepulauan Seribu are also characterized by much lower $\delta^{18}O$ values compared to other carbonate systems, due to high sea surface temperatures and low $\delta^{18}O_w$ in the Java Sea. Deep atmospheric convection leads to heavy precipitation and increased fluvial runoff of very ^{18}O depleted water to the semi enclosed Java Sea. The relatively low $\delta^{18}O$ of benthic foraminifers and bivalves from Kepulauan Seribu shows that the oxygen isotope signature can be used to distinguish foramol facies from oligophotic equatorial carbonates and cool water carbonates in the rock record.

CRediT Statement

Dwi Amanda Utami: funding acquisition, resources, investigation, formal analysis, visualization, writing – original draft, writing – review and editing. **Lars Reuning**: supervision, resources, conceptualization, formal analysis, validation, writing – original draft, writing – review and editing. **Maximillian Hallenberger:** investigation, writing – review and editing. **Sri Yudawati Cahyarini**: resources, writing – review and editing.

Acknowledgement

The authors are grateful to Lembaga Pengelola Dana Pendidikan (LPDP) who awarded a scholarship and dissertation fund to Dwi Amanda Utami Nasution. We are grateful to Prof. Miriam Pfeiffer for providing stable isotope data of *Porites* corals from the Seychelles and Chagos and for commenting an earlier version of the manuscript. Dr. Nils Andersen (Kiel) is acknowledged for stable isotope analysis. Uwe Wollenberg is thanked for his help with XRD measurement. We thank two anonymous reviewers for insightful comments on the manuscript. This work was partially supported by National Geographic Explorer grant no CP 087R 17. We acknowledge Google Earth for online imagery and QGIS (ver. 3.14.1-Pi) for GIS software.

References

Aharon, P. (1991) Recorders of reef environment histories: stable isotopes in corals, giant clams, and calcareous algae. *Coral Reefs*, **10**, 71–90.

Allison, N., **Tudhope, A.W.** and **Fallick, A.E.** (1996) Factors influencing the stable carbon and oxygen isotopic composition of Porites lutea coral skeletons from Phuket, South Thailand. *Coral Reefs*, **15**, 43–57.

Andrews, J.E. (1991) Geochemical indicators of depositional and early diagenetic facies in Holocene carbonate muds, and their preservation potential during stabilisation. *Chem. Geol.*, **93**, 267–289.

Atmadja, W.S. (1977) Notes on the Distribution of Red Algae (Rhodophyta) on the Coral Reef of Pari Islands, Seribu Islands. *Mar. Res. Indones.*, **17**, 15–20.

Bathurst, R.G.C. (1966) Boring algae, micrite envelopes and lithification of molluscan biosparites. *Geol. J.*, **5**, 15–32.

Baum, G., **Januar, H.I.**, **Ferse, S.C.A.** and **Kunzmann, A.** (2015) Local and Regional Impacts of Pollution on Coral Reefs along the Thousand Islands North of the Megacity Jakarta, Indonesia. *PLoS One*, **10**, e0138271.

Bemis, B.E., **Spero, H.J.**, **Bijma, J.** and **Lea, D.W.** (1998) Reevaluation of the oxygen isotopic composition of planktonic foraminifera: Experimental results and revised paleotemperature equations. *Paleoceanography*, **13**, 150–160.

Blackmon, P.D. and **Todd, R.** (1959) Mineralogy of some foraminifera as related to their classification and ecology. *J. Paleontol.* , **33**, 1–15.

Blott, S.J. and **Pye, K.** (2001) Gradistat: A grain size distribution and statistics package for the analysis of unconsolidated sediments. *Earth Surf. Process. Landforms*, **26**, 1237–1248.

Brachert, T.C. and **Dullo, W.C.** (2000) Shallow burial diagenesis of skeletal carbonates: Selective loss of aragonite shell material (Miocene to Recent, Queensland Plateau and Queensland Trough, NE Australia) - implications for shallow cool-water carbonates. *Sediment. Geol.*, **136**, 169–187.

Cahyarini, S.Y., **Zinke, J.**, **Troelstra, S.**, **Suharsono**, **Aldrian, E.** and **Hoeksema, B.W.** (2016) Coral Sr/Ca-based sea surface temperature and air temperature variability from the inshore and offshore corals in the Seribu Islands, Indonesia. *Mar. Pollut. Bull.*, **110**, 694–700.

Chave, K.E. (1954) Aspects of the Biogeochemistry of Magnesium 1. Calcareous Marine Organisms. *J. Geol.*, **62**, 266–283.

Damar, A., **Colijn, F.**, **Hesse, K.-J.** and **Wardiatno, Y.** (2012) The Eutrophication states of Jakarta, Lampung and Semangka Bays: Nutrient and Phytoplankton Dynamics in Indonesia Tropical Waters. *J. Trop. Biol. Conserv.*, **9**, 61–81.

Epstein, S. and **Mayeda, T.** (1953) Variation of O18 content of waters from natural sources. *Geochim. Cosmochim. Acta*, **4**, 213–224.

Fairbanks, R.G., **Evans, M.N.**, **Rubenstone, J.L.**, **Mortlock, R.A.**, **Broad, K.**, **Moore, M.D.** and **Charles, C.D.** (1997) Evaluating climate indices and their geochemical proxies measured in corals. *Coral Reefs*, **16**, 93–100.

Farhan, A.R. and **Lim, S.** (2012) Vulnerability assessment of ecological conditions in Seribu Islands, Indonesia. *Ocean Coast. Manag.*, **65**, 1–14.

Gallagher, S.J., **Reuning, L.**, **Himmler, T.**, **Henderiks, J.**, **De Vleeschouwer, D.**, **Groeneveld, J.**, **Rastegar Lari, A.**, **Fulthorpe, C.S.**, **Bogus, K.**, **Renema, W.**, **McGregor, H.V.**, **Kominz, M.A.**, **Auer, G.**, **Baranwal, S.**, **Castañeda, S.**, **Christensen, B.A.**, **Franco, D.R.**, **Gurnis, M.**, **Haller, C.**, **He, Y.**, **Ishiwa, T.**, **Iwatani, H.**, **Jatiningrum, R.S.**, **Korpanty, C.A.**, **Lee, E.Y.**, **Levin, E.**, **Mamo, B.L.**, **McHugh, C.M.**, **Petrick, B.F.**, **Potts, D.C.**, **Takayanagi, H.** and **Zhang, W.** (2018) The enigma of rare Quaternary oolites in the Indian and Pacific Oceans: A result of global oceanographic physicochemical conditions or a sampling bias? *Quat. Sci. Rev.*, **200**, 114–122.

Gillespie, J.L. and **Nelson, C.S.** (1997) Mixed Siliciclastic Skeletal Carbonate Facies on Wanganui Shelf, New Zealand: A Contribution to the Temperate Carbonate Model. In: *Cool-water Carbonates* (Ed. N.. James and J.. Clarke), *Special Publications of SEPM*, 127–140.

Ginsburg, R.N. (1956) Environmental Relationships of Grain Size and Constituent Particles in Some South Florida Carbonate Sediments. *Am. Assoc. Pet. Geol. Bull.*, **40**, 2384–2427.

Gischler, E. (2006) Sedimentation on Rasdhoo and Ari Atolls, Maldives, Indian ocean. *Facies*, **52**, 341–360.

Gischler, E. (2011) Sedimentary Facies of Bora Bora, Darwin's Type Barrier Reef

(Society Islands, South Pacific): The Unexpected Occurrence of Non-Skeletal Grains. *J. Sediment. Res.*, **81**, 1–17.

Gischler, E., **Dietrich, S.**, **Harris, D.**, **Webster, J.M.** and **Ginsburg, R.N.** (2013) A comparative study of modern carbonate mud in reefs and carbonate platforms: Mostly biogenic, some precipitated. *Sediment. Geol.*, **292**, 36–55.

Gischler, E. and **Lomando, A.J.** (1999) Recent sedimentary facies of isolated carbonate platforms, Belize-Yucatan system, Central America. *J. Sediment. Res.*, **69**, 747–763.

Gischler, E. and **Lomando, A.J.** (2005) Offshore sedimentary facies of a modern carbonate ramp, Kuwait, northwestern Arabian-Persian Gulf. *Facies*, **50**, 443–462.

Gischler, E., **Swart, P.K.** and **Lomando, A.J.** (2012) Stable Isotopes of Carbon and Oxygen in Modern Sediments of Carbonate Platforms, Barrier Reefs, Atolls and Ramps: Patterns and Implications. Perspect. Carbonate Geol. 41:61–74.

Gischler, E. and **Zingeler, D.** (2002) The origin of carbonate mud in isolated carbonate platforms of Belize, Central America. *Int. J. Earth Sci.*, **91**, 1054–1070.

González, L.A. and **Lohmann, K.C.** (1985) Carbon and oxygen isotopic composition of Holocene reefal carbonates. *Geology*, **13**, 811–814.

Grossman, E.L. and **Ku, T.-L.** (1986) Oxygen and carbon isotope fractionation in biogenic aragonite: Temperature effects. *Chem. Geol. Isot. Geosci. Sect.*, **59**, 59–74.

Grottoli, A.G. (2002) Effect of light and brine shrimp on skeletal δ13C in the Hawaiian coral Porites compressa: A tank experiment. *Geochim. Cosmochim. Acta*, **66**, 1955–1967.

Grottoli, A.G. and **Wellington, G.M.** (1999) Effect of light and zooplankton on skeletal δ 13 C values in the eastern Pacific corals Pavona clavus and Pavona gigantea. *Coral Reefs*, **18**, 29–41.

Hallenberger, M., **Reuning, L.**, **Gallagher, S.J.**, **Back, S.**, **Ishiwa, T.**, **Christensen, B.A.** and **Bogus, K.** (2019) Increased fluvial runoff terminated inorganic aragonite precipitation on the Northwest Shelf of Australia during the early Holocene. *Sci. Rep.*, **9**, 1–9.

Hammer, Ø., **Harper, D.A.T.** and **Ryan, P.D.** (2001) Past: Paleontological Statistics Software Package for Education and Data Analysis. *Palaeontol. Electron.*, **4**, 178.

Hamzah, F., **Agustiadi, T.**, **Susanto, R.D.**, **Wei, Z.**, **Guo, L.**, **Cao, Z.** and **Dai, M.** (2020) Dynamics of the Carbonate System in the Western Indonesian Seas During the Southeast Monsoon. *J. Geophys. Res. Ocean.*, **125**, 1–18.

Heikoop, J.M., **Risk, M.J.**, **Lazier, A.V.**, **Edinger, E.N.**, **Jompa, J.**, **Limmon, G.V.**, **Dunn, J.J.**, **Browne, D.R.** and **Schwarcz, H.P.** (2000) Nitrogen-15 Signals of Anthropogenic Nutrient Loading in Reef Corals. *Mar. Pollut. Bull.*, **40**, 628–636.

Husinec, A., **Loree, P.E.** and **Murphy, J.T.** (2019) Degrading windward patch reefs and processes influencing composition, mineralogy, and stable-isotope record of peri-reefal sediment, San Salvador Island, Bahamas. *Facies*, **65**, 39.

Ishiwa, T., **Yokoyama, Y.**, **Reuning, L.**, **McHugh, C.M.**, **De Vleeschouwer, D.** and **Gallagher, S.J.** (2019) Australian Summer Monsoon variability in the past 14,000 years revealed by IODP Expedition 356 sediments. *Prog. Earth Planet. Sci.*, **6**, 1–10.

James, N.P., **Bone, Y.** and **Kyser, T.K.** (2005) Where Has All the Aragonite Gone? Mineralogy of Holocene Neritic Cool-Water Carbonates, Southern Australia. *J. Sediment. Res.*, **75**, 454–463.

Jordan, C.F. (1998) The Sedimentology of Kepulauan Seribu: A Modern Patch Reef Complex in the West Java Sea, Indonesia. *Indones. Pet. Assoc.*, 1–81.

Keeling, C.D. (1979) The Suess effect: 13Carbon-14Carbon interrelations. *Environ. Int.*, **2**, 229–300.

Kendall, C.G.S.C. and **Skipwith, P.A.** (1969) Holocene Shallow-Water Carbonate and Evaporite Sediments of Khor al Bazam, Abu Dhabi, Southwest Persian Gulf. *Am. Assoc. Pet. Geol. Bull.*, **53**, 841–869.

Koropitan, A.F. and **Ikeda, M.** (2016) Influences of Physical Processes and Anthropogenic Influx on Biogeochemical Cycle in the Java Sea: Numerical Model Experiment. *Procedia Environ. Sci.*, **33**, 532–552.

Land, L.S. (1970) Carbonate mud; production by epibiont growth on Thalassia testudinum. *J. Sediment. Res.*, **40**, 1361–1363.

Lau, K.-M. and **Yang, S.** (2003) Walker Circulation. In: *Encyclopedia of Atmospheric Sciences* (Ed. J.R. Holton), *Academic Press*, 2505–2510.

Lebrato, M., **Garbe-Schönberg, D.**, **Müller, M.N.**, **Blanco-Ameijeiras, S.**, **Feely, R.A.**, **Lorenzoni, L.**, **Molinero, J.-C.**, **Bremer, K.**, **Jones, D.O.B.**, **Iglesias-Rodriguez, D.**, **Greeley, D.**, **Lamare, M.D.**, **Paulmier, A.**, **Graco, M.**, **Cartes, J.**, **Barcelos e Ramos, J.**, **de Lara, A.**, **Sanchez-Leal, R.**, **Jimenez, P.**, **Paparazzo, F.E.**, **Hartman, S.E.**, **Westernströer, U.**, **Küter, M.**, **Benavides, R.**, **da Silva, A.F.**, **Bell, S.**, **Payne, C.**, **Olafsdottir, S.**, **Robinson, K.**, **Jantunen, L.M.**, **Korablev, A.**, **Webster, R.J.**, **Jones, E.M.**, **Gilg, O.**, **Bailly du Bois, P.**, **Beldowski, J.**, **Ashjian, C.**, **Yahia, N.D.**, **Twining, B.**, **Chen, X.-G.**, **Tseng, L.-C.**, **Hwang, J.-S.**, **Dahms, H.-U.** and **Oschlies, A.** (2020) Global variability in seawater Mg:Ca and Sr:Ca ratios in the modern ocean. *Proc. Natl. Acad. Sci.*, **117**, 22281–22292.

Linsley, B.K., **Dunbar, R.B.**, **Dassié, E.P.**, **Tangri, N.**, **Wu, H.C.**, **Brenner, L.D.** and **Wellington, G.M.** (2019) Coral carbon isotope sensitivity to growth rate and water depth with paleo-sea level implications. *Nat. Commun.*, **10**, 2056.

Lumsden, D.N. (1979) Discrepancy Between Thin-Section and X-Ray Estimates of Dolomite in Limestone. *SEPM J. Sediment. Res.*, **Vol. 49**, 429–435.

Madden, R.H.C. and **Wilson, M.E.J.** (2012) Diagenesis of Neogene Delta-Front Patch Reefs: Alteration of Coastal, Siliciclastic-Influenced Carbonates from Humid Equatorial Regions. *J. Sediment. Res.*, **82**, 871–888.

Madduppa, H.H. (2013) Dynamics of fish diversity across an environmental gradient in the Seribu Islands reefs off Jakarta. *Biodiversitas, J. Biol. Divers.*, **14**, 17–24.

Maeda, A., **Fujita, K.**, **Horikawa, K.**, **Suzuki, A.**, **Yoshimura, T.**, **Tamenori, Y.** and **Kawahata, H.** (2017) Evaluation of oxygen isotope and Mg/Ca ratios in high-magnesium calcite from benthic foraminifera as a proxy for water temperature. *J. Geophys. Res. Biogeosciences*, **122**, 185–199.

McConnaughey, T. (1989) 13C and 18O isotopic disequilibrium in biological carbonates: I. Patterns. *Geochim. Cosmochim. Acta*, **53**, 151–162.

McConnaughey, T.A. (2003) Sub-equilibrium oxygen-18 and carbon-13 levels in biological carbonates: carbonate and kinetic models. *Coral Reefs*, **22**, 316–327.

McConnaughey, T.A. and **Gillikin, D.P.** (2008) Carbon isotopes in mollusk shell carbonates. *Geo-Marine Lett.*, **28**, 287–299.

Milliman, J.D., **Farnsworth, K.L.** and **Albertin, C.S.** (1999) Flux and fate of fluvial sediments leaving large islands in the East Indies. *J. Sea Res.*, **41**, 97–107.

Milliman, J.D., **Müller, G.** and **Förstner, U.** (1974) Recent Sedimentary Carbonates. *Springer Berlin Heidelberg*, Berlin, Heidelberg, 376 pp.

Miyajima, T., **Tsuboi, Y.**, **Tanaka, Y.** and **Koike, I.** (2009) Export of inorganic carbon from two Southeast Asian mangrove forests to adjacent estuaries as estimated by the stable isotope composition of dissolved inorganic carbon. *J. Geophys. Res.*, **114**, G01024.

Morse, J.W., **Wang, Q.** and **Tsio, M.Y.** (1997) Influences of temperature and Mg:Ca ratio on CaCO3 precipitates from seawater. *Geology*, **25**, 85–87.

Moyer, R.P. and **Grottoli, A.G.** (2011) Coral skeletal carbon isotopes (δ13C and Δ14C) record the delivery of terrestrial carbon to the coastal waters of Puerto Rico. *Coral Reefs*, **30**, 791–802.

O'Connell, L.G. and **James, N.P.** (2015) Composition and Genesis of Temperate, Shallow-Marine Carbonate Muds: Spencer Gulf, South Australia. *J. Sediment. Res.*, **85**, 1275–1291.

Park, R.K., **Crevello, P.D.** and **Hantoro, W.** (2010) Equatorial Carbonate Depositional Systems of Indonesia. In: *Cenozoic carbonate systems of Australasia* (Ed. W.A. Morgan, A.D. George, P.M. Harris, J.A. Kupecz, and J.F. Sarg), *SEPM Special Publication 95*, Tulsa, Oklahoma, 41–77.

Park, R.K., **Siemers, C.T.** and **Brown, A.A.** (1992) Holocene carbonate sedimentation, Pulau Seribu, Java Sea—the third dimension. In: *Carbonate Rocks and Reservoirs of Indonesia, A Core Workshop. Indonesian Petroleum Association, Jakarta*, 2–1 – 2–15.

Perry, C.T., **Salter, M.A.**, **Morgan, K.M.** and **Harborne, A.R.** (2019) Census Estimates of Algal and Epiphytic Carbonate Production Highlight Tropical Seagrass Meadows as Sediment Production Hotspots. *Front. Mar. Sci.*, **6**, 120.

Pfeiffer, M. and **Dullo, W.C.** (2006) Monsoon-induced cooling of the western equatorial Indian Ocean as recorded in coral oxygen isotope records from the Seychelles covering the period of 1840–1994AD. *Quat. Sci. Rev.*, **25**, 993–1009.

Pfeiffer, M., **Dullo, W.C.** and **Eisenhauer, A.** (2004) Variability of the Intertropical Convergence Zone recorded in coral isotopic records from the central indian

Ocean (Chagos Archipelago). *Quat. Res.*, **61**, 245–255.

Poerbandono (2016) Wind characteristics and the associated risk of erosion in Seribu Islands patch reef complexes, Java Sea, Indonesia. In: *The 5th International Symposium on Earthhazard and Disaster Mitigation. AIP Conf. Proc.*, 1730, 080001.

Purdy, E.G. (1963) Recent Calcium Carbonate Facies of the Great Bahama Bank. 1. Petrography and Reaction Groups. *J. Geol.*, **71**, 334–355.

Purdy, E.G. and **Gischler, E.** (2003) The Belize margin revisited: 1. Holocene marine facies. *Int. J. Earth Sci.*, **92**, 532–551.

Pusey, W.C. (1975) Holocene Carbonate Sedimentation on Northern Belize Shelf: Part 1. In: *Belize Shelf - Carbonate Sediments, Clastic Sediments, and Ecology*, *AAPG Special Volumes*, 146, 131–165.

Reid, R.P. and **Macintyre, I.G.** (2000) Microboring Versus Recrystallization: Further Insight into the Micritization Process. *SEPM J. Sediment. Res.*, **Vol. 70 (2**, 24–28.

Reijmer, J.J.G., **Swart, P.K.**, **Bauch, T.**, **Otto, R.**, **Reuning, L.**, **Roth, S.** and **Zechel, S.** (2009) A re-evaluation of facies on Great Bahama Bank I : new facies maps of western Great Bahama Bank. *Int. Assoc. Spec. Publ.*, **41**, 29–46.

Renema, W. (2008) Habitat selective factors influencing the distribution of larger benthic foraminiferal assemblages over the Kepulauan Seribu. *Mar. Micropaleontol.*, **68**, 286–298.

Romanek, C.S., **Grossman, E.L.** and **Morse, J.W.** (1992) Carbon isotopic fractionation in synthetic aragonite and calcite: Effects of temperature and precipitation rate. *Geochim. Cosmochim. Acta*, **56**, 419–430.

Rozanski, K., **Araguás-Araguás, L.** and **Gonfiantini, R.** (1993) Isotopic Patterns in Modern Global Precipitation. In: *Geophysical Monograph Series* (Ed. P.K. Swart, K.C. Lohmann, J. Mckenzie, and S. Savin), *AGU Books Board*, 78, 1–36.

Rubinson, M. and **Clayton, R.N.** (1969) Carbon-13 fractionation between aragonite and calcite. *Geochim. Cosmochim. Acta*, **33**, 997–1002.

Salter, M.A., **Harborne, A.R.**, **Perry, C.T.** and **Wilson, R.W.** (2017) Phase heterogeneity in carbonate production by marine fish influences their roles in sediment generation and the inorganic carbon cycle. *Sci. Rep.*, **7**, 1–15.

Salter, M.A., **Perry, C.T.**, **Stuart-Smith, R.D.**, **Edgar, G.J.**, **Wilson, R.W.** and **Harborne, A.R.** (2018) Reef fish carbonate production assessments highlight regional variation in sedimentary significance. *Geology*, **46**, 699–702.

Salter, M.A., **Perry, C.T.** and **Wilson, R.W.** (2012) Production of mud-grade carbonates by marine fish: Crystalline products and their sedimentary significance. *Sedimentology*, **59**, 2172–2198.

Saraswati, P.K., **Seto, K.** and **Nomura, R.** (2004) Oxygen and carbon isotopic variation in co-existing larger foraminifera from a reef flat at Akajima, Okinawa, Japan. *Mar. Micropaleontol.*, **50**, 339–349.

Sayani, H.R., **Cobb, K.M.**, **DeLong, K.**, **Hitt, N.T.** and **Druffel, E.R.M.** (2019) Intercolony δ18O and Sr/Ca variability among Porites spp. corals at Palmyra Atoll: Toward more robust coral-based estimates of climate. *Geochemistry, Geophys. Geosystems*, **20**, 5270–5284.

Schlager, W. (1992) Sedimentology and sequence stratigraphy of reefs and carbonate platforms. *The American Association of Petroleum Geologists; Continuing Education Course Note Series, 34*, Tulsa, Oklahoma, 77 pp.

Schmitt, D. and **Gischler, E.** (2017) Recent sedimentary facies of Roatan (Bay Islands, Honduras), a Caribbean oceanic barrier reef system. *Facies*, **63**, 5.

Schroeder, J.H. (1972) Fabrics and sequences of submarine carbonate cements in Holocene Bermuda cup reefs. *Geol. Rundschau*, **61**, 708–730.

Scrutton, M. (1976a) Aspects Carbonate Sedimentation in Indonesia. In: *Indonesian Petroleum Association, Proceeding 5th Annual Convention*, 179–193.

Scrutton, M. (1976b) Modern Reefs in the West Java Sea. In: *Indonesian Petroleum Association, Proceeding 5th Annual Convention*, 14–36.

Smith, S. V. and **Kroopnick, P.** (1981) Carbon-13 isotopic fractionation as a measure of aquatic metabolism. *Nature*, **294**, 252–253.

Sofian, I. and **Kozai, K.** (2007) Literature review of the climatology of the Java Sea. *Kobe Univ. Repos. Kernel*, 133–138.

Swart, P.K. (1983) Carbon and oxygen isotope fractionation in scleractinian corals: a review. *Earth-Science Rev.*, **19**, 51–80.

Swart, P.K., **Greer, L.**, **Rosenheim, B.E.**, **Moses, C.S.**, **Waite, A.J.**, **Winter, A.**, **Dodge, R.E.** and **Helmle, K.** (2010) The 13C Suess effect in scleractinian corals mirror changes in the anthropogenic CO2 inventory of the surface oceans. Geophys Res Lett. doi: 10.1029/2009GL041397

Swart, P.K. and **Kramer, P.A.** (1997) Geology of Mud Islands in Florida Bay. In: *Geology and Hydrogeology of Carbonate Islands. Developments in Sedimentology 54* (Ed. H.. Vacher and T. Quinn), *Elsevier B.V.*, 249–274.

Swart, P.K. and **Price, R.** (2002) Origin of salinity variations in Florida Bay. *Limnol. Oceanogr.*, **47**, 1234–1241.

Swart, P.K., **Reijmer, J.J.G.** and **Otto, R.** (2009) A Re-Evaluation of Facies on Great Bahama Bank II: Variations in the δ13C, δ18O and Mineralogy of Surface Sediments. In: *Perspectives in Carbonate Geology*, *John Wiley & Sons, Ltd*, Chichester, West Sussex, UK, 47–59.

Swart, P.K., **Sternberg, L.D.S.L.**, **Steinen, R.** and **Harrison, S.A.** (1989) Controls on the oxygen and hydrogen isotopic composition of the waters of Florida Bay, U.S.A. *Chem. Geol. Isot. Geosci. Sect.*, **79**, 113–123.

Tarutani, T., **Clayton, R.N.** and **Mayeda, T.K.** (1969) The effect of polymorphism and magnesium substitution on oxygen isotope fractionation between calcium carbonate and water. *Geochim. Cosmochim. Acta*, **33**, 987–996.

Tomascik, T., **Mah, A.J.**, **Nontji, A.** and **Moosa, M.K.** (1997) The Ecology of the

Indonesia Seas Volume VIII Part II. *Oxford University*, 1231–1239 pp.

Trumbull, W.J. (1988) Depositional History of a Windward Open Marginal Lagoon: Northern Great Bahama Bank. University of North Carolina

Urey, H. (1947) The thermodynamic properties of isotopic substances. *J. Chem. Soc.*, **99**, 562–581.

Utami, D.A., **Reuning, L.** and **Cahyarini, S.Y.** (2018) Satellite- and field-based facies mapping of isolated carbonate platforms from the Kepulauan Seribu Complex, Indonesia. *Depos. Rec.*, **4**, 255–273.

van der Meij, S.E.T., **Moolenbeek, R.G.** and **Hoeksema, B.W.** (2009) Decline of the Jakarta Bay molluscan fauna linked to human impact. *Mar. Pollut. Bull.*, **59**, 101–107.

Völpel, R., **Paul, A.**, **Krandick, A.**, **Mulitza, S.** and **Schulz, M.** (2017) Stable water isotopes in the MITgcm. *Geosci. Model Dev.*, **10**, 3125–3144.

Weber, J.N. and **Schmalz, R.F.** (1968) Factors Affecting the Carbon and Oxygen Isotopic Composition of Marine Carbonate Sediments, Part III, Eniwetok Atoll. *SEPM J. Sediment. Res.*, **38**, 1270–1279.

Weber, J.N. and **Woodhead, P.M.J.** (1972) Carbonate Lagoon and Beach Sediments of Tarawa Atoll, Gilbert Islands. *Atoll Res. Bull.*, **157**, 1–21.

Wefer, G. and **Berger, W.H.** (1991) Isotope paleontology: growth and composition of extant calcareous species. *Mar. Geol.*, **100**, 207–248.

Wefer, G., **Killingley, J.S.** and **Lutze, G.F.** (1981) Stable isotopes in recent larger foraminifera. *Palaeogeogr. Palaeoclimatol. Palaeoecol.*, **33**, 253–270.

Wilson, M.E.J. (2002) Cenozoic carbonates in Southeast Asia: Implications for equatorial carbonate development. *Sediment. Geol.*, **147**, 295–428.

Wilson, M.E.J. (2008) Global and regional influences on equatorial shallow-marine carbonates during the Cenozoic. *Palaeogeogr. Palaeoclimatol. Palaeoecol.*, **265**, 262–274.

Wilson, M.E.J. (2012) Equatorial carbonates: an earth systems approach. *Sedimentology*, **59**, 1–31.

Wilson, M.E.J. and **Vecsei, A.** (2005) The apparent paradox of abundant foramol facies in low latitudes: Their environmental significance and effect on platform development. *Earth-Science Rev.*, **69**, 133–168.

Chapter 4

Microplastic as a Sedimentary Component

4 Microplastics as a sedimentary component in reefs systems

Dwi Amanda Utami[1,2,3], Lars Reuning[2,1], Olga Konechnaya[4], Jan Schwarzbauer[4]
[1]Geological Institute, Energy and Mineral Resources Group, RWTH Aachen University, Germany
[2]Institute of Geosciences, Kiel University, Germany
[3]Geotechnology Research Center, Indonesian Institute of Sciences, Indonesia
[4]Institute of Geology and Geochemistry of Petroleum and Coal, RWTH Aachen University, Germany

Submitted to Sedimentology

Abstract

Only recently, microplastic pollution have been reported from coral reef systems all over the tropics. Exposure to microplastics have several negative impacts on coral health, such as bleaching, tissue necrosis or an impairment of the corals immune system. Despite this potential risk for reef systems, the controlling processes for microplastics dispersion and accumulation in reefs sediments are still largely understudied. Presented here is a study of microplastics distribution in two tropic atoll reef platforms in Kepulauan Seribu, Indonesia. Sediment samples were collected with a tube to a depth of 7 cm in the reef crest, sand apron, lagoon, and intertidal beach. Microplastics were concentrated using density floatation and characterized by light and scanning electron microscopy. Some particles were identified as polypropylene using micro Fourier transform infrared (µFT-IR) spectroscopy. All recovered microplastics were classified as secondary microplastics, likely derived from marine and local sources, with fibers as the most abundant type. Microplastics are showing similar transport and accumulation behaviour as fine siliciclastic grains. Abundance of microplastic is controlled by the proximity to the source area of larger plastic debris and hydrodynamic processes. Microplastics are not only present in low energy environment but also in high energy settings such as e.g. the reef crest. Processes that contribute to accumulation in reef sediments are biofouling, interlocking, and the creation of compound grains. Microplastics are present in sediment close to the seafloor (0-3.5 cm) but also in a depth between 3.5 and 7 cm. Microplastic particles below 3.5 cm are unlikely to be remobilized under modal weather conditions in the studied equatorial reefs. Subtidal reef sediment therefore can be regarded as a permanent sink for microplastics. The study shows that microplastics in coral reef environments deserve careful consideration, since microplastics poses an additional threat to corals and their ability as framework builders in reef systems.

Keywords: Coral reef, microfiber, sand apron, pollution, Indonesia, Anthropocene

4.1 Introduction

The worldwide accumulation of plastic litter in the marine environment has raised international awareness. Since the mass production of plastics in the 1950s, 6.3 billion tons of plastic is predicted to be waste (Geyer *et al.*, 2017) and a large number had entered the environment. Once introduced to the environment, plastic litter finally accumulates in the oceans (van Sebille *et al.*, 2015). In 2010, between 4.8 – 12.7 million tons of plastic waste entered the ocean and by 2025 this number is predicted to rise by one order of magnitude (Jambeck *et al.*, 2015). Ubiquitous litter in the marine environment consists of microplastics (Van Cauwenberghe *et al.*, 2015); plastic particles and fibers smaller than 5 mm (Arthur *et al.,* 2009 and many other) that were either directly manufactured or formed through breakdown of larger plastic waste (Andrady, 2011).

The marine ecosystem and its ecological function are reported to be threatened by microplastics (de Carvalho-Souza *et al.*, 2018). Coral reef ecosystems receive increased attention since the discovery that corals might capture and ingest microplastics due to their similarity in size to plankton (Hall *et al.*, 2015; Reichert *et al.*, 2018). Laboratory experiments have documented that ingestion of microplastics by corals can inhibit food intake (Hall *et al.*, 2015) and reduce their growth rate (Chapron *et al.*, 2018). Long term exposure and adhesion to microplastics may have negative effects on corals such as bleaching and necrosis (Reichert *et al.*, 2018). Furthermore, microplastics may promote the transmission of pathogens, which further increases the susceptibility of reef building corals to diseases (Zettler *et al.*, 2013; Lamb *et al.*, 2018). On the long run microplastics therefore pose a threat to reef corals and their ability to act as framework builders in coral reef systems.

Only recently, microplastic pollution have been reported from coral reef systems all over the tropics: The South China Sea (Ding *et al.*, 2019; Zhang *et al.*, 2019; Tan *et al.*, 2020), the Great Barrier Reef (Hall *et al.*, 2015), Maldives atolls (Imhof *et al.*, 2017; Saliu *et al.*, 2018, 2019), and the coast of India (Vidyasakar *et al.*, 2018). From popular tourist destinations to remote islands, reefs are affected by microplastic pollution (Imhof *et al.*, 2017; Tan *et al.*, 2020). Indonesia is part of the Indo-Pacific coral triangle, which represents one of the most diverse marine ecosystems. At the same time Indonesia is ranked as the second largest contributor of mismanaged plastic waste to the ocean (Jambeck *et al.*, 2015). In Indonesia, microplastics have been found in fish gut (Rochman *et al.*, 2015), coastal waters (Syakti *et al.*, 2017, 2018), river sediment (Alam *et al.*, 2019), estuaries (Firdaus *et al.*, 2020), deep sea sediment (Cordova & Wahyudi, 2016), and coral reef sediments (Cordova *et al.*, 2018). The Kepulauan Seribu patch reef system in Jakarta Bay is also at risk of microplastic pollution. Urban pressures and pollutants from rivers entering Jakarta Bay have been reported to cause environmental degradation of ecological conditions in Kepulauan Seribu (Farhan & Lim, 2012). Approximately 8 tons of plastic litter dominated by Styrofoam from the Greater Jakarta Area are entering Jakarta Bay on a daily basis (Cordova & Nurhati, 2019). Beach litter in Kepulauan Seribu is also generated from local island tourism or residents and passing ships. Altogether this has caused the spread of severe pollution even to more distant parts of the archipelago (Willoughby *et al.*, 1997).

Despite the global presence of microplastics, its distribution on the seafloor is poorly understood (Martin *et al.*, 2017; Kane & Clare, 2019). Half of all plastics have a density greater than seawater (Morét-Ferguson *et al.*, 2010) and therefore eventually sinks to the seafloor, which is considered to be a major sink for global plastic (Van Cauwenberghe *et al.*, 2013; Woodall *et al.*, 2014; Kowalski *et al.*, 2016). Integration of process based sedimentological knowledge with insights from modern sedimentary systems can provide crucial constraints on the transfer and distribution of microplastics to marine environments (Kane & Clare, 2019). However, the sedimentological processes that govern microplastics transport and distribution are still underexplored (Horton & Dixon, 2018; Kane & Clare, 2019). None of the aforementioned studies of microplastics distribution in reefal environments were taking the role of sedimentary processes or facies into account. This study wants to close this knowledge gap through the analyses of the distribution of microplastics in different environmental and sedimentary facies of a patch reef from Kepulauan Seribu. The sedimentary and environmental facies of this reef platform was previously investigated using a combination of grain size, mineralogical and compositional analysis in combination with ground-truthed satellite image analysis (Utami *et al.,* 2018; Utami *et al.,* accepted). New samples from the same reef system were taken to integrate microplastics analysis with sedimentological information.

4.2 Study area and environmental setting

Situated in the Java Sea, Kepulauan Seribu (Thousand islands) consists of more than 300 coral reef platforms. About a quarter of them possess islands ranging in size from a few meters across to a length greater than 7 km. From about 10 km off the northwest Java coastline, the island chain extends for about 40 km into the Java Sea. The patch reefs system of Kepulauan Seribu is located on the shallow Sunda Shelf where is rises from a water depth of 30 - 50 meters to the sea surface. A deep and several kilometers wide, east - west oriented channel separates Pari Island to the south from most other islands to its north (Fig. 4-1). It appears that this channel forms an important hydrologic barrier, channeling the sediment-laden coastal waters off Java and Kalimantan away from the reef (Tomascik *et al.*, 1997; Jordan, 1998).

Kepulauan Seribu is considered to be located in a relatively sheltered location protected from severe storms and ocean swell due to the fact that it is surrounded by major landmasses such as Sumatra, Java and Kalimantan (Fig. 4-1). The controlling influence on modern reef growth and morphology in Kepulauan Seribu is believed to be the seasonal change in wind and current directions which are controlled by the monsoonal climate (Scrutton, 1976). The Java Sea is characterized by monsoonal wind with a seasonal reversal between the Northwest (NW) Monsoon (December – February) and Southeast (SE) Monsoon (April – October). The seasonal SE Monsoon phase lasts longer but is characterized by lower maximum wind speeds compared to the NW Monsoon. On interannual timescale of more than 5-7 years this relationship reverses with higher wind magnitudes during the SE Monsoon (Poerbandono, 2016). The longer lasting winds of the SE Monsoon (eight months) are thought to be more important for beach erosion, despite the somewhat lower wind magnitudes on seasonal timescales (Poerbandono, 2016). The tidal range in Kepulauan Seribu is micro tidal, averaging about 52 cm with a range from 15 to 82 cm and a typical diurnal tidal cycle with one high and one low stand per day (Wyrtki, 1962).

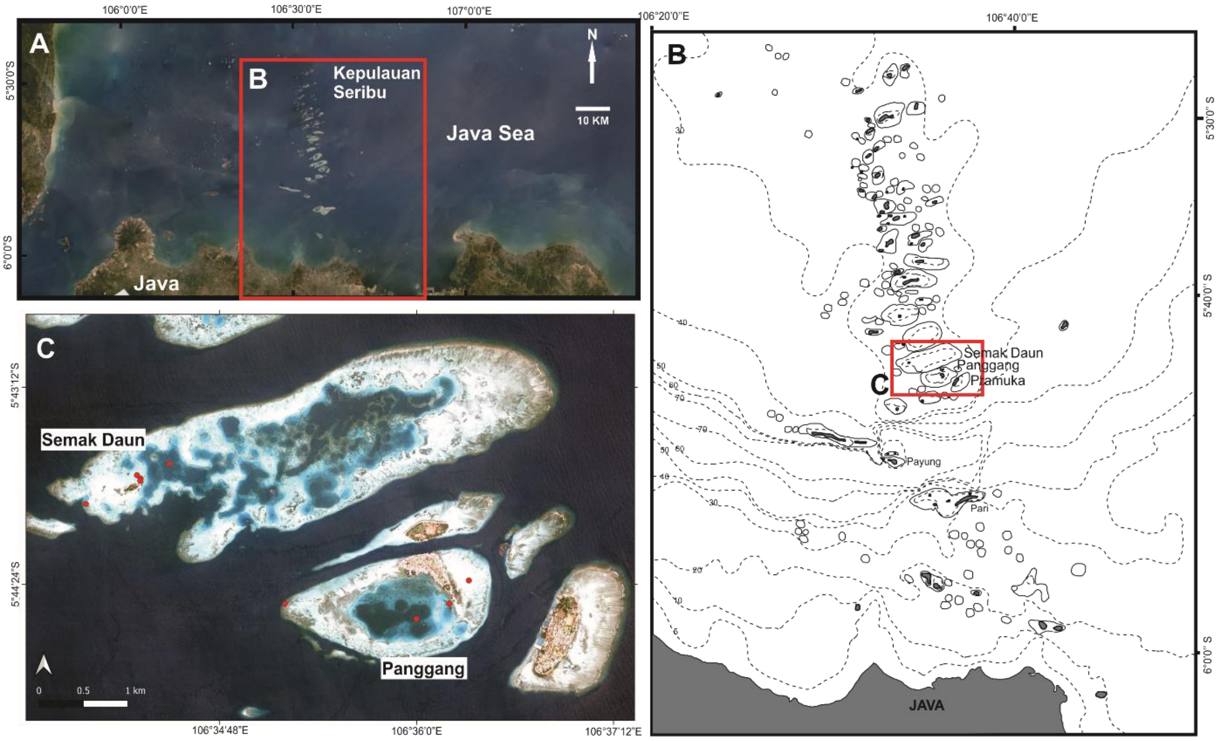

Figure 4-1. (A). Satellite image from the Java Sea showing turbid coastal waters caused by sediment-laden river runoff from northern Java and southeastern Sumatra (image credit: Allen Coral Atlas. The Satellite Coral Reef Mosaic is © *2019 Planet Labs and licensed CC BY_SA_NC 4.0*). (B). Bathymetry in the vicinity of the Seribu Platform (basemap from National Bathymetry, Indonesia Geospatial Information Agency. Available on http://tides.big.go.id/DEMNAS/. (C). Location of Semak Daun and Panggang as indicate in the red box. Sampling locations are in the red dots. Satellite image from Google Earth.

Focus of this study are the patch reef systems of Panggang and Semak Daun which are situated in the middle part of the Kepulauan Seribu chain (Fig. 4-1C). Panggang Island has the highest population density in Kepulauan Seribu, with almost 10.000 people per m^2. It is situated on the northeastern part of the sand apron, sheltering parts of the reef system from direct wave exposure from the Java Sea. (Fig. 4-1). Most of the inhabitants of Panggang Island work as fisherman and also practice aquaculture within the lagoon.

The Panggang reef platform has an atoll morphology with an approximate area of 3.2 km^2 and a central lagoon surrounded by reef and sand apron facies. From the reef flat, the water depth increases from about 1 m to about 20 m in the deepest part of the lagoon. Parts of the reef crest will be exposed during low tide, showing a coral assemblage dominated by platy Acropora and foliated corals. The sand apron on the eastern and western side of the lagoon is roughly two times wider compared to the sand apron on the northern and southern side. Only one small inlet traverses the sand aprons allowing only very limited connection between the lagoon and the open sea.

Semak Daun Island is a small, uninhabited island (Fig. 4-1) popular for local, unorganized tourism on a camping ground. The reef platform Semak Daun is characterized by an extensive reef flat surrounding a partially filled shallow lagoon with active coral growth in its center. Similar to Panggang, the reef flat in Semak Daun is expanded broadly on the eastern and western side, leaving a narrow reef flat on the northern and southern side. Water exchange between the lagoon and the Java Sea is restricted to few inlets on its western side, while the eastern side of Semak Daun is directly exposed to the Java Sea. Semak Down is separated from Panggang towards the south by a shallow inter reef channel (Fig. 4-1).

Surface sediments in the study area can be subdivided in four sedimentary facies: coral grainstone, coral packstone/grainstone, coral-mollusc packstone and mollusc wackestone (Utami *et al.*, 2018). The occurrence of mollusc wackestone in the lagoon is controlled by water depth, while the sand apron and reef front do not show significant facies separation with water depth. Environmental facies distribution is mainly controlled by water depth, density of seagrass cover and coral abundance (Utami *et al.*, 2018) (Tab. 4-1). The satellite derived environmental facies correlated only in the lagoon directly with sedimentary facies. No direct correlation of environmental facies to sedimentary facies exists in the sand apron due to the heterogeneity and complexity of the environment (Utami *et al.*, 2018).

Aragonite is the dominant mineral phase, while low magnesium calcite and high magnesium calcite occur in fairly similar amounts in all sedimentary facies. Small amount of siliciclastic minerals (quartz and smectite) are preferentially deposited in deeper waters below the wave base (Utami *et al.,* accepted).

4.3 Method

Sample Collection

Sediments were collected in July 2018 from different subtidal and intertidal environmental from Panggang and Semak Daun reef platforms (Utami *et al.*, 2018): beach, sand apron with dense seagrass and without seagrass, subtidal reef margin and the deeper part of the lagoon (Tab. 4-1). For each site, three replicate samples were taken within a radius of ~ 5 m. All the sampling sites were documented photographically by using an underwater camera and geographically using a Garmin map62s GPS. In shallow water, sediments were collected by hand. Below a water depth of 10 m, sediments were retrieved using a grab sampler. Water depth was measured using a folding rule or markers on the hand line of the grab sampler. The samples for microplastics extraction were taken by 'coring' the seabed or the sediment recovered with the grab sampler with a tube (3.5 cm diameter) made of a modified syringe (Romed Holland, Wilnis, Netherlands) to acquire 70 ml sediment from a depth of 7 cm *(Ling et al.,* 2017 with modification). The tube was immediately wrapped with an aluminium foil and fastened with a rubber band to avoid contamination. On land, each sample was split into two subsamples of 35 ml each: The lower and the upper 3.5 cm of the sediment column were transferred to separate foil trays. The environmental facies for each sampling site are derived from the facies map in Utami *et al.* (2018) and was ground-truthed with field observations.

Grain size analysis and sedimentary facies

Each samples of 35 ml were dried using an oven (Memmert, Schwabach, Germany) set to 70°C for 7 h. Dried samples were sieved through 125 µm, 250 µm, 500 µm, 1 mm and 2 mm sieves (Retsch GmbH, Haan, Germany). All individual grain-size fractions were weighed. Mean grain size and sorting were calculated using the software Gradistat (Blott & Pye, 2001). Sorting of samples was quantified as graphic standard deviation using the equation of Folk and Ward (1957). Values below 2 indicate moderate sorting, while values <4 and >4 indicate poor and very poor sorting, respectively. Point counting analysis was done on a minimum of 100 grains from the bulk fraction and compared with results from Utami *et al.* (2018) to derive the sedimentary facies for each sample.

Distribution analysis

All statistical analyses were performs using PAST (version 3.15) (Hammer *et al.*, 2001). The Levene´s test was used to check if homogeneity of variances was met. The non-parametric Mann-Whitney *U* test was used for pairwise comparisons between depth and density of microplastic. The non-parametric Kruskal-Wallis test for independent samples was used to examine the medians of microplastic distribution in different environmental facies. The significance level for all analysis was set at 95%. All samples used for microplastics analysis have an equal volume of 35 ml, but each sample has slightly different weight due to differences in porosity and composition. Microplastic concentration for all samples were normalized to a constant weight of one kg dry weight. To allow a better comparison to literature data the concentration was additionally normalized to volume (one liter) and area (one m^2).

Table 4-1. Sediment texture, sedimentary facies, and water depth for each environmental facies in Panggang, Pramuka and Semak Daun platform reef (Utami *et al.*, 2018). Dunham texture: GST = grainstone, PST = packstone, WST = wackestone. Environmental facies: DSPL/PM = deeper subtidal part of lagoon/platform margin, SSPL/PM = shallower subtidal part of lagoon/platform margin, SRM/SC = subtidal reef margin/sparse coral, SAWDSG = sand apron with dense seagrass, SAWSSG = sand apron with sparse seagrass, SAWSG = sand apron without seagrass. Sedimentary facies: CG = Coral Grainstone, CP/G= Coral Packstone/Grainstone, C-M P = Coral Mollusc Packstone, MW = Mollusc Wackestone.

Environmental facies	**mean grainsize (µm)**	**sorting (µm)**	**water depth (m)**	**Dunham**			**Sedimentary facies**			
				GST	**PST**	**WST**	**CG**	**CP/G**	**C-M P**	**MW**
DSPL/PM	84	5.5	9.6		38%	63%				100%
SSPL/PM	175	7.5	6.6		60%	40%			40%	60%
SRM/SC	441	4.6	14.3	33%	67%		17%	33%	50%	
SAWDSG	514	3.8	0.7	57%	43%		22%	65%	13%	
SAWSSG	585	3.6	0.6	71%	29%		18%	71%	11%	
SAWSG	614	3.6	0.7	64%	36%		55%	45%		

Procedural Contamination Protocol

A strict protocol for each procedure was followed to prevent potential post sampling contamination. Standard non-plastic laboratory equipment was used as much as possible. Clean cotton white lab coats and nitrile gloves were worn all the time during sample handling. All laboratory procedures were done inside a laminar fume hood. The laminar fume hood was cleaned thoroughly using filtered distilled water and a non-shedding lab paper before and after every microplastics extraction. All surfaces and laboratory equipment were cleaned three times with tap water and filtered distilled water, then covered with clean aluminium foil. Only new, filtered NaCl-solution was used for the density separation procedure. Airborne fibers were monitored by placing a damped filter paper pad inside the laminar fume hood for a 72 h period before and during each extraction (Martin *et al.*, 2017). Additionally, procedural blanks were analyzed to monitor background contamination, using the density separation protocol with NaCl-solution but without sediments. Blanks were analyzed prior to the first extraction and after every third sample (Coppock *et al.*, 2017). Fibers observed during monitoring were identified as cotton using SEM and were excluded from the data analysis. The lower size range of plastic examined in this study was limited to 125 µm, since particles below this size are increasingly difficult to identify by ATR-µFT-IR. The investigated size spectrum is overlapping with the size of zooplankton, which is ingested by reef corals as food (Houlbrèque *et al.*, 2009; Hall *et al.*, 2015) and microplastics used in feeding experiments of corals (Reichert *et al.*, 2018).

Microplastics Extraction

Sediment Microplastic Isolation (SMI) was constructed as an extraction tools that allows rapid, simple and efficient microplastics separation from sediment (Coppock *et al.*, 2017). SMI was chosen due to its practicality in single step decanting and cleaning to avoid cross contamination as well as its functionality and feasibility when processing numerous replicates of small samples. Two SMI units were used for extraction to minimize wear of the SMI units. Ball valves of both SMIs were check regularly to rule out PVC contamination (Nel *et al.*, 2019). The procedure for microplastics extraction from sediment follows Coppock *et al.* (2017) with one exception: Filtered, saturated sodium chloride (NaCl) solution with a density of 1.2 g/cm^3, instead of $ZnCl_2$ solution, was used for density separation. NaCl-solution has the advantage of being non-acidic, non-toxic and cheap. Other commonly used solutions, such as $ZnCl_2$-solution, have low pH, leading to reaction with the carbonate sediment and hampering an effective microplastics extraction. To evaluated the recovery rate of microplastics for this study, microplastics in the size range from 125 µm to 1 mm were produced by cutting a polypropylene rope and sieving the resulting fragments. These fragments were distinctive in both color and shape to ensure that they are distinguishable from non-spiked plastic. Fifty of these fragments, covering the complete size range, were added to every third sample prior to microplastics extraction. The mean recovery rate for the spiked microplastics was 89%, somewhat lower compared to the >95% reported by Coppock *et al.* (2017) for the SMI unit using $ZnCl_2$ solution as a flotation media.

Microplastics Identification

Visual identification based on morphological and physical characteristic is most widely utilized for microplastics identification in combination with other methods. An optical analysis of the particles recovered on the filters after density separation was performed using a stereomicroscope (Wild M3Z, Heerbrugg, Switzerland). Microplastic particles > 125 µm were identified and counted following protocols developed by Lusher *et al.* (2017). Unnatural colors and/or shininess and unnatural forms/structures were used as indicators of potential microplastics (Fries *et al.*, 2013; Martin *et al.*, 2017). Particles with potentially cellular or organic structures and translucent fibers were rejected as microplastics (Martin *et al.*, 2017). Translucent fibers and fibers that were not characterized by three-dimensional bending and uniform thickness were also rejected (Nuelle *et al.*, 2014; Martin *et al.*, 2017). Subsequently all identified, potential microplastic particles were counted according to shape and color and photographed.

Several potential microplastic fragments were chosen for micro Fourier transform infrared (µFT-IR) spectroscopy analysis. Attenuated total reflectance (ATR) µFT-IR analysis was carried out with a Spotlight™ 400 Series imaging system by Perkin Elmer (Waltham, Massachusetts, United States). The imaging system is equipped with a mercury cadmium telluride detector, operating in the 4000 – 650 cm^{-1} wave number range, and was run in reflectance mode. Spectrum 10.4.2 software is used to analyzed spectroscopy images. A library of the most commonly used polymers was self-generated to serve for comparison and identification of the polymer type according to their IR spectra. The plastics were provided from daily goods, the IR spectra were measured using the same FT-IR tool and verified with the resin identification code symbols on their surface. In addition, all spectra were also compared with published libraries. The spectrum analysis followed the method of Woodall *et al.* (2014). Matches with a quality index ≥0.7 were accepted. Matches with a quality index <0.7 but ≥0.6 were individually inspected and interpreted based on the proximity of their absorption frequencies to those of chemical bonds in the known polymers. Matches with a quality index <0.6 were rejected. ATR-µFT-IR analysis was restricted to fragments, while fibers commonly were too small to be analyzed by this method.

Fibers and some fragments were therefore further identified using Scanning Electron Microscopy (SEM). SEM is known to produce high resolution images and has been used in several studies for the identification of microplastics (Corcoran *et al.*, 2009; Fries *et al.*, 2013; Van Cauwenberghe *et al.*, 2013; Vianello *et al.*, 2013; Lusher *et al.*, 2017). Microplastics identification based on surface morphology and elemental chemistry were carried out using SEM with an energy dispersive X-ray spectrometer (SEM EDX) mounted on a FEG-SEM Zeiss SUPRA 55-VP (Carl Zeiss, Oberkochen, Germany). All particles were gold coated prior to analysis to prevent sample charging (Corcoran *et al.,* 2009). To obtain best image resolution, SEM was operated at 3kV in secondary electron (SE) mode. To obtain information on average atomic numbers and chemical composition of the sample the SEM was operated at 12 kV in back-scattered electron (BSE) mode combined with EDX (Vianello *et al.*, 2013).

4.4 Results

Microplastics characterization

Four microplastic particles with appropriate size were analysed by µFT-IR analysis. Three microplastic particles were confirmed to be polypropylene (Fig. 4-2). For one additional microplastic particle the polymer type could not be identified unequivocally but the µFT-IR analysis revealed a clear dibutyl phthalate signal. A detailed interpretation and comparison with reference spectra clearly allowed a differentiation from chemically similar polymers, in particular polyethylene terephthalate PET. Phthalates are known as plasticizers and as ingredients of microplastics in proportions up to 60% of the total plastic product weight (Teuten *et al.*, 2009). Saliu *et al.* (2019) found appreciable levels of phthalates in the tissue of corals from an atoll reef in the Maldives Archipelago. Samples containing dibutyl phthalate were found on the intertidal beach of Panggang, and were assumed to be fragments of chipped boat paint. Microplastic particles and fibers, which were too small for µFT-IR analysis were analyzed using SEM EDX (n = 17, 13%) to characterize their surface morphology and elemental chemistry. The remaining microplastic particles and fibers were accepted solely through visual identification (visual matches on color and physical form) to µFT-IR and SEM EDX confirmed microplastics from the same subsample or corresponding replicate.

Secondary microplastics were identified in samples from all facies and occurs predominantly as fibers (98%), while fragments (2%) and film (1%) are subordinate (Fig. 4-3). Most microplastic fibers and particles are either blue (44%) or black (36%). Less common colors are red (15%), white (4%), and transparent (1%).

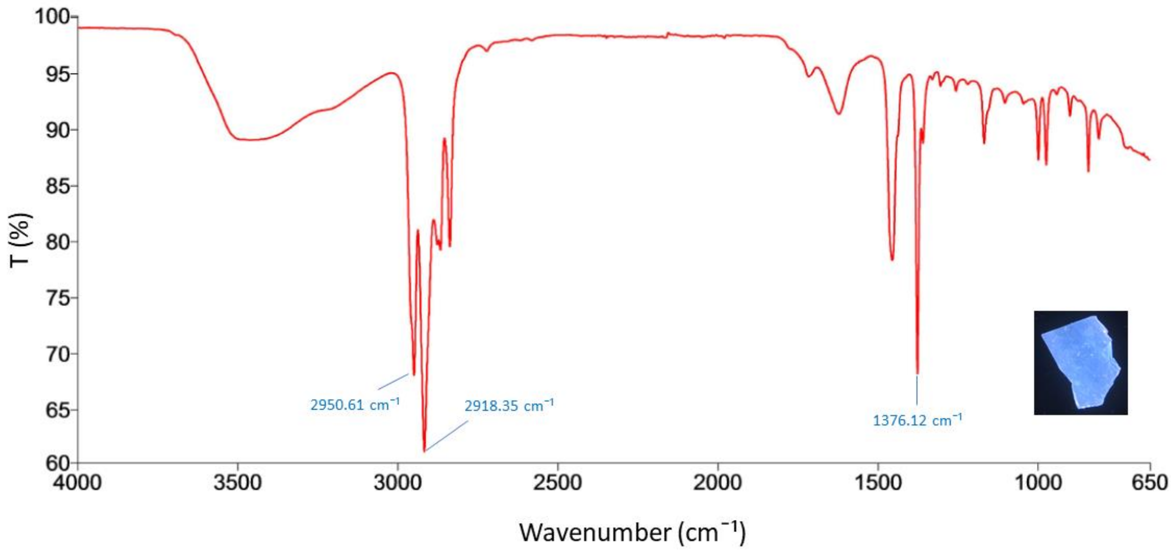

Figure 4-2. Detected microplastic particle from the beach of Panggang, identified as polypropylene based on its infrared spectrum.

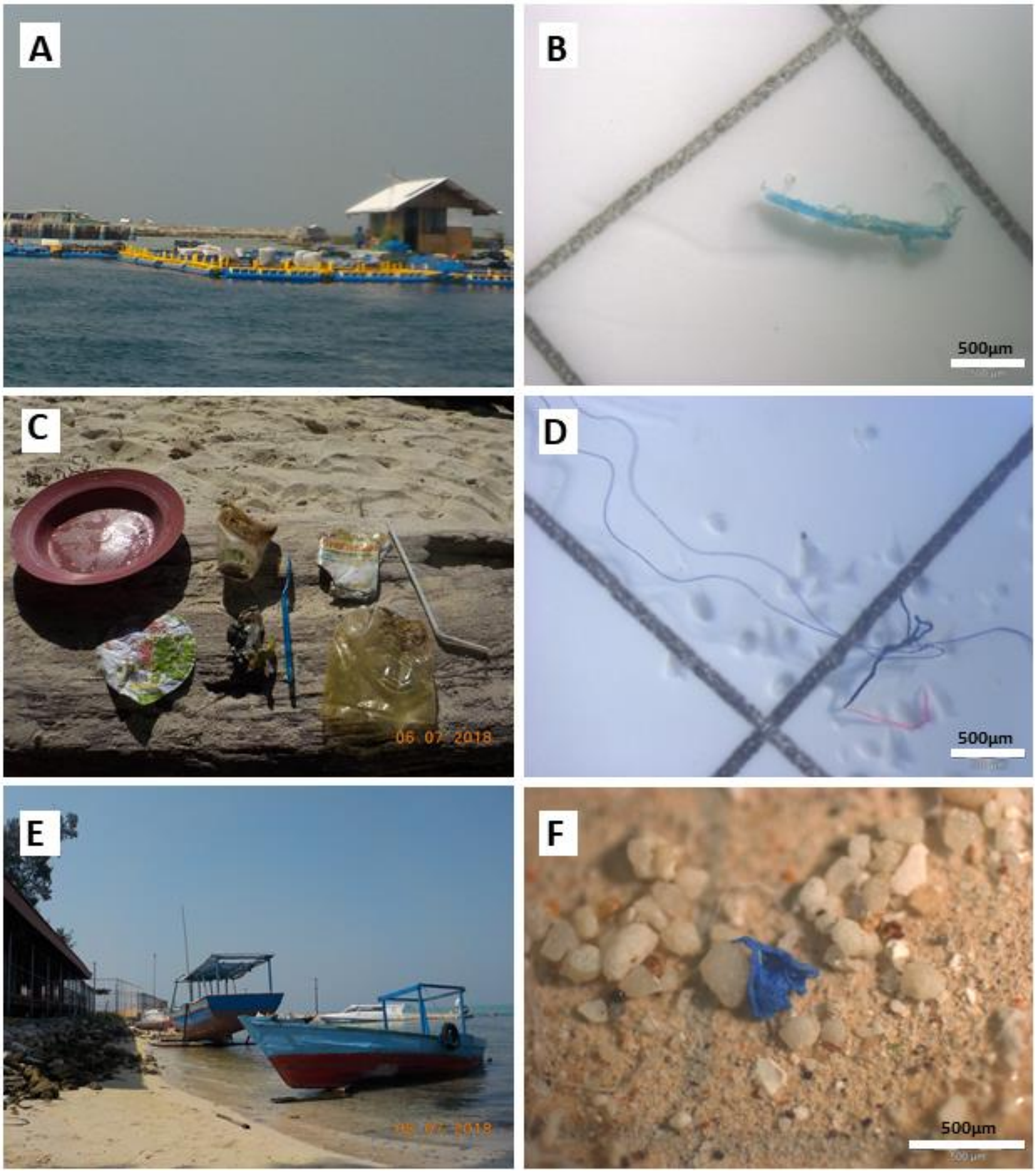

Figure 4-3. Local sources of contamination and microplastic particles found in the study area. (A). Fish farming in the lagoon of Panggang. (B). Microplastic fragment from the lagoon of Panggang (sample M07, 3.5-7 cm). (C) Plastic litter from unregimented camping found on the beach of Semak Daun. (D) Microplastic fibers with various lengths and color from the beach of Semak Daun (sample M19, 3.5-7 cm). (E) Boats on the beach of Panggang used for fishing and tourism. (F). Microplastic fragment from the beach of Panggang (sample M29, 3.5-7 cm).

Microplastics distribution

Most sediment samples in the study area are grain supported (83%) and can be categorized as grainstone (0-10% matrix) or packstone (10-50% matrix). Wackestone (50-90% matrix) is the only matrix-supported texture (17%). Sorting is generally poor (68%) or very poor (20%), but "moderately sorted" (7%) and "moderately well sorted" samples (3%) are also present. The grain size of the samples varies between 0.03 and 1.3 mm, with a mean grain size of 0.5 mm. The fine fraction (<125 µm) is most abundant in the lagoon, while coarser sediments are mostly found at the reef front of Panggang and Semak Daun (Fig. 4-4). The sediment composition is nearly identical to previous facies descriptions (Utami *et al.,* 2018, Utami *et al.,* accepted.) with corals and molluscs as the dominant skeletal components. Based on their grain size and composition all samples can be attributed to the sedimentary facies defined by Utami *et al.,* (2018). Samples from the two sites within the lagoons of Panggang and Semak Daun belong to the mollusc wackestone facies. The two sites from the reef crest yielded coral pack-/grainstone samples, while sediments from all other sites belonged to the coral grainstone facies (Fig. 4-4).

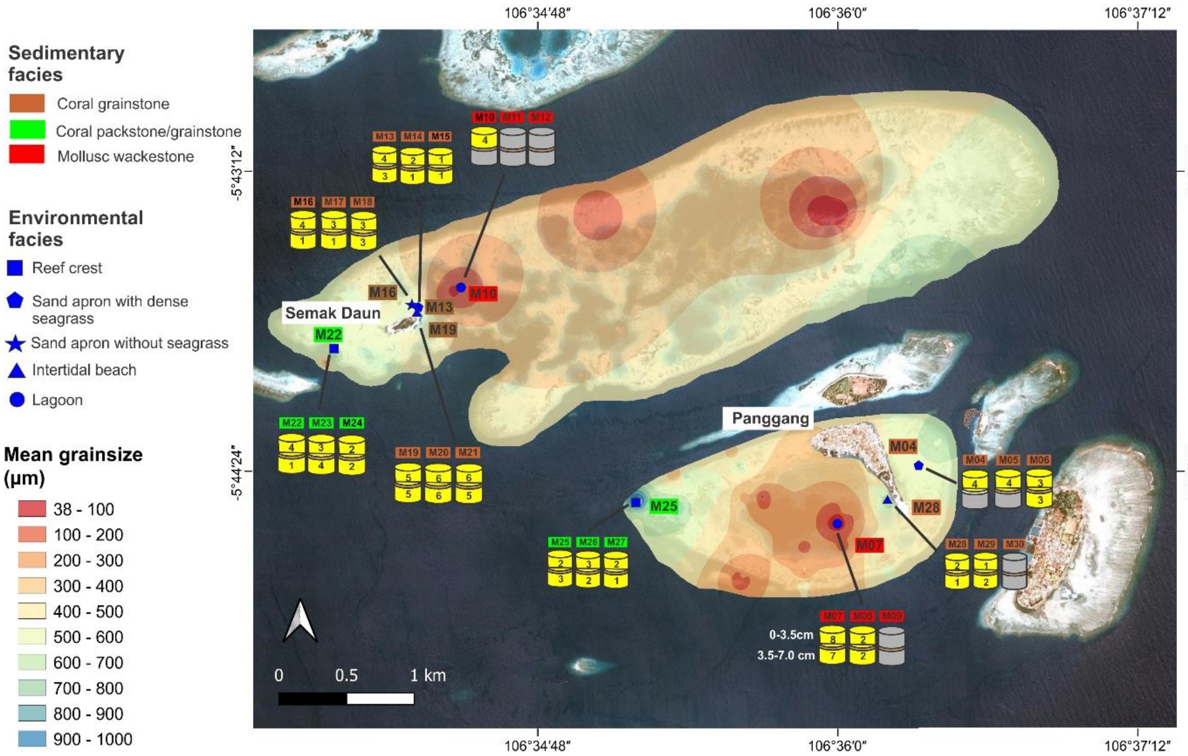

Figure 4-4. Locations of sample sites and microplastic abundance in bulk sediment samples (35ml) overlain with mean grainsize distribution (grainsize data acquired from this study and Utami *et al.,* 2018). Microplastic counts are shown within the boxes. Yellow boxes represent contaminated sediment subsample, grey boxes represent samples devoid of microplastics. Sample sites are chosen to represent environmental and sedimentary facies in the study area based on the results of Utami *et al.* (2018).

A total of 132 microplastic fragments and fibers were recovered from 43 subsamples (including replicates), while 11 subsamples were devoid of microplastic. Fibers are the majority of contaminants in the study area (98%) followed by chipped boat paints (1%) (Fig. 4-3). Microplastic abundance varied from 0 to 8 particles/subsample (Fig. 4-4). High microplastic concentrations were found on the beach of Semak Daun and in the lagoon of Panggang (Fig. 4-4). The concentration of microplastic shows a statistical significance difference with depth for subtidal facies in both reef platforms (Independent samples Mann-Whitney *U* test, $p < 0.05$) (Fig. 4-5). The beach environment is characterized by relatively constant concentrations with depth on both islands (Fig. 4-5). Overall, there is no significant difference in microplastic abundance between the uninhabited island of Semak Daun and the densely populated island of Panggang (Independent samples Mann-Whitney *U* test, $p = 0.258$). The mean concentration is higher at Semak Daun, while the highest absolute number is found in a sample from Panggang (Fig. 4-6). At Semak Daun, the microplastic concentration is significantly higher at the beach compared to all subtidal facies (Independent samples Kruskal Wallis test, $p < 0.05$) (Fig. 4-6). All subtidal facies at Panggang show higher concentrations compared to the beach, although the difference is not statistically significant (Independent samples Kruskal Wallis test, $p = 0.356$) (Fig. 4-6). Generally, high microplastic concentrations are restricted to samples with mean grain sizes < 100 µm and >50% fine fraction (<125 µm) content (Fig. 4-7).

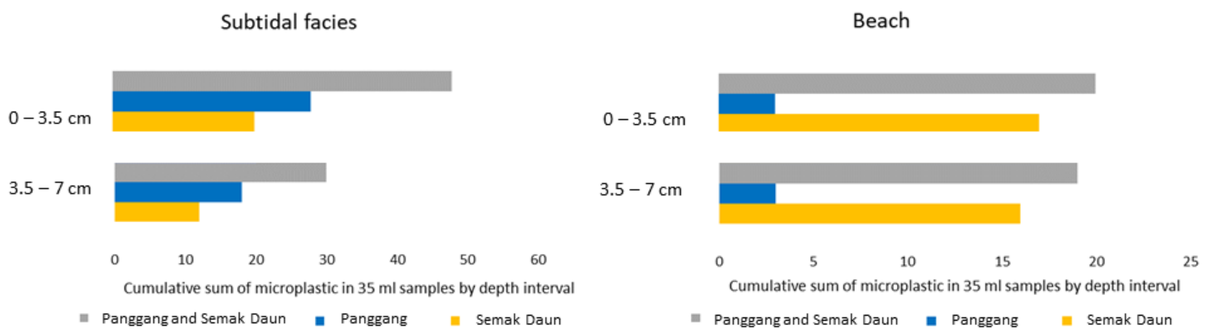

Figure 4-5. Depth profile of cumulative microplastic abundance in all beach (n = 12) and subtidal facies samples (n = 42) within the two reef platforms.

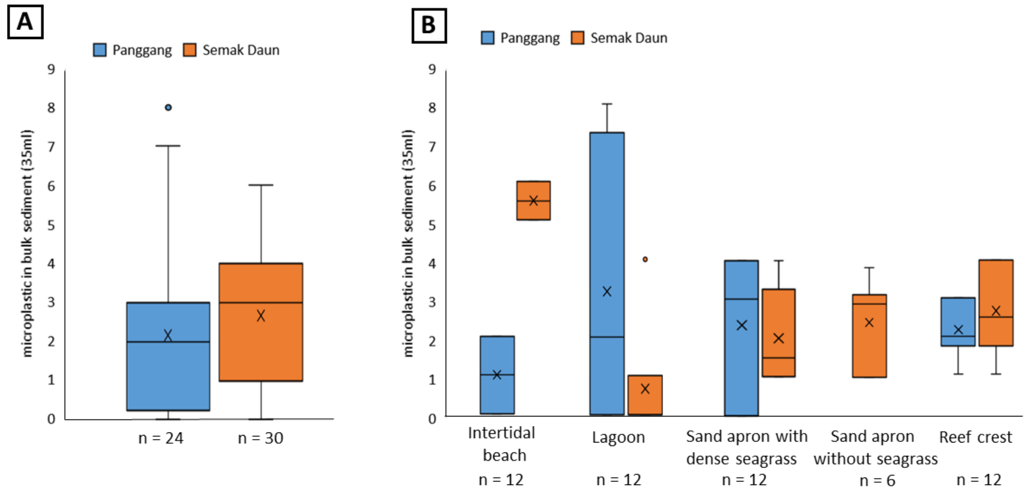

Figure 4-6. (A) Box plots and arithmetic mean (x) for microplastics in bulk sediment (35 ml) of Panggang and Semak Daun reef platforms. (B) Comparison of microplastic concentrations between environmental facies.

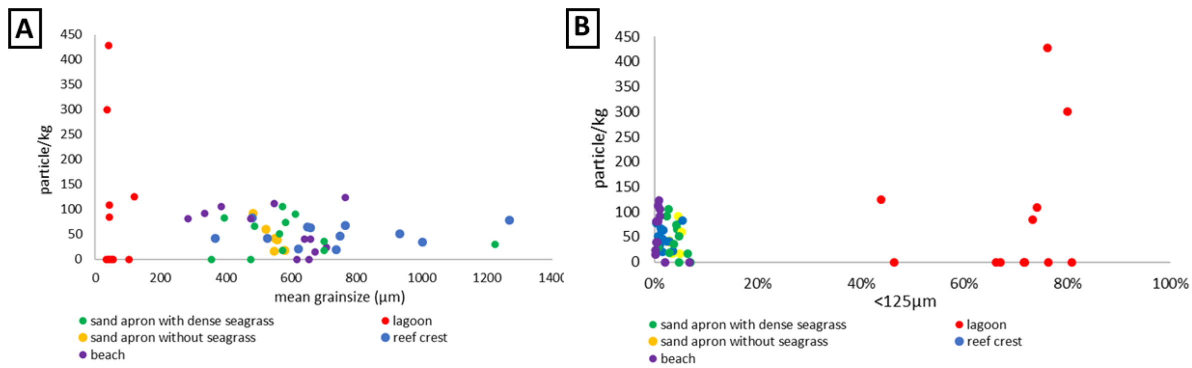

Figure 4-7. (A). Plot of microplastic concentration (particle/kg) with mean grainsize (µm) of bulk samples. Highest microplastic concentration occurs in the sediment with the finest mean grain size (< 100 µm). (B). Plot of microplastic concentration (particle/kg) with fine fraction content (< 125 µm) in the bulk sample. Highest microplastic concentration occurs in samples containing >50% fine sediment.

4.5 Discussion

Comparison with other reef environments

Information on the concentration of microplastic in reef environments is very limited. Saliu *et al.* (2018) studied microplastic abundance at the beach of a populated but remote island from the Maldives Archipelago. Cordova *et al.* (2018) and Zhang *et al.* (2019) studies the sediments from subtidal reef environments (Tab. 4-2). Microplastic concentration on the beaches of the study area are much higher compared to the example from the Maldives. This can be partly attributed to differences in the sampling protocol, since Saliu *et al.* (2018) was sampling a larger area (0.25 m^2 for < 1mm fraction) but only to a depth of 1 cm. Turra *et al.* (2015) noted that plastic items may occur to a depth of 2 m in beach environments, emphasized that depth of sampling is crucial for a comparison between sites when the abundance of particles is normalized to an area. This is supported by this study, which is showing similar concentration of microplastic in the upper and lower 3.5 cm of the beach samples (Fig. 4-5). Assuming a homogeneous distribution of microplastic within the sampled 7 cm, the concentration would be reduced to 149 and 842 particles/m^2 based solely on the uppermost 1 cm. However, even when these differences in sampling protocol are considered, the concentration of microplastic in Kepulauan Seribu is considerably higher compared to the Faavu Atoll in the Maldives. This likely results from the higher population density in Panggang and the effect of unregimented camping on Semak Daun.

Table 4-2. Comparison of microplastic concentration between different reef platforms.

Location	**Sampling site**	**Average microplastic concentration**		**References**
		/kg	**/m²**	
Beach				
Semak Daun, Indonesia	Atoll island	99	5891	this study
Panggang, Indonesia	Atoll island	19.8	1040	this study
Faavu Atoll, Maldives	Atoll island		22.7	(Saliu *et al.*, 2018)
Subtidal environments				
Semak Daun, Indonesia	Atoll	40	2036	this study
Panggang, Indonesia	Atoll	85	2657	this study
Lombok, Indonesia	Fringing reef	48		(Cordova *et al.*, 2018)
Nansha Island, South China Sea	Atoll	73		(Zhang *et al.*, 2019)
Weizhou Island, South China Sea	Fringing reef	75		(Zhang *et al.*, 2019)
Sanya LHT, South China Sea	Fringing reef	168		(Zhang *et al.*, 2019)
Xisha Island, South China Sea	Atoll	260		(Zhang *et al.*, 2019)

For subtidal environments the microplastic concentration is comparable to other reef systems. Semak Daun shows somewhat lower and Panggang somewhat higher values compared to Lombok or several reef systems in the South China Sea. Microplastic concentration between 40-90 particles/kg therefore seem to be the rule for subtidal reef environments, while much higher values from Sanya Lu Hui Tou and the Xisha Island (both in the South China Sea) seem to be exceptional.

Microplastics source and accumulation at the seafloor

The morphology of recovered microplastics indicate that breakdown of larger plastic items into secondary microplastics is the primary source of microplastics in the study area. Styrofoam, plastic cups and thin plastic wrap were reported as the most abundant land derived marine debris from the Greater Jakarta Area (Cordova & Nurhati, 2019). This is in contrast with the composition of the microplastic assemblage in Kepulauan

Seribu. Fibers and flakes of boat paint as the majority of microplastics indicate a local source of contamination from the islands or of marine origin, i.e. by fishing activity (Fig. 4-3), instead of a direct impact from the Greater Jakarta Area. A deep sub-marine channel to the north of Pari (Fig. 4-1) appear to act as important hydrologic barrier channeling the sediment-laden coastal waters off Java and Kalimantan away from the reef of Kepulauan Seribu (Tomascik *et al.*, 1997; Jordan, 1998). This seem to be in line with observations of other environmental stressors. Polluted water masses from the Greater Jakarta Area are considered to affect reefs in nearshore areas close to river mouths around Jakarta Bay, while localized effects of anthropogenic stressors are more important for reef in the northern Kepulauan Seribu (Farhan & Lim, 2012; Baum *et al.*, 2015). The lack of a statistically significant difference between samples from the densely populated (Panggang) and the unpopulated island (Semak Daun) is likely due to mismanaged plastic waste from tourism, as indicated by the abundance of microplastic found on the intertidal beach at Semak Daun which is known as a popular unregimented touristic campsite (Fig. 4-6).

The difference in abundance of microplastic between the environmental facies shows diverging patterns between the two reef platforms. At Panggang, the highest concentrations are observed in the lagoon, which is used for aquafarming. At Semak Daun, the highest concentrations also seem to be coupled to human activity on the beach of the touristically used island. Microplastic abundance therefore seem to be controlled to some extend by the proximity to the source area of larger plastic debris. However, the question remains why the microplastics are deposited and incorporated in the carbonate sediment at all. The microplastic fragments identified using µFT-IR analysis proved to be polypropylene (Fig. 4-2), which should be buoyant in sea water (Hidalgo-Ruz *et al.*, 2012). Biofouling is known to increase the density of microplastics to an extend that allows even buoyant polymers to sink to the seafloor (Kaiser *et al.*, 2017). Biofouling describes the process of buildup of organic matter and successive colonialization of plastic by organisms from bacteria to invertebrates. Fragments of diatoms were observed on microplastic fibers from the sand apron of Semak Daun (Fig. 4-8). Biofouling experiments from the Baltic Sea show that diatom fragments were abundant on microplastics after an incubation period of only six weeks (Kaiser *et al.*, 2017) and diatoms are also known to be among the first colonizers of seagrass blades (Corlett & Jones, 2007). Colonization by diatoms and generally biofouling therefore seems to be a relatively rapid process which allows even buoyant microplastics to settle to the seafloor.

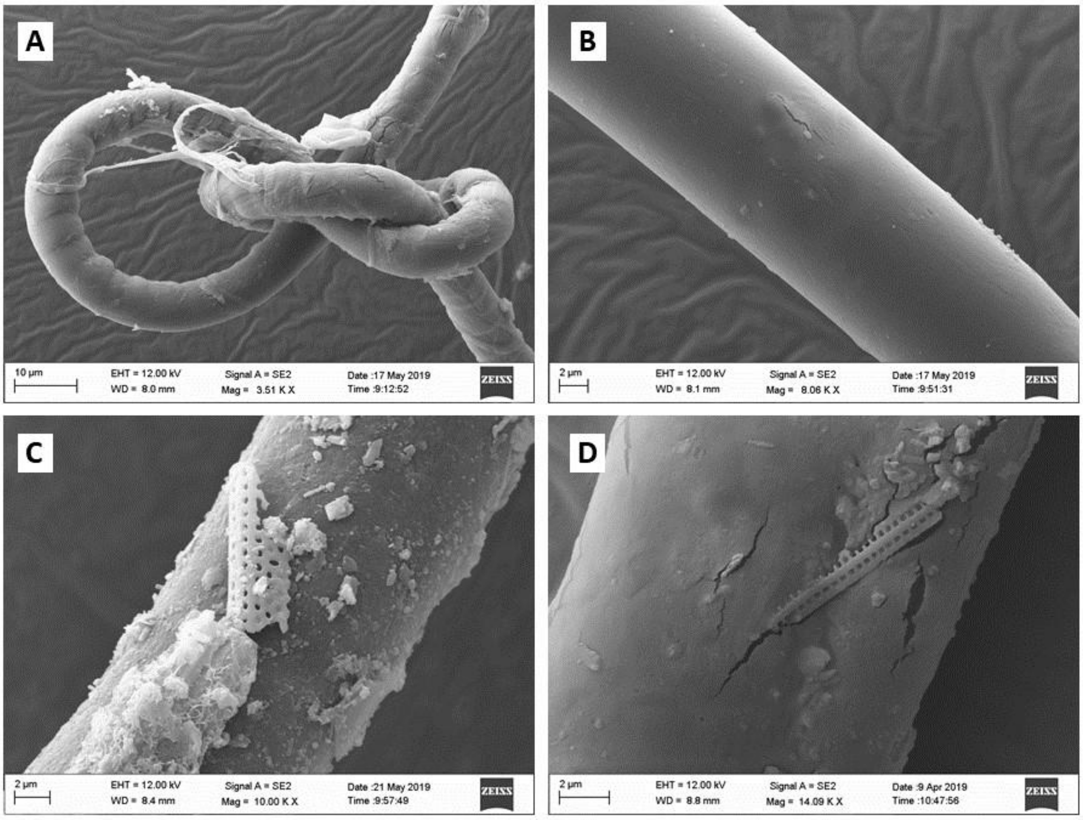

Figure 4-8. SEM images of synthetic fibers. (A). Fiber from the sand apron of Semak Daun (Sample M16). (B). Fiber from the intertidal beach of Semak Daun (Sample M19). (C). Biofouling of a fiber from the sand apron of Panggang (Sample M01). (D). Biofouling of a fiber from the sand apron of Semak Daun (Sample M18). SEM-EDX confirms that the test fragments in C and D are composed of silica. The fragments are interpreted to be derived from diatom tests, based on morphology and elemental composition.

Another process that is specific to reef environments is the trapping of floating and suspended sediment grains by coral mucus (Wild *et al.*, 2004). Mucus is a gel-like substance released by corals. It is used as a defense mechanism under stressed conditions, e.g. to prevent desiccation during air exposure (Wild *et al.*, 2004), but also to facilitate heterotrophic feeding (Lewis & Price, 1976). Mucus is known to accumulate to floats that drift from the reef towards the lagoon, before they sink to the seafloor. This process is known to effectively trap suspended sediments, which could include even the buoyant microplastics fraction.

Other polymers, that are slightly less dense compared to seawater, are thought to be transported similarly to e.g. clay minerals (Zalasiewicz *et al.*, 2016) and therefore could be easily winnowed from higher energy depositional environments. Plots of microplastic abundance vs. grain size of bulk sediment (Fig. 4-7) show a high variability but generally indicate that the highest microplastic concentration are limited to sediments with a mean grain size < 100 µm and fine fraction contents > 50%. These fine-grained sediments occur exclusively in the lagoon, indicating that the lagoon acts as a sink for microplastics once it has accumulated in this low energy environment. The assumption that microplastics are subject to similar transport and accumulation processes as fine grained siliciclastic is supported by increase values of siliciclastic and microplastics only occur in sample with 50% fine fraction (Fig. 4-9). There is no local source for siliciclastic phases on the reef platforms in the study area. Clay minerals (smectite) and fine-grained quartz therefore are thought to be derived from neighboring larger islands, such as Sumatra. Subsequently they are transported into the study area by oceanic currents (Utami *et al.,* accepted.). In the reef platforms they are concentrated below the local wave base, indicated by bulk fine fraction contents > 50% (Utami *et al.,* accepted.). A similar hydrodynamic control has been shown before for microplastic distribution in siliciclastic sediments in the Lagoon of Venice (Vianello *et al.*, 2013). Besides proximity to sources of plastic input, hydrodynamics therefore seems to be an important control for microplastic accumulation.

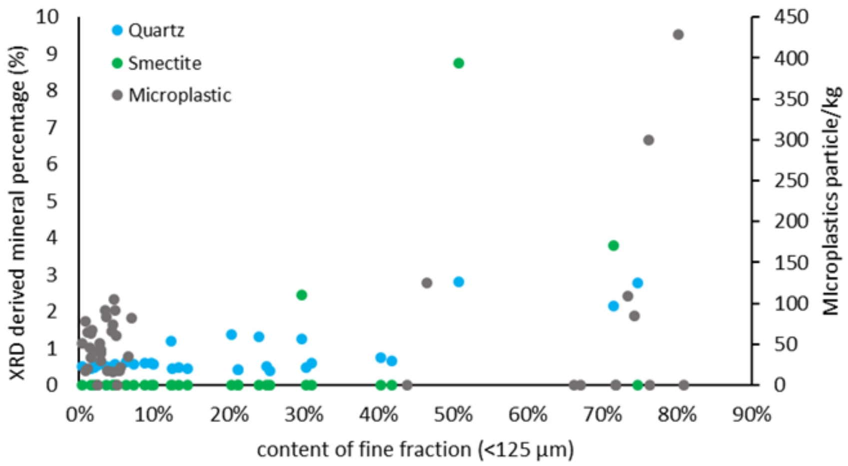

Figure 4-9. Plot of microplastics and siliciclastic mineral concentration with fine fraction (<125 µm) content in the bulk sample. Highest concentration of microplastic and siliciclastic minerals are found in sediment with >50% fine fraction content, indicating similar transport behavior. Mineralogy and associated bulk grain sizes are from Utami *et al.* (accepted).

It therefore is somewhat surprising that relatively high concentrations of low density microplastics have been observed in the relatively high energy environments of the reef crest and sand apron (Fig. 4-4) where carbonate sediments are characterized by relatively coarse grain sizes and are lacking clay minerals (Fig. 4-7). It is well known that seagrass baffles currents (Corlett & Jones, 2007; Utami *et al.*, 2018) demonstrated that the mean grain size of sediments on the sand apron of Panggang is reduced within dense seagrass meadows. Huang *et al.* (2020) showed that intertidal seagrass beds act as trap for microplastics, with a two- to threefold enrichment in sediments from seagrass beds compared to barren areas. The comparison of microplastic concentrations on the sand apron of Semak Daun shows no significant difference between the areas within and outside seagrass meadows (Independent samples Mann-Whitney *U* test, $p = 0.552$). However, this point should be studied with a larger dataset to evaluate the effect of subtidal seagrass beds on microplastics trapping conclusively.

The entrainment and resuspension of the microplastic particles might be hindered by armoring and interlocking effects (sensu Kench and McLean 1996). Bed armoring shields finer particles below coarse particles, limiting the capacity of currents for entrainment and transport (Reed *et al.*, 1999). This effect might be amplified by the shape of microplastic fibers. Entanglement of fibers with carbonate grains might contribute to an interlocking effect by which particles are tightly held by their neighbors. This process might even create compound grains (Fig. 4-10), consisting of mixed microplastic/carbonate particles with a density close to carbonate and a very irregular shape. The irregular shape and porous nature of reef sands might facilitate these entanglements, compared to more rounded and smoother siliciclastic grains. Another type of microplastic/carbonate compound grain was observed in beach sediments of Panggang (Fig. 4-10). Blue microplastics seem to partially cover carbonate grains. The color of the microplastics closely resembles the blue color of local fisher boats (Fig. 4-3), which are regularly painted at the beach. The grains are therefore interpreted to result from the contact of carbonate sand grains with fresh boat paint. Biofouling, armoring, interlocking and the creation of compound grains will all contribute to the sinking and accumulation of microplastics in relatively high energy environments as the beach, sand apron and reef crest. An alternative pathway for the incorporation of microplastics into carbonate grains in reefs would be the in vivo trapping within intraskeletal pores of the coral skeleton or the inclusion within the coral skeleton itself. Both processes have been described for suspended siliciclastic sediments (Barnard *et al.*, 1974; Risk & Edinger, 2011) and seem to be common for corals living in turbid water (Cortés & Risk, 1985). The same might apply for microplastics that is overgrown by coral tissue or ingested and retained by corals polyps. Microplastics within corals (tissue and/or skeleton) has been observed from the South China Sea (Ding *et al.*, 2019) but not in the study area.

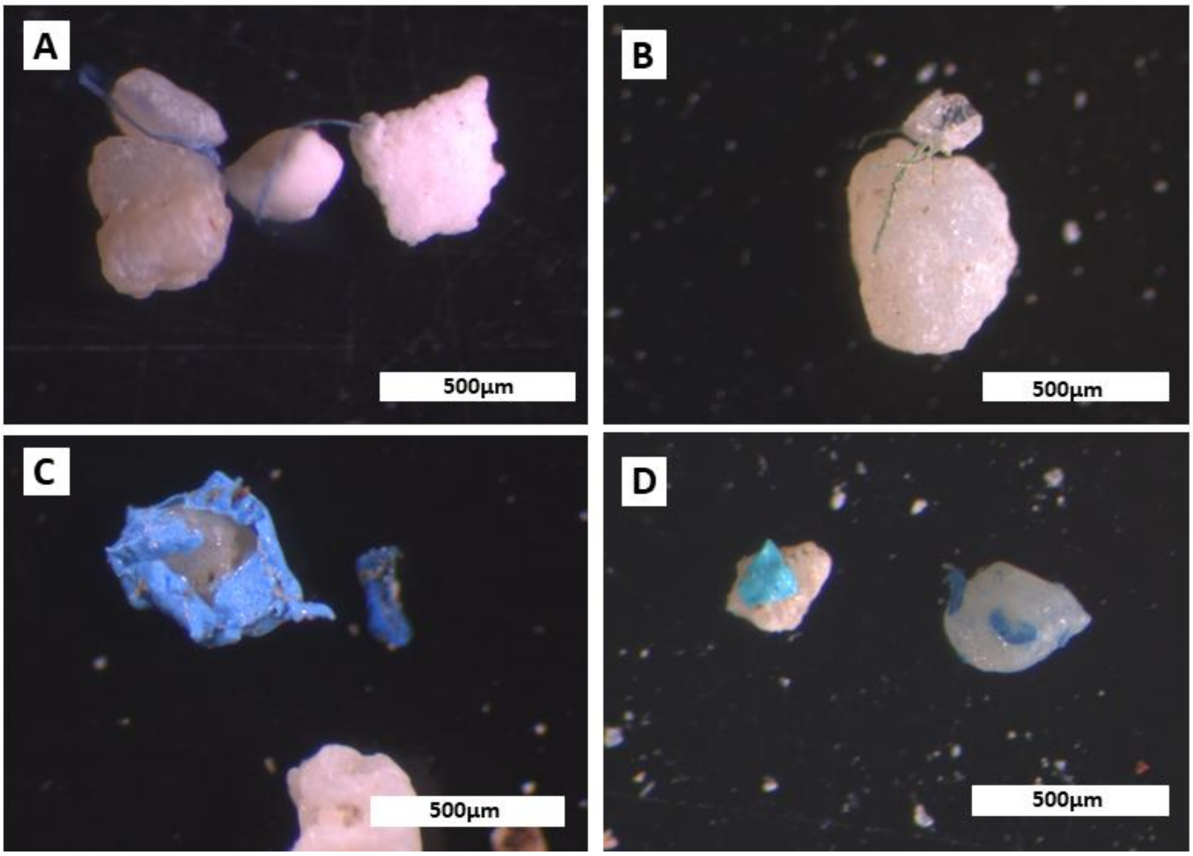

Figure 4-10. Entanglement of fibers and adhesion of paint creates compound grains. The higher density of these grains compared to pure microplastics facilitate their accumulation on the seafloor. (A). Entanglement of a fiber with carbonate sand grains (Sample M20, intertidal beach, Semak Daun). (B). Entanglement of a fiber with carbonate sand grains (Sample M29, intertidal beach, Panggang). (C). Microplastics, interpreted as remnants of paint droplets, wrapped around a sand grain (Sample M29, intertidal beach, Panggang). (D). Microplastics, interpreted as remnants of paint droplets, attached to the surface of sand grains (Sample M28, intertidal beach, Panggang).

Reef sediments as permanent sink for microplastics

Due to its widespread occurrence, microplastics are regarded as a good practical indicator of Anthropocene strata (Zalasiewicz *et al.*, 2016). However, the authors cautioned that shelf sediments might be depleted in microplastics due to the effect of currents transporting plastic offshore into deeper water. There is a shortage of studies investigating the depth distribution of microplastics in shallow subtidal sediments and a complete lack of data for reef systems. This study indicates that microplastics are not only common in sediments close to the surface (0-3.5 cm) but also in sediments between 3.5 and 7 cm depth.

The mixing depth is defined as the vertical thickness of a layer of active sediment exchange, below which lies an immobile bed (Sherman *et al.*, 1993). Besides hydrodynamic mechanism, sediment mixing depth is influenced by bioturbation. Jackson *et al.* (2005) found that bioturbation is responsible for an increased mixing depth in estuarine beaches. An experimental study by Näkki *et al.* (2017) revealed that bioturbation can distribute microplastics within the uppermost 5 cm of the sediment column in just three weeks. Martin *et al.* (2017) found that microplastics are ubiquitous in superficial sediment of the Irish continental shelf but only at depth less than 4 cm, inferring significant exposure of filter and deposit feeder. Bioturbation is pervasive on the sand apron of reef platforms in Kepulauan Seribu (Fig. 4-11) which could explain the presence of microplastics in depth > 3.5 cm.

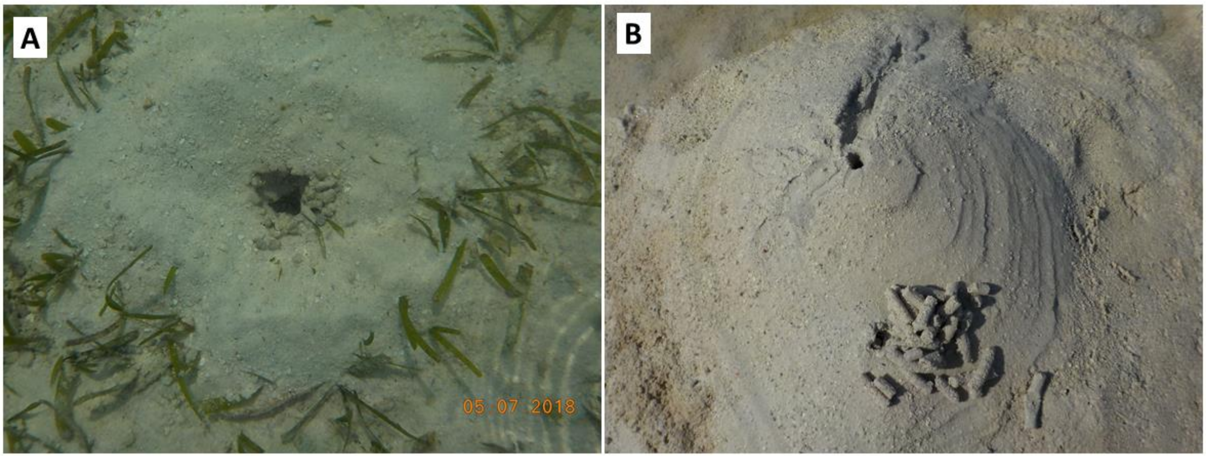

Figure 4-11. Bioturbation observed in the reef environment. (A). Subtidal sand apron of Panggang platform. (B). Intertidal sand apron of Pari platform. Diameter of the bioturbation burrow is approximately 2 cm in both cases.

Hydrodynamic transport of sediment grains on the sand apron of reef systems is an understudied topic. However, measurements on the sand apron of the high energy reef of One Tree Island, indicate mixing depth of < 2.5 cm under modal conditions (Vila-Concejo *et al.*, 2014). Microplastics in the interval below 3.5 cm therefore is unlikely to be remobilized under modal weather conditions. However, it is typically assumed that erosion and deposition on reef platforms is strongly influenced by high-energy events such as storms. This is especially true for reefs between 7-25° north and south of the equator, that are affected by tropical cyclones (Scoffin, 1993). In contrast, the reef platforms of Kepulauan Seribu belong to the equatorial carbonate systems (Park *et al.,* 2010; Utami *et al.,* accepted) and are mainly influenced by the monsoonal wind system (Umbgrove, 1947). Beach sediments of sand keys in Kepulauan Seribu are subject to erosion by the seasonally reversing monsoonal winds (Poerbandono, 2016). Microplastics in beach sediments therefore might be resuspended, likely resulting in a lower preservation potential of microplastics accumulate. However, analysis of wind strength over a 30-yrs interval for Kepulauan Seribu indicated maximum offshore significant wave heights of < 0.4 m (Poerbandono, 2016), which is much less compared to the average offshore significant wave heights of 1.15 m at One Tree Island (Hopley *et al.*, 2007). High energy events therefore are not likely to cause resuspension of microplastics from subtidal environments, which are therefore considered to be a permanent sink. Martin *et al.* (2019) observed that the concentration of floating microplastics in the Red Sea is unusually low. They attributed this to adhesion of microplastics to corals in the abundant reefs of the Red Sea. This study suggests that burial in reef sediments might be an alternative or additional mechanism to explain the relatively low concentrations.

Microplastics and reef health

Scleractinian corals are known to ingest microplastics that they confuse with natural prey (Hall *et al.*, 2015; Allen *et al.*, 2017; Reichert *et al.*, 2019) and microplastics adhere passively on the surface of reef corals (Ding *et al.*, 2019; Martin *et al.*, 2019). Only a relatively small fraction of the ingested microplastics are retained by the corals, which use similar rejection mechanisms for microplastics as for other sedimentary grains (Stafford-Smith & Ormond, 1992; Reichert *et al.*, 2018). However, egestion of microplastics and other rejection mechanisms are thought to be energetically costly (Reichert *et al.*, 2019). Most laboratory experiments show that exposure to microplastics have several negative impacts on coral health, such as bleaching, tissue necrosis or an impairment of the corals immune system (Reichert *et al.*, 2018; Tang *et al.*, 2018; Syakti *et al.*, 2019). No effect on calcification rates were observed for 28 days under laboratory conditions (Lanctôt *et al.*, 2020), but species-specific reduction of growth rates was shown for chronic exposure to microplastics over a period of six month (Reichert *et al.*, 2019). Plastic debris can also be the carrier of pathogens or chemical contaminants (Saliu *et al.*, 2019; Feng *et al.*, 2020), increasing the probability of coral disease by 4–89% (Lamb *et al.*, 2018). Phthalic acid esters or phthalates, a common group of plastic additives, were found in the tissue of 95% coral samples from an atoll in the Maldivian archipelago (Saliu *et al.*, 2019; Montano *et al.*, 2020). This was the first indication that microplastics might transfer plastic additives into reef corals within their natural environment (Saliu *et al.*, 2019; Montano *et al.*, 2020). It is therefore noteworthy that in this study phthalates were detected on the surface of two microplastic particles, making the contaminants bioavailable to corals after ingestion. The widespread presence of microplastics in all facies zones and water depth is in line with the finding of Montano *et al.* (2020), who did not find significant differences in phthalates concentration in coral tissue from different water depth. In Kepulauan Seribu partly of the reef are exposed subaerially during low tide. This would allow a direct exposure to microplastics floating on the sea surface. Moreover, the data of this study shows that appreciable amounts of microplastics are sinking to the seafloor in all facies zones, including the reef crest (Fig. 4-4). Here microplastic particles could adhere to the coral tissue or be resuspended, increasing the likelihood of direct contact with corals. Microplastic concentration at the reef crest of Panggang is even significantly higher compared to the beach. This could indicate that the risk to microplastics exposure for coral reefs is hitherto underestimated, since most sediment studies are limit to the beach environment (Imhof *et al.*, 2017; Saliu *et al.*, 2018).

Globally coral reefs are suffering from anthropogenic stressors. Microplastics in coral reef environment therefor deserve careful consideration, since microplastics poses an additional threat to corals and their ability as framework builders in reef systems.

4.6 Conclusion

Microplastics are present as sedimentary component in two reef platforms from the island chain of Kepulauan Seribu, about 30 km north of the Greater Jakarta Area. One of the reef platforms, Panggang, hosts a densely populated island. A small unpopulated island on the reef platform of Semak Daun is intensively used for unregimented touristic camping. The microplastic contamination in both reef systems is related to marine and local, coastal anthropogenic factors. Abundance of microplastic in sediment is controlled to some extend by the proximity to the source area of larger plastic debris.

Processes of microplastics transport and accumulation are thought to be similar to fine siliciclastic grains in the reef system. Microplastics are partly winnowed from high energy environment of the reef system and accumulates in low energy environment, such as lagoons. This emphasizes that hydrodynamic controls are important for microplastics distribution.

However, microplastic contamination was also found in high energy environments such as the beach, sand apron and reef crest. One of the mechanisms that allows buoyant microplastics to sink to the seafloor is density modification through biofouling. In the sand apron, bed armoring and interlocking effects could entrain and resuspended microplastics by shielding finer particles below coarse particles. This effect might be amplified by the shape of microplastic fibers. Entanglement of fibers with carbonate grains also contributes to an interlocking effect by which particles are tightly held by their neighbors. Furthermore, entanglement might create compound grains, consisting of mixed microplastic/carbonate particles with a density close to carbonate and a very irregular shape. These processes principally can operate in different sedimentary environments but might be promoted by the irregular shape and porous nature of bioclastic carbonate grains. A process, which is specific to reef environments, is the trapping of sedimentary grains and potentially microplastics by the mucus produced by corals.

Microplastics are not only present in the surface layer (0-3.5 cm), but also in a depth between 3.5 and 7 cm. Transport of microplastics to deeper sediment layers likely is controlled by bioturbation, which is pervasive on the reef platforms of Kepulauan Seribu. Microplastics below a depth of 3.5 cm is unlikely to be remobilized from subtidal sediments under modal weather conditions. Subtidal environments are therefore considered to be a permanent sink for microplastics in equatorial reef systems that are not affected by high energy events, such as tropical cyclones. For this reason, microplastics in subtidal reef environments from the equatorial zone can be a good practical indicator of Anthropocene strata. The influence of storm events on the accumulation of microplastics need further investigation.

The reef crest in the study area is partially exposed subaerially during low tide, allowing a direct contact to microplastics floating on the sea surface. Microplastics are also abundant in surface sediments of all reef environments, including the reef crest. Resuspension therefore can lead to the repeated exposure to microplastic, which is energetically costly for corals. Phthalates, a common plastic additive, was detected on the surface of microplastic particles in the study area. This demonstrates that contaminants associated with microplastics could become bioavailable to corals after ingestion. Microplastics in coral reef environments therefor deserves careful consideration, since microplastics poses an additional threat to corals and their ability as framework builders in reef systems.

CRediT Statement

Dwi Amanda Utami: funding acquisition, resources, methodology, investigation, formal analysis, visualization, writing – original draft, writing – review and editing. **Lars Reuning**: supervision, resources, conceptualization, methodology, formal analysis, validation, writing – original draft, writing – review and editing. **Olga Konechnaya**: investigation, writing – review and editing. **Jan Schwarzbauer**: resources, validation, writing – review and editing.

Acknowledgement

The authors are grateful to Lembaga Pengelola Dana Pendidikan (LPDP) who awarded a scholarship and dissertation fund to Dwi Amanda Utami Nasution. Karina Sujatmiko and Endang Lili are thanked for their aid during field work. Philipp Binger is thanked for assisting laboratory sampling. Larissa Dsikowitzky is thanked for supporting µFT-IR measurement. Uwe Wollenberg is thanked for helping with SEM EDX measurements. Google Earth software (http://www.google.com/earth) and QGIS 3.14.1-Pi was used extensively.

Conflict of Interest

We declare that we have no commercial or associative aim that might represent a conflict of interest in connection with the work submitted.

Data Availability Statement

The data that support the findings of this study are available on the supplement.

References

Alam, F.C., **Sembiring, E.**, **Muntalif, B.S.** and **Suendo, V.** (2019) Microplastic distribution in surface water and sediment river around slum and industrial area (case study: Ciwalengke River, Majalaya district, Indonesia). *Chemosphere*, **224**, 637–645.

Allen, A.S., **Seymour, A.C.** and **Rittschof, D.** (2017) Chemoreception drives plastic consumption in a hard coral. *Mar. Pollut. Bull.*, **124**, 198–205.

Andrady, A.L. (2011) Microplastics in the marine environment. *Mar. Pollut. Bull.*, **62**, 1596–1605.

Arthur, C., **Baker, J.** and **H. Bamford** (2009) Proceedings of the International Research Workshop on the Occurrence, Effects, and Fate of Microplastic Marine Debris. Sept 9-11, 2008. In: *NOAA Technical Memorandum NOS-OR&R-30*,

Barnard, L.A., **Macintyre, I.G.** and **Pierce, J.W.** (1974) Possible environmental index in tropical reef corals. *Nature*, **252**, 219–220.

Baum, G., **Januar, H.I.**, **Ferse, S.C.A.** and **Kunzmann, A.** (2015) Local and Regional Impacts of Pollution on Coral Reefs along the Thousand Islands North of the Megacity Jakarta, Indonesia. *PLoS One*, **10**, e0138271.

Chapron, L., **Peru, E.**, **Engler, A.**, **Ghiglione, J.F.**, **Meistertzheim, A.L.**, **Pruski, A.M.**, **Purser, A.**, **Vétion, G.**, **Galand, P.E.** and **Lartaud, F.** (2018) Macro- and microplastics affect cold-water corals growth, feeding and behaviour. *Sci. Rep.*, **8**, 15299.

Coppock, R.L., **Cole, M.**, **Lindeque, P.K.**, **Queirós, A.M.** and **Galloway, T.S.** (2017) A small-scale, portable method for extracting microplastics from marine sediments. *Environ. Pollut.*, **230**, 829–837.

Corcoran, P.L., **Biesinger, M.C.** and **Grifi, M.** (2009) Plastics and beaches: A degrading relationship. *Mar. Pollut. Bull.*, **58**, 80–84.

Cordova, M.R., **Hadi, T.A.** and **Prayudha, B.** (2018) Occurrence and abundance of microplastics in coral reef sediment: a case study in Sekotong, Lombok-Indonesia. *AES Bioflux*, **10**, 23–29.

Cordova, M.R. and **Nurhati, I.S.** (2019) Major sources and monthly variations in the release of land-derived marine debris from the Greater Jakarta area, Indonesia. *Sci. Rep.*, **9**, 18730.

Cordova, M.R. and **Wahyudi, A.J.** (2016) Microplastic in the deep sea sediment of southwestern Sumatran waters. *Mar. Res. Indones.*, **41**, 27–35.

Corlett, H. and **Jones, B.** (2007) Epiphyte communities on Thalassia testudinum from Grand Cayman, British West Indies: Their composition, structure, and contribution to lagoonal sediments. *Sediment. Geol.*, **194**, 245–262.

Cortés, J.N. and **Risk, M.J.** (1985) A reef under siltation stress: Cahuita, Costa Rica: Ingenta Connect. *Bull. Mar. Sci.*, **36**, 339-356(18).

de Carvalho-Souza, G.F., **Llope, M.**, **Tinôco, M.S.**, **Medeiros, D. V**, **Maia-Nogueira, R.** and **Sampaio, C.L.** (2018) Marine litter disrupts ecological processes in reef systems. *Mar. Pollut. Bull.*, **133**, 464–471.

Ding, J., **Jiang, F.**, **Li, J.**, **Wang, Z.**, **Sun, C.**, **Wang, Z.**, **Fu, L.**, **Ding, N.X.** and **He, C.** (2019) Microplastics in the Coral Reef Systems from Xisha Islands of South China Sea. *Environ. Sci. Technol.*, **53**, 8036–8046.

Farhan, A.R. and **Lim, S.** (2012) Vulnerability assessment of ecological conditions in Seribu Islands, Indonesia. *Ocean Coast. Manag.*, **65**, 1–14.

Feng, L., **He, L.**, **Jiang, S.**, **Chen, J.**, **Zhou, C.**, **Qian, Z.-J.**, **Hong, P.**, **Sun, S.** and **Li, C.** (2020) Investigating the composition and distribution of microplastics surface biofilms in coral areas. *Chemosphere*, **252**, 126565.

Firdaus, M., **Trihadiningrum, Y.** and **Lestari, P.** (2020) Microplastic pollution in the sediment of Jagir Estuary, Surabaya City, Indonesia. *Mar. Pollut. Bull.*, **150**, 110790.

Fries, E., **Dekiff, J.H.**, **Willmeyer, J.**, **Nuelle, M.-T.**, **Ebert, M.** and **Remy, D.** (2013) Identification of polymer types and additives in marine microplastic particles using pyrolysis-GC/MS and scanning electron microscopy. *Environ. Sci. Process. Impacts*, **15**, 1949.

Geyer, R., **Jambeck, J.R.** and **Law, K.L.** (2017) Production, use, and fate of all plastics ever made. *Sci. Adv.*, **3**, e1700782.

Hall, N.M., **Berry, K.L.E.**, **Rintoul, L.** and **Hoogenboom, M.O.** (2015) Microplastic ingestion by scleractinian corals. *Mar. Biol.*, **162**, 725–732.

Hammer, Ø., **Harper, D.A.T. a. T.** and **Ryan, P.D.** (2001) PAST: Paleontological Statistics Software Package for Education and Data Analysis. *Palaeontol. Electron.*, **4(1)**, 1–9.

Hidalgo-Ruz, V., **Gutow, L.**, **Thompson, R.C.** and **Thiel, M.** (2012) Microplastics in the Marine Environment: A Review of the Methods Used for Identification and Quantification. *Environ. Sci. Technol.*, **46**, 3060–3075.

Hopley, D., **Smithers, S.G.** and **Parnell, K.** (2007) The Geomorphology of the Great Barrier Reef: Development, Diversity and Change. *Cambridge University Press*.

Horton, A.A. and **Dixon, S.J.** (2018) Microplastics: An introduction to environmental transport processes. *Wiley Interdiscip. Rev. Water*, **5**, e1268.

Houlbrèque, F., **Meibom, A.**, **Cuif, J.-P.**, **Stolarski, J.**, **Marrocchi, Y.**, **Ferrier-Pagès, C.**, **Domart-Coulon, I.** and **Dunbar, R.B.** (2009) Strontium-86 labeling experiments show spatially heterogeneous skeletal formation in the scleractinian coral *Porites porites*. *Geophys. Res. Lett.*, **36**, L04604.

Huang, Y., **Xiao, X.**, **Xu, C.**, **Perianen, Y.D.**, **Hu, J.** and **Holmer, M.** (2020) Seagrass beds acting as a trap of microplastics - Emerging hotspot in the coastal region? *Environ. Pollut.*, **257**, 113450.

Imhof, H.K., **Sigl, R.**, **Brauer, E.**, **Feyl, S.**, **Giesemann, P.**, **Klink, S.**, **Leupolz, K.**, **Löder, M.G.J.**, **Löschel, L.A.**, **Missun, J.**, **Muszynski, S.**, **Ramsperger, A.F.R.M.**, **Schrank, I.**, **Speck, S.**, **Steibl, S.**, **Trotter, B.**, **Winter, I.** and **Laforsch, C.** (2017) Spatial and temporal variation of macro-, meso- and microplastic abundance on a remote coral island of the Maldives, Indian Ocean. *Mar. Pollut. Bull.*, **116**, 340–347.

Jackson, N.L., **Nordstrom, K.F.** and **Smith, D.R.** (2005) Influence of waves and horseshoe crab spawning on beach morphology and sediment grain-size characteristics on a sandy estuarine beach. *Sedimentology*, **52**, 1097–1108.

Jambeck, J.R., **Geyer, R.**, **Wilcox, C.**, **Siegler, T.R.**, **Perryman, M.**, **Andrady, A.**, **Narayan, R.** and **Law, K.L.** (2015) Plastic waste inputs from land into the ocean. *Science (80-.).*, **347**, 768–771.

Jordan, C.F. (1998) The Sedimentology of Kepulauan Seribu: A Modern Patch Reef Complex in the West Java Sea, Indonesia. 1–81.

Kaiser, D., **Kowalski, N.** and **Waniek, J.J.** (2017) Effects of biofouling on the sinking behavior of microplastics. *Environ. Res. Lett.*, **12**, 124003.

Kane, I.A. and **Clare, M.A.** (2019) Dispersion, Accumulation, and the Ultimate Fate of Microplastics in Deep-Marine Environments: A Review and Future Directions. *Front. Earth Sci.*, **7**, 80.

Kench, P. and **McLean, R.** (1996) Hydraulic characteristics of bioclastic deposits: new possibilities for environmental interpretation using settling velocity fractions. *Sedimentology*, **43**, 561–570.

Kowalski, N., **Reichardt, A.M.** and **Waniek, J.J.** (2016) Sinking rates of microplastics and potential implications of their alteration by physical, biological, and chemical factors. *Mar. Pollut. Bull.*, **109**, 310–319.

Lamb, J.B., **Willis, B.L.**, **Fiorenza, E.A.**, **Couch, C.S.**, **Howard, R.**, **Rader, D.N.**, **True, J.D.**, **Kelly, L.A.**, **Ahmad, A.**, **Jompa, J.** and **Harvell, C.D.** (2018) Plastic waste associated with disease on coral reefs. *Science (80-.).*, **359**, 460–462.

Lanctôt, C.M., **Bednarz, V.N.**, **Melvin, S.**, **Jacob, H.**, **Oberhaensli, F.**, **Swarzenski, P.W.**, **Ferrier-Pagès, C.**, **Carroll, A.R.** and **Metian, M.** (2020) Physiological stress response of the scleractinian coral Stylophora pistillata exposed to polyethylene microplastics. *Environ. Pollut.*, **263**, 114559.

Lewis, J.B. and **Price, W.S.** (1976) Patterns of ciliary currents in Atlantic reef corals and their functional significance. *J. Zool.*, **178**, 77–89.

Ling, S.D., **Sinclair, M.**, **Levi, C.J.**, **Reeves, S.E.** and **Edgar, G.J.** (2017) Ubiquity of microplastics in coastal seafloor sediments. *Mar. Pollut. Bull.*, **121**, 104–110.

Lusher, A.L., **Welden, N.A.**, **Sobral, P.** and **Cole, M.** (2017) Sampling, isolating and identifying microplastics ingested by fish and invertebrates. *Anal. Methods*, **9**, 1346–1360.

Martin, C., **Corona, E.**, **Mahadik, G.A.** and **Duarte, C.M.** (2019) Adhesion to coral surface as a potential sink for marine microplastics. *Environ. Pollut.*, **255**, 113281.

Martin, J., **Lusher, A.**, **Thompson, R.C.** and **Morley, A.** (2017) The Deposition and Accumulation of Microplastics in Marine Sediments and Bottom Water from the Irish Continental Shelf. *Sci. Rep.*, **7**, 10772.

Montano, S., **Seveso, D.**, **Maggioni, D.**, **Galli, P.**, **Corsarini, S.** and **Saliu, F.** (2020) Spatial variability of phthalates contamination in the reef-building corals Porites lutea, Pocillopora verrucosa and Pavona varians. *Mar. Pollut. Bull.*, **155**, 111117.

Morét-Ferguson, S., **Law, K.L.**, **Proskurowski, G.**, **Murphy, E.K.**, **Peacock, E.E.** and **Reddy, C.M.** (2010) The size, mass, and composition of plastic debris in the western North Atlantic Ocean. *Mar. Pollut. Bull.*, **60**, 1873–1878.

Näkki, P., **Setälä, O.** and **Lehtiniemi, M.** (2017) Bioturbation transports secondary microplastics to deeper layers in soft marine sediments of the northern Baltic Sea. *Mar. Pollut. Bull.*, **119**, 255–261.

Nel, H., **Krause, S.**, **Sambrook Smith, G.H.** and **Lynch, I.** (2019) Simple yet effective modifications to the operation of the Sediment Isolation Microplastic unit to avoid polyvinyl chloride (PVC) contamination. *MethodsX*, **6**, 2656–2661.

Nuelle, M.-T., **Dekiff, J.H.**, **Remy, D.** and **Fries, E.** (2014) A new analytical approach for monitoring microplastics in marine sediments. *Environ. Pollut.*, **184**, 161–169.

Park, R.K., **Crevello, P.D.** and **Hantoro, W.** (2010) Equatorial Carbonate Depositional Systems of Indonesia. In: *Cenozoic carbonate systems of Australasia* (Ed. W.A. Morgan, A.D. George, P.M. Harris, J.A. Kupecz, and J.F. Sarg), *SEPM Special Publication 95*, Tulsa, Oklahoma, 41–77.

Poerbandono (2016) Wind characteristics and the associated risk of erosion in Seribu Islands patch reef complexes, Java Sea, Indonesia. In: *The 5th International Symposium on Earthhazard and Disaster Mitigation. AIP Conf. Proc.*, 1730, 080001.

Reed, C.W., **Niedoroda, A.W.** and **Swift, D.J.P.** (1999) Modeling sediment entrainment and transport processes limited by bed armoring. *Mar. Geol.*, **154**, 143–154.

Reichert, J., **Arnold, A.L.**, **Hoogenboom, M.O.**, **Schubert, P.** and **Wilke, T.** (2019) Impacts of microplastics on growth and health of hermatypic corals are species-specific. *Environ. Pollut.*, **254**, 113074.

Reichert, J., **Schellenberg, J.**, **Schubert, P.** and **Wilke, T.** (2018) Responses of reef building corals to microplastic exposure. *Environ. Pollut.*, **237**, 955–960.

Risk, M.J. and **Edinger, E.** (2011) Impacts of Sediment on Coral Reefs. 575–586.

Rochman, C.M., **Tahir, A.**, **Williams, S.L.**, **Baxa, D. V.**, **Lam, R.**, **Miller, J.T.**, **Teh, F.-C.**, **Werorilangi, S.** and **Teh, S.J.** (2015) Anthropogenic debris in seafood: Plastic debris and fibers from textiles in fish and bivalves sold for human consumption. *Sci. Rep.*, **5**, 14340.

Saliu, F., **Montano, S.**, **Garavaglia, M.G.**, **Lasagni, M.**, **Seveso, D.** and **Galli, P.** (2018) Microplastic and charred microplastic in the Faafu Atoll, Maldives. *Mar. Pollut. Bull.*, **136**, 464–471.

Saliu, F., **Montano, S.**, **Leoni, B.**, **Lasagni, M.** and **Galli, P.** (2019) Microplastics as a threat to coral reef environments: Detection of phthalate esters in neuston and scleractinian corals from the Faafu Atoll, Maldives. *Mar. Pollut. Bull.*, **142**, 234–241.

Scoffin, T.P. (1993) The geological effects of hurricanes on coral reefs and the interpretation of storm deposits. *Coral Reefs*, **12**, 203–221.

Scrutton, M. (1976) Aspects Carbonate Sedimentation in Indonesia. In: *Indonesian Petroleum Association, Proceeding 5th Annual Convention*, 179–193.

Sherman, D.J., **Short, A.D.** and **Takeda, I.** (1993) Sediment Mixing-Depth and Bedform Migration in RIP Channels. *J. Coast. Res. Spec. Issue No. 15. Beach Surf Zo. Morphodynamics.*, 39–48.

Stafford-Smith, M. and **Ormond, R.** (1992) Sediment-rejection mechanisms of 42 species of Australian scleractinian corals. *Mar. Freshw. Res.*, **43**, 683.

Syakti, A.D., **Bouhroum, R.**, **Hidayati, N.V.**, **Koenawan, C.J.**, **Boulkamh, A.**, **Sulistyo, I.**, **Lebarillier, S.**, **Akhlus, S.**, **Doumenq, P.** and **Wong-Wah-Chung, P.** (2017) Beach macro-litter monitoring and floating microplastic in a coastal area of Indonesia. *Mar. Pollut. Bull.*, **122**, 217–225.

Syakti, A.D., **Hidayati, N.V.**, **Jaya, Y.V.**, **Siregar, S.H.**, **Yude, R.**, **Suhendy**, **Asia, L.**, **Wong-Wah-Chung, P.** and **Doumenq, P.** (2018) Simultaneous grading of microplastic size sampling in the Small Islands of Bintan water, Indonesia. *Mar. Pollut. Bull.*, **137**, 593–600.

Syakti, A.D., **Jaya, J.V.**, **Rahman, A.**, **Hidayati, N.V.**, **Raza'i, T.S.**, **Idris, F.**, **Trenggono, M.**, **Doumenq, P.** and **Chou, L.M.** (2019) Bleaching and necrosis of staghorn coral (Acropora formosa) in laboratory assays: Immediate impact of LDPE microplastics. *Chemosphere*, **228**, 528–535.

Tan, F., **Yang, H.**, **Xu, X.**, **Fang, Z.**, **Xu, H.**, **Shi, Q.**, **Zhang, X.**, **Wang, G.**, **Lin, L.**, **Zhou, S.**, **Huang, L.** and **Li, H.** (2020) Microplastic pollution around remote uninhabited coral reefs of Nansha Islands, South China Sea. *Sci. Total Environ.*, **725**, 138383.

Tang, J., **Ni, X.**, **Zhou, Z.**, **Wang, L.** and **Lin, S.** (2018) Acute microplastic exposure raises stress response and suppresses detoxification and immune capacities in the scleractinian coral Pocillopora damicornis. *Environ. Pollut.*, **243**, 66–74.

Teuten, E.L., **Saquing, J.M.**, **Knappe, D.R.U.**, **Barlaz, M.A.**, **Jonsson, S.**, **Björn, A.**, **Rowland, S.J.**, **Thompson, R.C.**, **Galloway, T.S.**, **Yamashita, R.**, **Ochi, D.**, **Watanuki, Y.**, **Moore, C.**, **Viet, P.H.**, **Tana, T.S.**, **Prudente, M.**, **Boonyatumanond, R.**, **Zakaria, M.P.**, **Akkhavong, K.**, **Ogata, Y.**, **Hirai, H.**, **Iwasa, S.**, **Mizukawa, K.**, **Hagino, Y.**, **Imamura, A.**, **Saha, M.** and **Takada, H.** (2009) Transport and release of chemicals from plastics to the environment and to wildlife. *Philos. Trans. R. Soc. B Biol. Sci.*, **364**, 2027–2045.

Tomascik, T., **Mah, A.J.**, **Nontji, A.** and **Moosa, M.K.** (1997) The Ecology of the Indonesia Seas Volume VIII Part II. *Oxford University*, 1231–1239 pp.

Turra, A., **Manzano, A.B.**, **Dias, R.J.S.**, **Mahiques, M.M.**, **Barbosa, L.**, **Balthazar-Silva, D.** and **Moreira, F.T.** (2015) Three-dimensional distribution of plastic pellets in sandy beaches: shifting paradigms. *Sci. Rep.*, **4**, 4435.

Umbgrove, J.H.F. (1947) Coral Reefs of the East Indies. *Bull. Geogr. Sociaty Am.*, **58**, 729–778.

Utami, D.A., **Reuning, L.** and **Cahyarini, S.Y.** (2018) Satellite- and field-based facies mapping of isolated carbonate platforms from the Kepulauan Seribu Complex, Indonesia. *Depos. Rec.*, **4**, 255–273.

Van Cauwenberghe, L., **Devriese, L.**, **Galgani, F.**, **Robbens, J.** and **Janssen, C.R.** (2015) Microplastics in sediments: A review of techniques, occurrence and effects. *Mar. Environ. Res.*, **111**, 5–17.

Van Cauwenberghe, L., **Vanreusel, A.**, **Mees, J.** and **Janssen, C.R.** (2013) Microplastic pollution in deep-sea sediments. *Environ. Pollut.*, **182**, 495–499.

van Sebille, E., **Wilcox, C.**, **Lebreton, L.**, **Maximenko, N.**, **Hardesty, B.D.**, **van Franeker, J.A.**, **Eriksen, M.**, **Siegel, D.**, **Galgani, F.** and **Law, K.L.** (2015) A global inventory of small floating plastic debris. *Environ. Res. Lett.*, **10**, 124006.

Vianello, A., **Boldrin, A.**, **Guerriero, P.**, **Moschino, V.**, **Rella, R.**, **Sturaro, A.** and **Da Ros, L.** (2013) Microplastic particles in sediments of Lagoon of Venice, Italy: First observations on occurrence, spatial patterns and identification. *Estuar. Coast. Shelf Sci.*, **130**, 54–61.

Vidyasakar, A., **Neelavannan, K.**, **Krishnakumar, S.**, **Prabaharan, G.**, **Sathiyabama Alias Priyanka, T.**, **Magesh, N.S.**, **Godson, P.S.** and **Srinivasalu, S.** (2018) Macrodebris and microplastic distribution in the beaches of Rameswaram Coral Island, Gulf of Mannar, Southeast coast of India: A first report. *Mar. Pollut. Bull.*, **137**, 610–616.

Vila-Concejo, A., **Harris, D.L.**, **Power, H.E.**, **Shannon, A.M.** and **Webster, J.M.** (2014) Sediment transport and mixing depth on a coral reef sand apron. *Geomorphology*, **222**, 143–150.

Wild, C., **Huettel, M.**, **Klueter, A.**, **Kremb, S.G.**, **Rasheed, M.Y.M.** and **Jørgensen, B.B.** (2004) Coral mucus functions as an energy carrier and particle trap in the reef ecosystem. *Nature*, **428**, 66–70.

Willoughby, N.G., **Sangkoyo, H.** and **Lakaseru, B.O.** (1997) Beach litter: an increasing and changing problem for Indonesia. *Mar. Pollut. Bull.*, **34**, 469–478.

Woodall, L.C., **Sanchez-Vidal, A.**, **Canals, M.**, **Paterson, G.L.J.**, **Coppock, R.**, **Sleight, V.**, **Calafat, A.**, **Rogers, A.D.**, **Narayanaswamy, B.E.** and **Thompson, R.C.** (2014) The deep sea is a major sink for microplastic debris. *R. Soc. Open Sci.*, **1**, 140317.

Wyrtki, K. (1962) Physical Oceanography of the Southeast Asian Waters By Klaus Wyrtki NAGA Report Volume 2. Scientific Results of Marine Investigations of the South China Sea and the Gulf of Thailand, 1959–1961. S.I.O., La Jolla, Calif., 1961. *J. Mar. Biol. Assoc. United Kingdom*, **42**, 707.

Zalasiewicz, J., **Waters, C.N.**, **Ivar do Sul, J.A.**, **Corcoran, P.L.**, **Barnosky, A.D.**, **Cearreta, A.**, **Edgeworth, M.**, **Gałuszka, A.**, **Jeandel, C.**, **Leinfelder, R.**, **McNeill, J.R.**, **Steffen, W.**, **Summerhayes, C.**, **Wagreich, M.**, **Williams, M.**, **Wolfe, A.P.** and **Yonan, Y.** (2016) The geological cycle of plastics and their use as a stratigraphic indicator of the Anthropocene. *Anthropocene*, **13**, 4–17.

Zettler, E.R., **Mincer, T.J.** and **Amaral-Zettler, L.A.** (2013) Life in the “Plastisphere”: Microbial Communities on Plastic Marine Debris. *Environ. Sci. Technol.*, **47**, 7137–7146.

Zhang, L., **Zhang, S.**, **Wang, Y.**, **Yu, K.** and **Li, R.** (2019) The spatial distribution of microplastic in the sands of a coral reef island in the South China Sea: Comparisons of the fringing reef and atoll. *Sci. Total Environ.*, **688**, 780–786.

Chapter 5

General Conclusions and Outlook

5 General conclusions and outlook

5.1 Conclusions

The reef platforms of Kepulauan Seribu represent the shallow water, photozoan-dominated part of a humid equatorial carbonate system. The characteristic of their surface sediments are distinct from most other carbonate systems and likely are representative for many SE Asian reef systems affected by river runoff.

Kepulauan Seribu reef platforms are largely composed of biogenic debris from corals and molluscs, with minor components include benthic foraminifers, echinoderms, red algae and the green algae *Halimeda*. Non-skeletal grains are very rare, restricted to faecal pellets and aggregates due to cementation by red algae or serpulids. Statistical analysis based on texture and composition reveal four sedimentary facies in the shallow waters (< 20m) of the Kepulauan Seribu: coral grainstone, coral packstone/grainstone, coral-mollusc packstone and mollusc wackestone. The occurrence of mollusc wackestone in the lagoon is controlled by water depth, while the sand apron and reef front do not show significant facies separation with water depth. Environmental facies maps were derived from remote sensing data. The sand apron can be subdivided into three facies with either no, sparse, or dense seagrass cover. One facies is further characterized by active coral growth. The deeper water zone can be separated into a shallow and a deep subtidal part of lagoons and platform margins. Distribution is therefore mainly controlled by water depth, density of seagrass cover and coral abundance. The satellite derived environmental facies correlated only in the lagoon directly with sedimentary facies. No direct correlation of environmental facies to sedimentary facies exists in the sand apron due to the heterogeneity and complexity of the environment.

The dominant mineral phase in Kepulauan Seribu is aragonite, mainly contributed from corals and to a lesser degree by molluscs. LMC and HMC occur in fairly similar amounts in all facies. Bivalves (calcitic and bimineralic) and some rotaliid foraminifers (e.g. *Amphistegina* and *Elphidium*) contribute to LMC. Most red algae (e.g. *Amphiroa*), echinoderms, and benthic foraminifers (e.g. *Calcarina* and *Operculina*) are important sources for HMC. Small amounts of siliciclastic minerals (quartz and smectite) are preferentially deposited in deeper waters below the wave base. This shows that despite its relatively isolated position, Kepulauan Seribu is affected by sediment laden river runoff.

The main mineralogical difference between carbonates from Kepulauan Seribu and most other reefal systems in the tropic western Atlantic and Indo Pacific Warm Pool area is the widespread presence of > 10% LMC content in the shallow water sediment. The LMC is contributed by organisms that are not or less light dependent (bivalves and some rotaliid foraminifers) and therefore can thrive under oligophotic conditions. The suspended particulate matter from terrestrial runoff likely limits the depth of the euphotic zone. This is reflected in the deposition of foramol facies below a depth of ~28m (Jordan, 1998), but seems to already affect the sediments in the upper 20m. Compared to similar foramol facies from higher latitudes, the Mg-content in HMC components from Kepulauan Seribu is much higher due to the different water temperature between both regions.

The $\delta^{13}C$ signature of carbonates from Kepulauan Seribu is considerably more negative compared to nearly all other platform and reef systems. This is likely due to the combination of low $\delta^{13}C_{DIC}$ in surface waters and the lack of green algal grains and inorganically precipitated carbonates. Carbonates from Kepulauan Seribu are also characterized by much lower $\delta^{18}O$ values compared to other carbonate systems, due to high sea surface temperatures and low $\delta^{18}O_w$ in the Java Sea. The relatively low $\delta^{18}O$ of benthic foraminifers and bivalves from Kepulauan Seribu shows that the oxygen isotope signature can be used to distinguish foramol facies from oligophotic equatorial carbonates and cool water carbonates in the rock record.

Recently, microplastics are present as sedimentary component in Kepulauan Seribu reef platforms. The source of microplastics contamination is related to marine and local, coastal anthropogenic factors. Abundance of microplastic in sediment is controlled to some extend by the proximity to the source area of larger plastic debris. Processes of microplastics transport and accumulation are thought to be similar to that of fine siliciclastic grains in the reef system. Microplastics are partly winnowed from high energy environment of the reef system and accumulate in the low energy environment, which emphasizes that hydrodynamic controls are important for microplastics distribution. However, microplastic contamination was also found in high energy environments such as the beach, sand apron and reef crest. One of the mechanisms that allows buoyant microplastics to sink to the seafloor is density modification through biofouling. In the sand apron, bed armoring and interlocking effects could hinder entrainment and resuspension of microplastics. Entanglement of fibers with carbonate grains also contributes to an interlocking effect.

In Kepulauan Seribu, microplastics are not only present in the surface layer but down to a depth of 7 cm. Transport of microplastics to deeper sediment layers likely is controlled by bioturbation. Microplastics below a depth of 3.5 cm is unlikely to be remobilized from subtidal sediments under modal weather conditions. Subtidal environments are therefore considered to be a permanent sink for microplastics in equatorial reef systems that are not affected by high energy events, such as tropical cyclones. For this reason, microplastics in subtidal reef environments from the equatorial zone can be a good practical indicator of Anthropocene strata.

5.2 Outlook

Surface sediment data has shown that equatorial carbonates from SE Asia are different from their subtropical counterparts and therefore should be re-examined as distinct depositional systems. A potential improvement for modern analogues of buried carbonate systems in SE Asia could be made by incorporating 'morphometric' analysis. Size and shape, i.e. so called 'morphometric' analysis is a useful tool for facies prediction in newly explored areas and for conditioning geologic and reservoir models (Purkis *et al.*, 2012, 2015). Acquiring and incorporating seismic reflection and GIS mapping therefor offer a better quantitative understanding of morphometric patterns within modern carbonate depositional systems.

On a broader context, this study could be expanded by studying physical processes that governs dynamics of coral sands in Kepulauan Seribu with respect to prevailing wind and wind-generated wave. Basic understanding of many physical processes can be initiated by observing the displacement or changes of position of any related features with respect to its spatial setting. Moreover, morphostratigraphic analysis based on core data also deemed useful to understand the reef island formation in relation to reef platform development and mid-Holocene sea level rise (Kench *et al.*, 2012). Kepulauan Seribu as well as other low-lying reef islands are subject to erosion, shoreline change, and sea level rise. The study will provide a rich information source to reconsider landuse planning in the context of climate change adaptation and even develop essential recovery programs for the region.

This study has filled in the knowledge gap related to process-based sedimentology with regard to transport, deposit, and burial of microplastics in reef environments. An improvement of the methodology on microplastic polymer identification could enhance our understanding of how microplastic may enter marine systems. The nature of the entry-point is critical to know how terrestrially sourced microplastic are transferred to marine sediment (Kane & Clare, 2019).

This study proposed that microplastics in subtidal reef environments from the equatorial zone can be a good practical indicator of Anthropocene strata. A study on the physical mechanism of sediment transport on a subtidal sand apron is important to improve our understanding of microplastics dispersion and accumulation in the reef systems. An investigation of sediment mixing depth can be performed over intensive field campaigns which covers both spring and neap tides, including measurements of waves, currents, and suspended sediment.

This study also highlights the presence of phthalate (a common group of plastic additives) in the reef sediment, which demonstrates that contaminants associated with microplastics could become bioavailable to corals after ingestion. A major improvement can be undertaken, considering that field studies of microplastics in the marine systems are limited. Investigation of phthalate presence in scleractinian corals (e.g. *Acropora*) in reef environments can be beneficial, as the presence of phthalates in coral tissues can be used as an indicator for microplastic contaminants. The study will therefor raise our awareness, since microplastics poses an additional threat to corals and their ability as framework builders in reef systems.

References

Jordan, C.F. (1998) The Sedimentology of Kepulauan Seribu: A Modern Patch Reef Complex in the West Java Sea, Indonesia. *Indones. Pet. Assoc.*, 1–81.

Kane, I.A. and **Clare, M.A.** (2019) Dispersion, Accumulation, and the Ultimate Fate of Microplastics in Deep-Marine Environments: A Review and Future Directions. *Front. Earth Sci.*, **7**, 80.

Kench, P.S., **Smithers, S.G.** and **McLean, R.F.** (2012) Rapid reef island formation and stability over an emerging reef flat: Bewick cay, northern Great Barrier Reef, Australia. *Geology*, **40**, 347–350.

Purkis, S., **Casini, G.**, **Hunt, D.** and **Colpaert, A.** (2015) Morphometric patterns in Modern carbonate platforms can be applied to the ancient rock record: Similarities between Modern Alacranes Reef and Upper Palaeozoic platforms of the Barents Sea. *Sediment. Geol.*, **321**, 49–69.

Purkis, S.J., **Harris, P.M.** and **Ellis, J.** (2012) Patterns of Sedimentation In the Contemporary Red Sea As An Analog for Ancient Carbonates In Rift Settings. *J. Sediment. Res.*, **82**, 859–870.

Supplementary information

Supplement 2-1. Sediment grain size and sorting. Sorting: MS = moderately sorted, PS = poorly sorted, VPS = very poorly sorted.

Sampel	Latitude	Longitude	Water Depth (m)	< 125 µm (%)	125-250 µm (%)	250-500 µm (%)	0.5-1 mm (%)	1-2 mm (%)	> 2mm (%)	mean grainsize (µm)	sorting (µm)	
Panggang Island												
MPG 11C	-5.7467	106.6033	0.5	7.3	29.3	13.9	12.8	12.7	23.9	551	3.66	PS
MPG 11E	-5.7463	106.6032	0.3	9.7	25.5	17.5	12.4	13.6	21.3	525	3.99	PS
MPG 11I	-5.7459	106.6030	1.2	14.6	27.3	19.6	17.7	20.1	0.8	371	3.65	PS
MPG 11K	-5.7457	106.6030	0.7	21.2	22.8	13.8	15.7	13.7	12.9	313	5.59	VPS
MPG 11O	-5.7453	106.6027	0.5	4.7	18.4	21.2	18.4	14.5	22.9	640	2.92	PS
MPG 12A	-5.7483	106.5978	1.6	4.5	36.0	29.2	6.1	5.6	18.5	467	3.02	PS
MPG 12F	-5.7476	106.5977	0.5	12.4	20.6	17.4	20.3	15.9	13.4	499	4.05	VPS
MPG 12K	-5.7468	106.5977	0.7	31.1	19.9	14.4	14.7	12.3	7.6	191	6.51	VPS
MPG 12M	-5.7465	106.5977	0.4	25.5	16.7	12.1	14.4	10.5	20.8	307	6.79	VPS
MPG 12O	-5.7463	106.5977	0.4	25.0	17.8	14.6	12.1	10.2	20.2	300	6.70	VPS
MPG 14C	-5.7485	106.5980	2	24.0	22.7	14.2	15.4	10.7	13.0	267	6.05	VPS
MPG 14E	-5.7484	106.5980	3	20.4	20.4	17.5	14.5	14.1	13.1	332	5.44	VPS
MPG 21F	-5.7425	106.5885	0.5	6.3	14.6	19.1	20.5	14.0	25.5	680	3.26	PS
MPG 21G	-5.7424	106.5888	0.3	4.9	12.7	17.6	26.2	19.3	19.3	712	2.75	PS
MPG 21H	-5.7424	106.5892	0.4	2.5	16.9	10.7	18.8	16.2	34.9	818	2.85	PS
MPG 21P	-5.7417	106.5915	0.5	9.9	23.6	18.7	17.7	13.2	16.9	519	3.93	PS
MPG 22C	-5.7396	106.5933	0.6	4.9	19.5	21.2	16.7	16.5	21.2	623	2.93	PS
MPG 22E	-5.7400	106.5936	0.5	13.4	21.2	13.2	19.4	16.7	16.1	529	4.29	VPS
MPG 22I	-5.7411	106.5941	0.5	12.3	31.2	20.1	24.8	11.5	0.1	335	3.18	PS
MPG 23A	-5.7436	106.5864	21	4.4	16.8	25.8	20.9	17.2	14.9	598	2.75	PS
MPG 23C	-5.7435	106.5865	15	5.0	15.3	17.0	19.7	17.0	25.9	714	2.91	PS
MPG 23E	-5.7435	106.5865	12	17.8	18.1	13.9	16.4	13.5	20.3	456	5.14	VPS
MPG 24E	-5.7388	106.5929	15	14.9	21.2	18.7	14.8	15.6	14.9	469	4.37	VPS
MPG 24F	-5.7388	106.5929	12	23.9	25.6	11.1	12.7	9.5	17.2	276	6.40	VPS
MPG 31B	-5.7382	106.6065	0.7	2.0	19.8	30.9	20.0	10.7	16.6	579	2.76	PS
MPG 31C	-5.7384	106.6063	0.5	0.4	23.3	21.4	20.0	18.4	16.4	619	2.76	PS
MPG 31D	-5.7386	106.6061	0.5	1.5	19.4	21.7	16.2	21.5	19.6	674	2.77	PS
MPG 31J	-5.7377	106.6069	19	5.5	15.5	19.5	18.5	20.6	20.4	675	3.00	PS
MPG 31L	-5.7378	106.6069	15	3.6	13.8	21.2	21.7	16.1	23.6	721	2.76	PS
MPG 31N	-5.7379	106.6068	12	3.9	20.9	23.8	23.2	17.4	10.8	540	2.67	PS
MPG 32A	-5.7450	106.6003	4	30.3	21.5	15.6	20.1	12.1	0.4	172	5.57	VPS
MPG 32D	-5.7451	106.5977	3	40.4	13.5	13.0	15.6	10.0	7.5	152	7.14	VPS
MPG 32K	-5.7422	106.5950	10	41.7	15.9	8.9	10.0	7.5	16.0	174	8.53	VPS
MPG 32M	-5.7417	106.5949	6	50.8	15.3	12.5	15.0	4.4	2.1	96	6.23	VPS
MPG 33D	-5.7431	106.6000	10	71.4	6.5	9.3	10.2	1.8	0.7	53	5.67	VPS
MPG 33G	-5.7435	106.5997	8	74.7	8.4	9.7	5.1	1.4	0.8	44	5.04	VPS
MPG 33J	-5.7426	106.6004	7	29.7	16.8	12.9	12.1	12.4	16.1	248	7.28	VPS
MPG 41G	-5.7403	106.5898	1.2	3.7	12.0	33.0	19.2	13.0	19.1	654	2.66	PS
MPG 41I	-5.7409	106.5916	0.5	8.8	17.9	17.7	20.7	13.7	21.2	600	3.79	PS
MPG 41O	-5.7417	106.5937	0.5	21.2	26.1	15.5	15.2	13.4	8.6	274	5.22	VPS
MPG 42D	-5.7472	106.5935	15	51.1	16.0	10.9	9.5	5.2	7.3	101	7.10	VPS
MPG 42G	-5.7470	106.5936	10	31.0	17.0	14.2	13.3	10.1	14.4	226	7.24	VPS
MPG 42L	-5.7402	106.5889	18	18.2	24.7	14.9	14.1	13.0	15.2	380	5.06	VPS
MPG 42O	-5.7402	106.5891	15	21.0	24.6	8.9	8.6	13.9	23.0	350	5.95	VPS
MPG 42R	-5.7402	106.5892	12	21.4	23.2	13.3	16.5	13.4	12.2	305	5.56	VPS
Pramuka Island												
PR 21A	-5.7499	106.6092	1.2	9.0	20.9	29.2	10.4	16.0	14.5	492	3.69	PS
PR 21C	-5.7499	106.6099	0.8	10.5	29.0	15.2	14.6	10.3	20.5	499	4.10	VPS
PR 21E	-5.7498	106.6106	0.5	11.4	14.9	15.0	15.6	15.8	27.3	639	4.19	VPS
PR 21G	-5.7496	106.6111	0.4	12.2	15.9	12.5	19.9	12.2	27.3	617	4.30	VPS
PR 21I	-5.7496	106.6115	0.4	12.8	15.0	15.3	16.6	15.7	24.7	602	4.33	VPS
PR 22A	-5.7514	106.6151	1.5	5.2	18.2	29.5	13.6	9.9	23.7	582	2.99	PS
PR 22C	-5.7511	106.6149	1	10.2	15.2	15.5	17.7	12.8	28.7	646	4.03	VPS
PR 22E	-5.7507	106.6148	0.8	9.7	16.8	15.6	22.6	14.9	20.4	605	3.90	PS
PR 22G	-5.7503	106.6147	0.6	13.2	18.2	13.8	18.8	17.7	18.3	557	4.31	VPS
PR 22I	-5.7500	106.6145	0.4	8.7	19.8	12.2	16.9	15.2	27.3	648	3.85	PS
PR 22K	-5.7496	106.6142	0.4	10.4	15.5	14.5	20.5	17.6	21.5	623	3.99	PS
PR 22M	-5.7493	106.6140	0.3	1.0	28.2	15.4	16.2	18.5	20.7	626	2.90	PS
PR 22O	-5.7490	106.6138	0.3	9.0	22.5	12.5	18.0	19.8	18.3	589	3.81	PS
PR 23A	-5.7470	106.6198	1.5	1.3	21.5	29.2	19.0	10.9	18.1	585	2.78	PS
PR 23C	-5.7470	106.6193	1	6.5	26.9	16.9	15.3	10.8	23.7	561	3.45	PS
PR 23E	-5.7469	106.6186	0.8	0.6	18.3	59.1	16.4	1.4	4.1	372	1.80	MS
PR 23G	-5.7469	106.6182	0.6	6.8	18.8	18.0	21.3	10.1	25.1	626	3.44	PS
PR 23I	-5.7468	106.6177	0.6	4.0	20.6	14.9	23.4	14.3	22.8	656	2.92	PS
PR 23K	-5.7467	106.6171	0.4	8.2	17.0	15.9	16.8	13.8	28.1	658	3.74	PS
PR 23M	-5.7466	106.6165	0.3	13.8	17.4	16.0	16.5	18.0	18.3	544	4.37	VPS
PR 23O	-5.7465	106.6158	0.3	5.1	23.9	13.7	17.3	21.1	18.8	622	2.98	PS
PR 24A	-5.7403	106.6150	1.5	14.2	17.1	13.8	18.3	18.0	18.6	554	4.41	VPS

PR 24C	-5.7407	106.6150	1	1.9	11.4	39.2	16.5	7.4	23.6	654	2.63	PS
PR 24E	-5.7410	106.6151	0.8	8.7	16.7	21.7	16.7	20.3	16.0	576	3.66	PS
PR 24G	-5.7414	106.6150	0.6	9.9	17.7	20.4	24.6	12.4	15.0	541	3.80	PS
PR 24I	-5.7418	106.6150	0.4	8.9	18.9	16.1	17.2	16.9	22.1	611	3.82	PS
PR 31A	-5.7405	106.6147	5	11.5	22.8	21.0	21.2	15.8	7.7	437	3.68	PS
PR 31C	-5.7400	106.6147	15	24.2	28.9	17.3	7.6	4.9	17.0	263	6.45	VPS
PR 31E	-5.7396	106.6147	15	15.4	29.1	15.2	6.7	13.1	20.6	445	4.58	VPS
PR 32A	-5.7496	106.6091	5	18.0	29.4	15.1	6.2	5.3	26.0	379	5.27	VPS
PR 32C	-5.7498	106.6086	12	20.2	20.3	22.7	15.7	8.6	12.5	312	5.20	VPS
PR 32E	-5.7500	106.6081	20	4.4	15.5	17.9	14.3	15.3	32.6	767	2.90	PS
Semak Daun Island												
SD 11A	-5.7321	106.5666	1	2.8	18.5	25.1	15.5	15.2	22.9	642	2.84	PS
SD 11C	-5.7320	106.5668	0.8	5.2	15.2	16.3	25.9	29.3	8.0	622	2.68	PS
SD 11E	-5.7318	106.5669	0.7	12.3	23.2	15.6	17.2	13.3	18.5	518	4.25	VPS
SD 11G	-5.7317	106.5671	0.6	14.1	20.0	15.4	22.5	18.9	9.1	472	4.03	VPS
SD 11I	-5.7317	106.5673	0.5	10.1	19.5	14.4	20.5	21.5	14.0	562	3.82	PS
SD 11K	-5.7316	106.5674	0.4	9.9	27.4	14.7	13.7	19.9	14.5	501	3.88	PS
SD 11M	-5.7316	106.5675	0.4	9.8	18.2	14.0	24.0	20.9	13.2	567	3.74	PS
SD 11O	-5.7315	106.5677	0.5	11.8	20.1	14.3	22.1	19.8	11.9	520	3.95	PS
SD 12A	-5.7323	106.5664	2	2.4	19.6	19.2	9.0	16.7	33.0	779	2.90	PS
SD 12C	-5.7325	106.5661	8	7.9	21.7	13.5	13.8	16.0	27.1	641	3.73	PS
SD 12E	-5.7327	106.5659	16	25.0	23.8	19.8	15.1	10.0	6.2	212	5.40	VPS
SD 13A	-5.7285	106.5729	5	26.9	23.2	12.0	18.2	10.5	9.2	214	6.07	VPS
SD 13C	-5.7283	106.5736	10	40.5	22.6	17.0	9.4	6.0	4.5	120	6.13	VPS
SD 13E	-5.7280	106.5743	15	65.2	15.3	11.3	6.8	1.4	0.1	54	5.08	VPS
SD 14A	-5.7227	106.5989	15	75.5	9.4	9.1	4.9	1.1	0.0	42	4.77	VPS
SD 14C	-5.7228	106.5999	10	78.2	9.0	7.0	4.7	1.0	0.0	38	4.57	VPS
SD 14E	-5.7230	106.5839	5	50.5	10.8	9.8	8.1	3.0	17.9	143	9.24	VPS
SD 15A	-5.7275	106.6048	1.8	0.7	5.4	45.2	5.4	5.4	37.8	702	2.49	PS
SD 15C	-5.7275	106.6048	1.7	2.5	9.2	33.2	14.4	9.0	31.7	745	2.65	PS
SD 15E	-5.7274	106.6047	1.5	2.2	22.5	48.5	10.6	7.8	8.4	412	2.33	PS
SD 15G	-5.7272	106.6046	1	3.6	17.5	22.2	14.7	11.7	30.2	690	2.90	PS
SD 15I	-5.7270	106.6044	0.7	5.9	16.9	16.4	14.5	13.4	32.9	721	3.25	PS
SD 15K	-5.7268	106.6043	0.5	7.8	20.0	13.5	11.7	10.7	36.3	694	3.76	PS
SD 15M	-5.7267	106.6041	0.5	6.6	26.6	13.1	15.4	14.1	24.3	597	3.48	PS
SD 15O	-5.7266	106.6039	0.4	10.8	22.2	14.2	18.8	18.5	15.5	543	3.99	PS

Supplement 2-2. Sediment composition of carbonate facies in Kepulauan Serib including sediment texture and environmental facies. Dunham textures: GST = grainstone, PST = packstone, WST = wackestone. Environmental facies: DSPL/PM = deeper subtidal part lagoon/platform margin, SSPL/PM = shallower subtidal part lagoon/platform margin, SRM/SC = subtidal reef margin/sparse coral, SAWDSG = sand apron with dense sea grass, SAWSSG = sand apron with sparse sea grass, SAWSG = sand apron without sea grass.

Sample	Coral (%)	Red Algae (%)	*Halimeda* (%)	Mollusk (%)	Foram (%)	Echinoderm (%)	Non Skeletal (%)	other (%)	Fines (%)	Dunham	Environmental Facies	water depth (m)
Coral Grainstone												
MPG 1-2A	52.5	10.5	1.3	11.9	7.6	5.7	4.0	1.9	4.5	GST	-	1.6
MPG 2-1G	58.3	3.5	0.3	22.8	7.9	2.2	0	0	4.9	GST	SAWSSG	0.3
MPG 2-4E	51.6	3.4	0.9	17	6.8	4	0	1.4	14.9	PST	-	15
MPG 3-1C	58.1	3.3	4	21.6	7.6	4	0	1	0.4	GST	SAWSSG	0.5
PR 22A	54.2	2.2	8.9	17.8	9.2	2.5	0	0	5.2	GST	SAWDSG	1.5
PR 22E	56.1	0.6	7.2	14.4	10.6	1.4	0	0	9.7	GST	SAWSSG	0.8
PR 22I	54.5	1.1	10.9	17.6	5.3	2	0	0	8.7	GST	SAWSG	0.4
PR 22M	70	1.2	3.3	18.2	5.1	1.2	0	0	1	GST	SAWSG	0.3
PR 23A	56.6	8.6	4.9	9.2	18.4	1	0	0	1.3	GST	-	1.5
PR 23M	53.4	1.4	4.5	17	6.2	3.7	0	0	13.8	PST	SAWDSG	0.3
PR 24A	53.7	5.7	3.2	13.6	8.4	1.2	0	0	14.2	PST	SRM/SC	1.5
PR 24I	63.4	1.1	0.9	20.9	1.7	2.9	0.3	0	8.9	GST	SAWDSG	0.4
PR 32E	66.4	3.2	3.7	14.1	6.4	1.6	0.3	0	4.4	GST	-	20
SD 11A	71.2	4.4	3.8	10.4	5.5	1.9	0	0	2.8	GST	SAWDSG	1
SD 11C	59.7	3.1	3.8	17	5.2	5.9	0	0	5.2	GST	SAWDSG	0.8
SD 11I	53.8	1.7	6.4	15.6	7.8	4.6	0	0	10.1	PST	SAWSG	0.5
SD 11M	57.2	0	1.2	19.1	3.9	7.7	1.2	0	9.8	GST	SAWSSG	0.4
SD 11O	60.9	1.5	0.9	16.5	2.9	5.3	0.3	0	11.8	PST	SAWSG	0.5
SD 12A	76.6	1.9	2.2	6.9	6.9	3	0	0	2.4	GST	-	2
SD 15A	58.8	2.9	5.1	23.8	6.4	2.2	0	0	0.7	GST	SAWSG	1.8
SD 15C	61.5	2.1	4.2	21.2	4.9	3.5	0	0	2.5	GST	SAWSG	1.7
SD 15I	61	1.1	4.7	19	5.2	3	0	0	5.9	GST	SAWSSG	0.7
mean	59.5	2.9	3.9	16.6	6.8	3.2	0.3	0.2	6.5			2.4
STDDEV	6.6	2.5	2.7	4.4	3.3	1.8	0.9	0.5	4.6			5.0
min - max											0.3	20
Coral Packstone/Grainstone												
MPG 1-1C	45.4	0	2.5	21	2.5	5.6	1.9	13.9	7.3	GST	SAWSSG	0.5
MPG 1-1E	48.2	1.5	6.6	25.6	2.1	4.2	0	2.1	9.7	GST	SAWDSG	0.3
MPG 1-1O	42.9	3.8	5.4	21.6	4.1	3.2	2.9	11.4	4.7	GST	SAWSSG	0.5
MPG 1-2F	49.7	0	0	25.4	5.3	6.4	0	0.9	12.4	PST	SAWDSG	0.5
MPG 2-1F	52.4	3.4	2.2	27.2	5.3	3.1	0	0	6.3	GST	SAWSSG	0.5
MPG 2-1H	55.2	2.6	3.6	27.6	4.2	4.2	0	0	2.5	GST	SAWSSG	0.4
MPG 2-1P	50.4	2.7	6	26.7	1.8	2.4	0	0	9.9	GST	SAWSSG	0.5
MPG 2-2C	53.9	1.9	2.5	29.8	3.8	3.2	0	0	4.9	GST	SAWSSG	0.6
MPG 2-2E	46.2	0.9	1.7	32.6	3.2	2	0	0	13.4	PST	SAWSSG	0.5
MPG 2-2I	52.6	2	0	30.1	1.5	1.5	0	0	12.3	PST	SAWDSG	0.5
MPG 2-3A	49.4	3.5	7.6	22.9	6.4	5.7	0	0	4.4	GST	SRM/SC	21
MPG 2-3C	50.6	5.7	8.5	22.8	4.1	3.2	0	0	5	GST	-	15
MPG 2-3E	44.6	6	3.6	20.5	3.3	4.1	0	0	17.8	PST	-	12
MPG 3-1B	42.5	6.2	1.6	21.9	10.8	5.9	0	9.1	2	GST	SAWDSG	0.7
MPG 3-1D	54.2	3.6	3.6	26.3	8.5	2.3	0	0	1.5	GST	SAWSSG	0.5
MPG 3-1J	48.8	4.4	0	29.6	4.4	5.7	0	1.6	5.5	GST	SRM/SC	19
MPG 3-1L	56.2	5.1	2.6	25.7	4.2	1.3	0	1.3	3.6	GST	-	15
MPG 3-1N	56.4	3.5	0	26.3	4.8	4.5	0	0.6	3.9	GST	-	12
MPG 4-1G	49.8	2.9	1.6	32.1	6.7	3.2	0	0	3.7	GST	SAWSSG	1.2
MPG 4-1I	48.6	2.7	5.5	28	4.9	1.5	0	0	8.8	GST	SAWSSG	0.5
PR 21A	48.9	3.8	7.3	28.1	3	0	0	0	9	GST	SAWSSG	1.2
PR 21C	48.9	1.8	9.7	22	3.9	3.1	0	0	10.5	PST	SAWDSG	0.8
PR 21E	46.4	2	6.6	27.6	2.8	2.6	0.6	0	11.4	PST	SAWSG	0.5
PR 21G	46.6	1	7.4	25.2	5.4	2.2	0	0	12.2	PST	SAWSSG	0.4
PR 21I	51.8	3.3	6.8	22	2.5	0.8	0	0	12.8	PST	SAWDSG	0.4
PR 22C	48.1	2.4	7.8	18.4	11.6	1.4	0	0	10.2	PST	SAWDSG	1
PR 22G	51.6	1.4	6	21.8	4	2	0	0	13.2	PST	SAWSG	0.6
PR 22K	44.3	0.7	9.1	28.1	5.4	1	1	0	10.4	PST	SAWSSG	0.4
PR 22O	56.2	1.1	3.7	26.2	2.4	1.3	0	0	9	GST	SAWDSG	0.3

PR 23C	38.5	1.9	13.1	22.7	17.4	0	0	0	6.5	GST	SAWDSG	1
PR 23E	49	2.6	5.1	20.8	19.9	1.9	0	0	0.6	GST	SAWDSG	0.8
PR 23G	46.6	1.2	9.3	24.2	8.7	3.1	0	0	6.8	GST	SAWDSG	0.6
PR 23I	50.1	2.8	7.3	23.2	8.3	4.3	0	0	4	GST	SAWSSG	0.6
PR 23K	47.8	0.9	12.6	22	7.3	1.2	0	0	8.2	GST	SAWSG	0.4
PR 23O	54.2	2	3.1	25.7	7.3	2.5	0	0	5.1	GST	SAWSSG	0.3
PR 24C	58.7	2.2	5.2	28	1.9	2.2	0	0	1.9	GST	SAWSSG	1
PR 24E	54.3	1.9	5.9	24.9	2.9	1.3	0	0	8.7	GST	SAWDSG	0.8
PR 24G	53.4	1.8	4.2	27.9	2.1	0.6	0	0	9.9	GST	SAWSSG	0.6
PR 31A	44.1	6.8	5.2	20.7	9.5	2.2	0	0	11.5	PST	-	4
PR 32A	50.1	2.8	3.8	22.3	1.5	1.5	0	0	18	PST	-	3
PR 32C	48.9	2.4	6.5	16.5	3.4	2.1	0	0	20.2	PST	-	12
SD 11E	48.6	2.4	7.4	19.3	3	5.6	1.5	0	12.3	PST	SAWSSG	0.7
SD 11G	47.6	1.8	5.5	19.3	7.5	3.9	0.4	0	14.1	PST	SAWSSG	0.6
SD 11K	46.8	2	5.1	23.3	3.9	9.1	0	0	9.9	GST	SAWSG	0.4
SD 12C	48.3	2.4	3	33.2	1.5	3.3	0.3	0	7.9	GST	-	8
SD 15E	46.9	3.6	11.6	19.5	8.9	7.3	0	0	2.2	GST	SAWDSG	1.5
SD 15G	38	2	12.1	23.3	12.4	8.6	0	0	3.6	GST	SAWSSG	1
SD 15K	48.1	0.3	4.3	21.3	10.3	7.9	0	0	7.8	GST	SAWDSG	0.5
SD 15M	44.2	3	10.1	23.1	8.6	4.4	0	0	6.6	GST	SAWSG	0.5
SD 15O	42.6	0.6	6.2	21.1	12.4	6.2	0	0	10.8	PST	SAWDSG	0.4
mean	49.0	2.5	5.5	24.5	5.8	3.3	0.2	0.8	8.3			2.9
STDDEV	4.4	1.5	3.3	3.8	4.0	2.2	0.5	2.8	4.5			5.3
min - max											0.3	21
Coral-Mollusk Packstone												
MPG 1-1I	22.2	0	8.5	35.6	3.4	4.8	3.2	7.6	14.6	PST	SAWSSG	1.2
MPG 1-1K	34.1	1.8	6	22.3	3.4	4.5	0	6.6	21.2	PST	SAWSSG	0.7
MPG 1-2K	34.9	2.1	3.9	18.4	3.2	3	0	3.4	31.1	PST	SAWDSG	0.7
MPG 1-2M	45	1	2.2	22.6	0.7	3	0	0	25.5	PST	SAWSSG	0.4
MPG 1-2O	38	1.5	1.2	25.5	4	4.7	0	0	25	PST	SAWDSG	0.4
MPG 1-4C	29.6	6.8	0	17.7	6.6	5.1	4.8	5.3	24	PST	-	2
MPG 1-4E	33.2	9.3	0	17.2	8	8	0	4	20.4	PST	-	3
MPG 2-4F	42.6	2.8	0	20	5.6	5.1	0	0	23.9	PST	-	12
MPG 3-3J	35.1	0	0.9	27.2	2.3	4.7	0	0	29.7	PST	SSPL/PM	7
MPG 4-1O	43.3	1.1	2.1	27.1	2.9	2.1	0	0.3	21.2	PST	SAWDSG	0.5
MPG 4-2G	43	3	1.1	15.4	3	3.4	0	0	31	PST	SRM/SC	10
MPG 4-2L	41.2	2.7	0.5	17.7	5.2	3.5	0	10.9	18.2	PST	SRM/SC	18
MPG 4-2O	40.8	3.7	0.5	16.3	4.5	6.6	0	6.6	21	PST	-	15
MPG 4-2R	32.7	5	0	18.3	6.8	6.5	0	9.2	21.4	PST	-	13
PR 31C	33.8	5	5.6	22.1	7.7	1.6	0	0	24.2	PST	-	15
PR 31E	38.4	6	8	24.2	6.5	1.5	0	0	15.4	PST	-	15
SD 12E	40.6	1.2	3.8	10.4	9.7	9.3	0	0	25	PST	SRM/SC	16
SD 13A	40.9	0.2	0	23.5	3.6	4.9	0	0	26.9	PST	SSPL/PM	5
mean	37.2	3.0	2.5	21.2	4.8	4.6	0.4	3.0	23.3			7.5
STDDEV	5.8	2.6	2.8	5.7	2.3	2.1	1.3	3.8	4.7			6.6
min - max											0.4	18
Mollusk Wackestone												
MPG 3-2A	8.1	0	0	23.9	1.6	2.3	3.5	30.2	30.3	PST	DSPL/PM	4
MPG 3-2D	22.4	0	0	31.8	1.2	3.2	0	1	40.4	PST	DSPL/PM	3
MPG 3-2K	7.8	0	0	31.1	3.9	5.8	2.4	7.3	41.7	PST	SSPL/PM	10
MPG 3-2M	22.8	4.4	2.8	14	2.3	3	0	0	50.8	WST	SSPL/PM	6
MPG 3-3D	0	0	0	5.7	0	0	0	22.9	71.4	WST	DSPL/PM	12
MPG 3-3G	0	0	0	17.7	0	0.8	0	6.8	74.7	WST	DSPL/PM	8
MPG 4-2D	20.4	0	0	13.9	3.3	4.1	2.3	5	51.1	WST	-	15
SD 13C	30.6	0.3	0	18.9	2.4	4.5	0	2.7	40.5	PST	DSPL/PM	10
SD 13E	9.8	0.1	0	16.8	0.3	5.2	0	2.5	65.2	WST	DSPL/PM	15
SD 14A	0.8	0	0.1	14.9	1	5.3	0	2.4	75.5	WST	DSPL/PM	15
SD 14C	2.1	0.2	0	11.8	0.4	4.8	0	2.5	78.2	WST	DSPL/PM	10
SD 14E	28.7	0.5	0.6	14.5	1.6	1.3	0	2.4	50.5	WST	SSPL/PM	5
mean	12.8	0.5	0.3	17.9	1.5	3.4	0.7	7.1	55.9			9.4
STDDEV	11.5	1.3	0.8	7.6	1.3	1.9	1.3	9.4	16.4			4.3
min - max											3	15

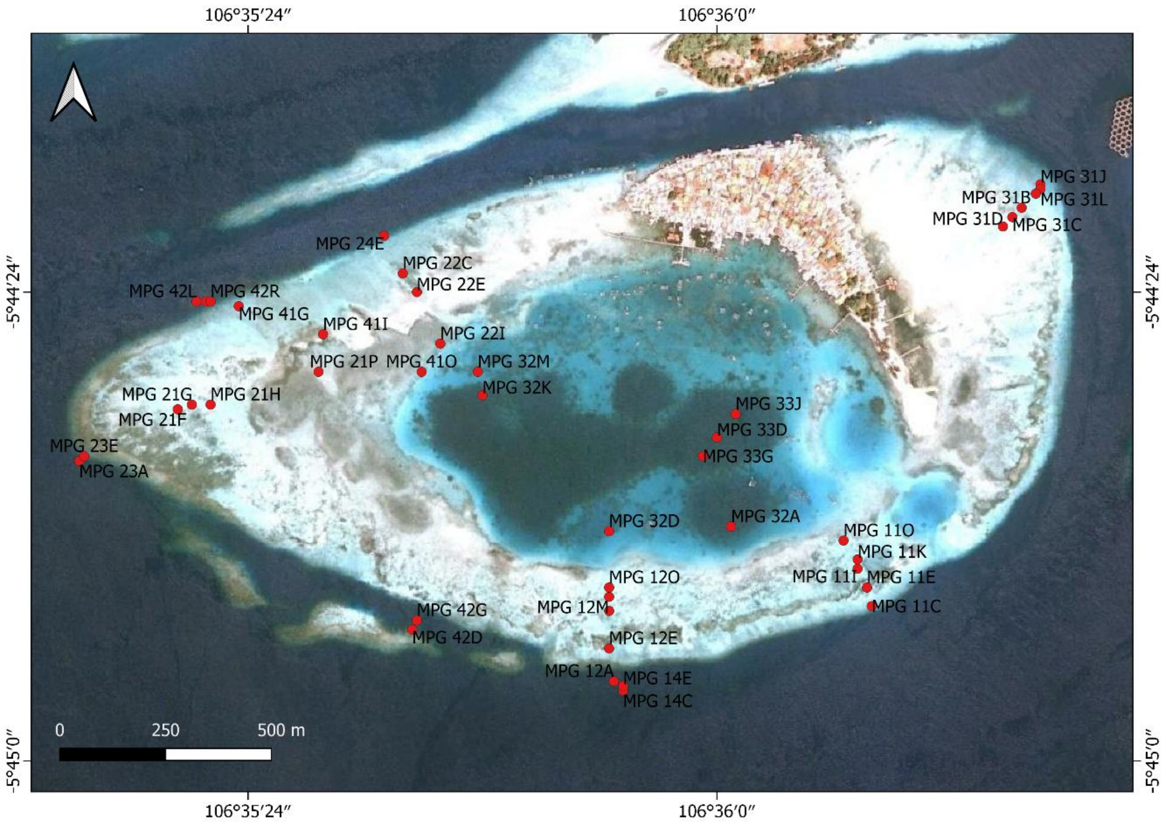

Supplement 3-1. Sampling location in Panggang reef platform, Kepulauan Seribu.

Supplement 3-2. Mineralogy of Panggang reef, Kepulauan Seribu.

Sample	Aragonite	Calcite	CalciteMg	Quartz	Smectite	d-Value	MgCO3 (mol%)
MPG 11C	83.7	9.4	5.7	0.6	0.0	3.0	12.0
MPG 11E	82.8	10.7	5.3	0.6	0.0	3.0	14.3
MPG 11I	83.4	10.3	5.3	0.5	0.0	3.0	12.3
MPG 11K	85.7	8.8	5.1	0.4	0.0	3.0	13.7
MPG 11O	82.0	10.7	6.1	0.5	0.0	3.0	13.3
MPG 12A	81.9	9.8	7.8	0.5	0.0	3.0	14.3
MPG 12E	78.9	9.4	11.3	0.5	0.0	3.0	13.3
MPG 12K	79.5	11.4	8.6	0.6	0.0	3.0	13.7
MPG 12M	80.7	10.2	8.7	0.4	0.0	3.0	14.3
MPG 12O	79.2	9.4	10.5	0.5	0.0	3.0	13.3
MPG 14C	77.6	9.3	11.2	1.3	0.0	3.0	13.0
MPG 14E	76.8	10.2	10.6	1.4	0.0	3.0	13.0
MPG 21F	72.1	14.0	12.7	0.6	0.0	3.0	14.7
MPG 21G	74.0	9.1	15.4	0.6	0.0	3.0	14.7
MPG 21H	71.6	11.6	15.9	0.5	0.0	3.0	14.7
MPG 21P	81.8	9.3	8.0	0.6	0.0	3.0	14.7
MPG 22C	82.3	7.0	9.6	0.4	0.0	3.0	14.7
MPG 22E	80.1	8.7	9.9	0.5	0.0	3.0	15.0
MPG 22I	82.4	7.0	9.0	1.2	0.0	3.0	15.3
MPG 23A	81.6	7.5	9.3	0.7	0.0	3.0	15.0
MPG 23C	82.3	7.2	8.7	0.9	0.0	3.0	14.0
MPG 23E	77.3	12.8	7.2	1.7	0.0	3.0	13.7
MPG 24E	81.7	10.7	6.2	0.7	0.0	3.0	13.7

MPG 24F	84.5	8.8	5.4	0.7	0.0	3.0	13.7
MPG 31B	86.7	6.2	5.7	0.5	0.0	3.0	15.3
MPG 31C	84.0	8.6	6.0	0.5	0.0	3.0	14.0
MPG 31D	86.6	6.4	5.7	0.5	0.0	3.0	14.3
MPG 31J	87.2	6.2	4.8	0.7	0.0	3.0	12.7
MPG 31L	87.2	6.1	5.5	0.4	0.0	3.0	14.7
MPG 31N	87.4	5.1	5.9	0.6	0.0	3.0	14.3
MPG 32A	84.4	8.6	5.9	0.5	0.0	3.0	14.7
MPG 32D	82.8	8.0	7.9	0.8	0.0	3.0	14.0
MPG 32K	80.6	10.8	7.6	0.7	0.0	3.0	12.7
MPG 32M	63.3	14.8	8.0	2.8	8.8	3.0	12.7
MPG 33D	72.5	10.6	10.0	2.2	3.8	3.0	11.7
MPG 33G	72.5	12.7	11.2	2.8	0.0	3.0	12.7
MPG 33J	76.5	10.9	8.1	1.3	2.4	3.0	13.3
MPG 41G	80.7	8.5	9.6	0.5	0.0	3.0	14.7
MPG 41I	81.6	8.2	8.9	0.6	0.0	3.0	14.0
MPG 41O	81.8	8.4	9.0	0.4	0.0	3.0	16.0
MPG 42D	81.9	7.9	7.7	1.8	0.0	3.0	13.0
MPG 42G	83.6	6.5	8.2	1.0	0.0	3.0	14.3
MPG 42L	79.4	8.8	8.7	2.1	0.0	3.0	14.0
MPG 42O	80.3	6.9	11.4	0.9	0.0	3.0	14.7
MPG 42R	81.1	9.0	8.5	0.8	0.0	3.0	13.3
MPG 33D <125µm	64.2	11.7	12.7	2.6	8.8	3.0	14.0
MPG 14C <125µm	65.5	10.9	12.7	4.2	6.7	3.0	15.3
MPG 32D <125µm	62.3	7.7	10.9	3.8	14.3	3.0	11.7
MPG 42L <125µm	62.4	8.1	11.0	4.5	11.5	3.0	14.0
MPG 33G <125µm	63.7	10.7	13.5	2.4	8.1	3.0	13.3

Supplement 3-3. $\delta^{13}C$ and $\delta^{18}O$ (‰) values of Panggang reef, Kepulauan Seribu

Sample	$\delta^{13}C$	±	$\delta^{18}O$	±
MPG 1-2A	-0.06	0.01	-4.62	0.01
MPG 1-4C	-0.84	0.01	-4.34	0.01
MPG 1-4C <125 µm	-0.45	0.01	-4.35	0.02
MPG 2-1F	0.65	0.01	-4.20	0.01
MPG 2-1G	0.73	0.01	-4.10	0.01
MPG 2-2C	0.66	0.00	-4.32	0.01
MPG 2-4E	-0.49	0.01	-4.39	0.01
MPG 3-1C	-0.20	0.00	-4.60	0.02
MPG 3-1D	-0.38	0.01	-4.78	0.01
MPG 3-1J	-1.32	0.01	-4.90	0.02
MPG 3-2A	0.70	0.00	-4.06	0.01
MPG 3-2M	-0.21	0.01	-4.12	0.02
MPG 3-3D	0.86	0.00	-3.46	0.01
MPG 3-3D <125 µm	0.81	0.01	-3.96	0.01
MPG 3-3G	0.90	0.02	-3.49	0.06
MPG 3-3G <125 µm	0.90	0.00	-3.87	0.02
MPG 4-2D	-0.71	0.01	-4.69	0.02
MPG 4-2D <125 µm	-0.42	0.01	-4.46	0.01
MPG 4-2L	-0.54	0.01	-4.42	0.02
MPG 4-2L <125 µm	-0.19	0.02	-4.34	0.05

Supplement 3-4. $\delta^{13}C$ and $\delta^{18}O$ (‰) values of Porites coral from Bidadari Island, Kepulauan Seribu

Sample	$\delta^{13}C$	$\delta^{18}O$	Sample	$\delta^{13}C$	$\delta^{18}O$	Sample	$\delta^{13}C$	$\delta^{18}O$
Bi-72	-2.5	-5.2	Bi-123	-2.3	-6.0	Bi-78	-4.1	-5.9
Bi-137	-3.1	-5.2	Bi-234	-3.5	-6.0	Bi-74	-3.7	-5.9
Bi-150	-1.9	-5.3	Bi-94	-2.6	-6.0	Bi-237	-2.1	-5.9
Bi-98	-3.3	-5.5	Bi-37	-4.0	-6.0	Bi-110	-2.4	-5.9
Bi-138	-2.7	-5.5	Bi-242	-2.3	-6.0	Bi-29	-3.8	-5.9
BI-187	-1.8	-5.5	BI-182	-2.5	-6.0	Bi-155	-2.2	-5.9
Bi-69	-3.4	-5.5	BI-174	-3.2	-6.0	Bi-249	-3.0	-5.9
Bi-245	-3.6	-5.5	Bi-60	-2.9	-6.0	Bi-313	-2.1	-5.9
Bi-135	-3.1	-5.5	BI-179	-2.8	-6.0	Bi-250	-2.9	-5.9
Bi-97	-2.6	-5.6	Bi-104	-2.1	-6.0	BI-188	-2.9	-5.9
Bi-108	-2.9	-5.6	Bi-146	-2.5	-6.0	Bi-233	-4.0	-5.9
Bi-46	-2.6	-5.6	Bi-309	-2.7	-6.0	Bi-80	-3.5	-5.9
Bi-151	-2.4	-5.6	Bi-35	-2.3	-6.0	Bi-296	-1.6	-5.9
Bi-316	-2.6	-5.6	Bi-292	-2.9	-6.0	Bi-132	-2.3	-5.9
BI-210	-2.3	-5.6	Bi-239	-2.6	-6.0	BI-189	-2.8	-5.9
Bi-47	-3.4	-5.6	Bi-25	-4.3	-6.0	Bi-86	-4.0	-5.9
Bi-75	-3.7	-5.6	Bi-298	-2.5	-6.0	Bi-103	-2.6	-5.9
Bi-77	-3.1	-5.6	Bi-240	-2.7	-6.0	Bi-50	-3.6	-5.9
BI-170	-2.3	-5.6	Bi-238	-2.4	-6.0	Bi-31	-3.2	-5.9
Bi-317	-1.8	-5.6	Bi-3	-3.6	-6.1	Bi-231	-2.9	-5.9
Bi-23	-4.1	-5.6	Bi-12	-3.8	-6.1	Bi-41	-2.9	-6.0
Bi-140	-2.9	-5.7	Bi-159	-2.9	-6.1	Bi-34	-3.5	-6.0
Bi-79	-3.9	-5.7	Bi-349	-2.8	-6.1	Bi-352	-2.4	-6.0
Bi-60	-3.2	-5.7	Bi-1	-3.9	-6.1	Bi-236	-2.2	-6.0
Bi-106	-2.1	-5.7	Bi-16	-4.2	-6.1	Bi-63	-4.5	-6.0
Bi-297	-1.7	-5.7	Bi-222	-2.1	-6.1	Bi-68	-3.9	-6.0
Bi-22	-4.4	-5.7	Bi-54	-3.7	-6.1	Bi-306	-1.6	-6.0
Bi-24	-3.7	-5.7	Bi-350	-3.8	-6.1	Bi-83	-3.1	-6.0
Bi-76	-3.6	-5.7	Bi-48	-3.4	-6.1	Bi-30	-3.5	-6.0
Bi-264	-2.6	-5.7	Bi-129	-2.6	-6.1	Bi-66	-2.5	-6.0
Bi-82	-2.3	-5.7	BI-164	-2.6	-6.1	Bi-261	-2.7	-6.0
Bi-227	-3.0	-5.7	Bi-269	-1.9	-6.1	Bi-57	-3.5	-6.0
Bi-88	-3.3	-5.7	Bi-241	-2.6	-6.1	Bi-90	-3.5	-6.0
Bi-130	-1.8	-5.7	Bi-307	-1.7	-6.1	Bi-17	-3.8	-6.0
Bi-107	-2.6	-5.7	Bi-156	-2.1	-6.1	BI-192	-2.5	-6.0
Bi-259	-2.5	-5.7	Bi-295	-2.9	-6.1	BI-180	-2.6	-6.0
Bi-232	-3.4	-5.7	Bi-225	-2.3	-6.1	Bi-15	-4.7	-6.0
BI-166	-2.6	-5.7	Bi-143	-2.5	-6.1	Bi-95	-2.7	-6.0
Bi-279	-1.7	-5.7	BI-178	-2.5	-6.1	Bi-27	-4.0	-6.0
Bi-84	-3.7	-5.7	Bi-147	-3.4	-6.1	Bi-91	-3.2	-6.0
Bi-256	-2.5	-5.7	Bi-125	-2.4	-6.1	Bi-71	-3.2	-6.0
Bi-223	-2.4	-5.7	Bi-119	-3.2	-6.1	Bi-351	-3.5	-6.0

Bi-235	-2.8	-5.7	Bi-229	-2.8	-6.1	Bi-243	-2.5	-6.0
Bi-226	-3.0	-5.8	Bi-39	-3.1	-6.1	Bi-145	-2.4	-6.3
Bi-87	-3.4	-5.8	Bi-257	-2.3	-6.1	Bi-348	-2.8	-6.3
Bi-255	-2.6	-5.8	Bi-19	-2.7	-6.1	BI-177	-2.5	-6.3
Bi-105	-2.1	-5.8	Bi-294	-2.3	-6.2	Bi-36	-3.6	-6.3
Bi-149	-2.4	-5.8	Bi-304	-2.1	-6.2	Bi-283	-2.8	-6.4
Bi-118	-2.6	-5.8	Bi-284	-2.4	-6.2	Bi-20	-3.9	-6.4
Bi-13	-4.2	-5.8	Bi-312	-1.8	-6.2	Bi-282	-3.1	-6.4
Bi-248	-2.7	-5.8	Bi-288	-2.3	-6.2	Bi-114	-3.0	-6.4
Bi-310	-2.4	-5.8	Bi-26	-3.8	-6.2	BI-198	-3.3	-6.4
Bi-49	-4.2	-5.8	Bi-122	-3.1	-6.2	Bi-56	-4.2	-6.4
Bi-318	-1.9	-5.8	Bi-116	-2.3	-6.2	Bi-230	-2.5	-6.4
Bi-148	-3.6	-5.8	Bi-65	-2.5	-6.2	Bi-299	-2.8	-6.4
Bi-102	-2.9	-5.8	Bi-273	-3.3	-6.2	Bi-128	-3.7	-6.4
Bi-262	-2.4	-5.8	BI-176	-2.5	-6.2	Bi-347	-3.3	-6.4
Bi-85	-3.8	-5.8	BI-184	-2.8	-6.2	Bi-109	-3.2	-6.4
Bi-131	-1.8	-5.8	Bi-267	-2.8	-6.2	Bi-8	-4.2	-6.4
Bi-254	-2.8	-5.8	Bi-271	-2.2	-6.2	Bi-51	-3.5	-6.5
Bi-45	-2.8	-5.8	Bi-2	-3.7	-6.2	Bi-42	-3.3	-6.5
Bi-59	-3.6	-5.8	Bi-134	-3.5	-6.2	Bi-7	-3.0	-6.5
Bi-291	-3.0	-5.8	Bi-38	-3.3	-6.2	Bi-55	-3.7	-6.5
Bi-67	-3.3	-5.8	Bi-127	-3.2	-6.2	Bi-275	-2.4	-6.5
Bi-136	-3.4	-5.8	Bi-322	-2.6	-6.2	Bi-44	-3.1	-6.5
Bi-314	-2.4	-5.8	Bi-158	-3.0	-6.2	Bi-302	-2.3	-6.5
Bi-252	-2.9	-5.9	Bi-142	-3.0	-6.2	Bi-300	-2.1	-6.5
Bi-260	-2.6	-5.9	Bi-28	-3.7	-6.2	BI-195	-3.5	-6.5
Bi-70	-3.1	-5.9	Bi-92	-3.3	-6.2	Bi-120	-3.5	-6.5
BI-169	-2.8	-5.9	BI-200	-2.9	-6.2	BI-185	-3.1	-6.5
Bi-221	-2.7	-5.9	Bi-32	-3.0	-6.2	Bi-219	-2.2	-6.5
Bi-253	-3.0	-5.9	Bi-274	-2.5	-6.3	Bi-272	-2.9	-6.6
Bi-53	-3.5	-5.9	Bi-133	-3.4	-6.3	Bi-157	-2.5	-6.6
Bi-270	-1.7	-5.9	BI-161	-3.1	-6.3	Bi-281	-3.0	-6.6
Bi-115	-2.5	-5.9	Bi-301	-2.1	-6.3	Bi-315	-4.3	-6.6
Bi-244	-3.9	-5.9	Bi-228	-3.3	-6.3	Bi-345	-3.8	-6.6
BI-173	-2.4	-5.9	Bi-305	-2.6	-6.3	Bi-285	-3.7	-6.6
Bi-308	-1.9	-5.9	Bi-96	-3.1	-6.3	Bi-303	-2.6	-6.7
BI-183	-2.7	-5.9	Bi-52	-3.1	-6.3	Bi-277	-2.4	-6.7
Bi-139	-2.8	-5.9	Bi-4	-3.8	-6.3	Bi-10	-3.4	-6.7
Bi-81	-2.5	-5.9	Bi-6	-4.1	-6.3	Bi-289	-2.3	-6.7
Bi-266	-3.0	-5.9	Bi-21	-4.3	-6.3	Bi-246	-2.6	-6.8
Bi-61	-4.5	-7.1	Bi-141	-3.1	-7.3	Bi-286	-3.5	-6.8

Supplement 4-1. Water depth and grainsize of the sediment samples in Panggang, Kepulauan Seribu

No	Sample	water depth (m)	< 125 µm mud	125 - 250 µm fine sand	250 - 500 µm medium sand	500 - 1 mm coarse sand	1 - 2 mm very coarse	> 2mm gravel	FOLK AND WARD METHOD (Geometric µm) MEAN	SORTING	SKEWNESS	KURTOSIS	D10 (mm):	D50 (mm):	D90 (mm):
1	M04_1 upper	0.5	2%	14%	26%	26%	23%	8%	613.6	2.4	0.0	0.8	181.3	604.5	1881.1
2	M04_2 lower	0.5	5%	21%	28%	26%	14%	7%	475.7	2.5	0.1	0.9	149.2	463.2	1702.2
3	M05_1 upper	0.44	5%	23%	33%	26%	10%	2%	395.7	2.3	0.0	0.9	144.9	394.1	1167.4
4	M05_2 lower	0.44	7%	29%	31%	23%	9%	2%	357.1	2.6	0.0	1.2	134.6	345.8	1033.2
5	M06_1 upper	0.5	4%	18%	24%	22%	18%	13%	582.8	2.7	0.0	0.8	156.2	557.2	2172.2
6	M06_2 lower	0.5	5%	17%	30%	28%	13%	7%	487.9	2.4	0.1	1.0	155.6	477.2	1681.5
7	M07_1 upper	15	76%	10%	12%	2%	0%	0%	40.3	4.5	0.1	0.8	6.2	38.0	312.0
8	M07_2 lower	15	80%	8%	9%	2%	0%	0%	36.1	4.3	0.1	0.8	6.0	34.0	294.4
9	M08_1 upper	14	74%	10%	12%	3%	0%	0%	43.3	4.6	0.1	0.8	6.2	40.4	343.3
10	M08_2 lower	14	73%	11%	12%	3%	0%	0%	44.3	4.7	0.1	0.8	6.3	41.5	354.1
11	M09_1 upper	14	76%	9%	11%	3%	0%	0%	40.8	4.5	0.1	0.8	6.1	37.8	329.4
12	M09_2 lower	14	72%	10%	12%	4%	1%	1%	46.8	4.9	0.1	0.8	6.3	43.6	391.3
13	M10_1 upper	11	44%	15%	16%	16%	4%	5%	119.4	6.6	-0.2	0.8	8.6	165.0	967.2
14	M10_2 lower	11	47%	16%	17%	13%	6%	1%	104.7	6.0	-0.2	0.8	8.2	144.9	851.1
15	M11_1 upper	11	72%	16%	7%	5%	1%	0%	43.1	4.6	0.0	0.8	6.3	43.8	323.9
16	M11_2 lower	11	66%	15%	12%	6%	1%	0%	52.1	5.0	0.0	0.8	6.6	53.6	418.0
17	M12_1 upper	12	81%	10%	5%	3%	0%	1%	34.2	4.1	0.1	0.9	6.0	33.3	231.3
18	M12_2 lower	12	67%	11%	11%	11%	0%	0%	55.8	5.5	0.1	0.8	6.5	51.7	557.2
19	M13_1 upper	0.43	3%	16%	26%	26%	22%	6%	573.7	2.4	0.0	0.8	171.1	571.5	1790.3
20	M13_2 lower	0.43	5%	15%	23%	28%	23%	6%	565.2	2.5	-0.1	0.8	158.8	589.4	1755.9
21	M14_1 upper	0.36	4%	10%	18%	31%	28%	9%	702.1	2.4	-0.2	0.9	192.6	750.3	1965.7
22	M14_2 lower	0.36	7%	13%	21%	31%	23%	6%	574.2	2.8	-0.2	1.1	150.6	621.4	1754.9
23	M15_1 upper	0.4	1%	3%	10%	17%	37%	32%	1225.7	2.0	-0.4	0.9	379.2	1426.5	2520.2
24	M15_2 lower	0.4	3%	14%	18%	24%	27%	13%	701.4	2.6	-0.2	0.8	177.5	769.4	2182.0
25	M16_1 upper	0.73	5%	18%	29%	27%	18%	3%	484.7	2.4	0.0	0.9	153.9	478.2	1542.4
26	M16_2 lower	0.73	3%	16%	27%	27%	21%	6%	549.0	2.4	0.0	0.9	165.5	547.3	1724.6
27	M17_1 upper	0.9	5%	17%	25%	25%	21%	5%	523.7	2.6	-0.1	0.9	150.8	527.5	1726.6
28	M17_2 lower	0.9	5%	15%	23%	26%	24%	8%	580.0	2.6	-0.1	0.8	157.5	603.4	1864.6
29	M18_1 upper	0.85	3%	17%	27%	25%	22%	6%	551.2	2.4	0.0	0.8	166.1	546.0	1750.7

30	M18_2 lower	0.85	3%	16%	27%	29%	20%	5%	557.0	2.4	0.0	0.9	171.4	558.1	1701.7
31	M19_1 upper	1	1%	4%	28%	24%	36%	7%	766.9	2.1	-0.1	0.7	281.5	817.0	1895.4
32	M19_2 lower	1	1%	4%	55%	33%	7%	0%	477.1	1.7	0.3	0.9	268.4	445.0	956.6
33	M20_1 upper	0.9	1%	16%	73%	8%	2%	0%	334.6	1.5	-0.1	1.4	181.5	340.4	498.4
34	M20_2 lower	0.9	1%	6%	41%	33%	18%	1%	548.8	1.9	0.1	0.9	262.2	517.6	1396.2
35	M21_1 upper	1	1%	25%	44%	18%	1%	11%	386.2	2.2	0.2	1.3	159.9	362.5	2042.4
36	M21_2 lower	1	0%	34%	60%	6%	1%	0%	285.2	1.6	-0.1	0.9	152.5	301.0	478.5
37	M22_1 upper	0.65	5%	16%	41%	18%	9%	11%	480.2	2.7	0.2	1.2	152.7	407.4	2052.5
38	M22_2 lower	0.65	4%	13%	36%	16%	10%	21%	622.1	2.7	0.3	0.7	173.2	470.6	2385.4
39	M23_1 upper	0.95	2%	7%	31%	33%	18%	9%	649.4	2.3	0.1	1.0	254.8	613.2	1935.1
40	M23_2 lower	0.95	1%	5%	24%	34%	24%	12%	765.3	2.2	0.0	0.9	281.6	751.4	2115.1
41	M24_1 upper	0.9	2%	30%	39%	15%	9%	4%	368.0	2.2	0.2	1.1	148.8	339.7	1225.4
42	M24_2 lower	0.9	3%	26%	31%	12%	11%	18%	528.3	2.9	0.3	0.7	151.5	401.2	2313.5
43	M25_1 upper	0	1%	6%	18%	24%	24%	26%	933.2	2.4	-0.2	0.8	277.9	1016.2	2464.5
44	M25_2 lower	0	0%	3%	10%	19%	30%	38%	1268.0	2.0	-0.4	0.9	396.9	1516.3	2562.3
45	M26_1 upper	0	1%	13%	30%	24%	18%	14%	659.6	2.5	0.1	0.8	197.6	591.8	2212.5
46	M26_2 lower	0	2%	11%	26%	22%	17%	22%	750.1	2.6	0.0	0.7	211.6	708.4	2395.2
47	M27_1 upper	0	1%	8%	15%	17%	26%	33%	1001.7	2.5	-0.4	0.8	254.5	1263.5	2529.2
48	M27_2 lower	0	2%	14%	22%	20%	26%	17%	739.0	2.6	-0.1	0.7	190.0	779.0	2296.4
49	M28_1 upper	0	0%	8%	22%	43%	25%	1%	659.2	2.0	-0.1	1.0	262.6	681.7	1570.3
50	M28_2 lower	0	0%	8%	22%	43%	20%	6%	672.4	2.1	0.0	1.1	261.6	679.8	1752.1
51	M29_1 upper	0	0%	1%	15%	67%	15%	1%	709.1	1.6	0.0	1.4	373.2	707.8	1336.7
52	M29_2 lower	0	1%	2%	25%	54%	17%	2%	641.3	1.8	0.0	1.1	306.3	665.1	1407.6
53	M30_1 upper	0	2%	5%	25%	43%	23%	2%	655.2	2.0	-0.1	1.0	273.8	667.5	1566.9
54	M30_2 lower	0	7%	10%	21%	37%	13%	12%	617.4	2.9	-0.2	1.4	155.9	624.1	2100.9

Supplement 4-2. Microplastic counts in the sediment of Panggang reef platform, Kepulauan Seribu

No	Sample	Recovery	Fibres				Fragments	Film	Total	sediment volume (ml)	Weight dry sediment (g)	normalize plastic/kg	normalize plastic/liter	normalize plastic/m²	Environment	Island
			Black	Blue	Red	White	blue	transparent								
1	M04_Upper	94%	3		1				4	35.0	43.9	91.1	114.3	4158	sand apron with dense seagrass	Panggang
2	M04_Lower								0	35.0	34.9	0.0	0.0	0	sand apron with dense seagrass	Panggang
3	M05_upper		1	2	1				4	35.0	48.6	82.3	114.3	4158	sand apron with dense seagrass	Panggang
4	M05_lower								0	35.0	49.9	0.0	0.0	0	sand apron with dense seagrass	Panggang
5	M06_upper	90%	1	1	1				3	35.0	40.5	74.0	85.7	3119	sand apron with dense seagrass	Panggang
6	M06_lower			3					3	35.0	45.3	66.3	85.7	3119	sand apron with dense seagrass	Panggang
7	M07_upper		3	3	1	1			8	35.0	18.7	428.0	228.6	8316	lagoon	Panggang
8	M07_lower		1	2	3		1		7	35.0	23.4	299.7	200.0	7277	lagoon	Panggang
9	M08_upper	92%		1		1			2	35.0	18.4	109.0	57.1	2079	lagoon	Panggang
10	M08_lower			2					2	35.0	23.6	84.6	57.1	2079	lagoon	Panggang
11	M09_upper								0	35.0	23.1	0.0	0.0	0	lagoon	Panggang
12	M09_lower								0	35.0	20.1	0.0	0.0	0	lagoon	Panggang
13	M10_upper		2			2			4	35.0	32.1	124.8	114.3	4158	lagoon	Semak Daun
14	M10_lower								0	35.0	34.8	0.0	0.0	0	lagoon	Semak Daun
15	M11_upper								0	35.0	51.9	0.0	0.0	0	lagoon	Semak Daun
16	M11_lower	92%							0	35.0	50.5	0.0	0.0	0	lagoon	Semak Daun
17	M12_upper								0	35.0	29.8	0.0	0.0	0	lagoon	Semak Daun
18	M12_lower								0	35.0	24.2	0.0	0.0	0	lagoon	Semak Daun

19	M13_upper	82%		4					4	35.0	37.9	105.5	114.3	4158	sand apron with dense seagrass	Semak Daun
20	M13_lower		1	1	1				3	35.0	58.4	51.4	85.7	3119	sand apron with dense seagrass	Semak Daun
21	M14_upper			1	1				2	35.0	56.6	35.4	57.1	2079	sand apron with dense seagrass	Semak Daun
22	M14_lower				1				1	35.0	57.7	17.3	28.6	1040	sand apron with dense seagrass	Semak Daun
23	M15_upper	86%		1					1	35.0	33.5	29.8	28.6	1040	sand apron with dense seagrass	Semak Daun
24	M15_lower			1					1	35.0	56.0	17.9	28.6	1040	sand apron with dense seagrass	Semak Daun
25	M16_upper		1	2	1				4	35.0	43.4	92.1	114.3	4158	sand apron without seagrass	Semak Daun
26	M16_lower		1						1	35.0	61.8	16.2	28.6	1040	sand apron without seagrass	Semak Daun
27	M17_upper	88%	2	1					3	35.0	49.7	60.3	85.7	3119	sand apron without seagrass	Semak Daun
28	M17_lower					1			1	35.0	57.2	17.5	28.6	1040	sand apron without seagrass	Semak Daun
29	M18_upper		1	2					3	35.0	70.4	42.6	85.7	3119	sand apron without seagrass	Semak Daun
30	M18_lower			2	1				3	35.0	76.5	39.2	85.7	3119	sand apron without seagrass	Semak Daun
31	M19_upper	80%	1	3	1				5	35.0	40.6	123.1	142.9	5198	intertidal beach	Semak Daun
32	M19_lower		2	1	2				5	35.0	73.8	67.7	142.9	5198	intertidal beach	Semak Daun
33	M20_upper		1	5					6	35.0	65.2	92.1	171.4	6237	intertidal beach	Semak Daun
34	M20_lower		4	2					6	35.0	53.6	111.9	171.4	6237	intertidal beach	Semak Daun
35	M21_upper		3	2	1				6	35.0	57.1	105.2	171.4	6237	intertidal beach	Semak Daun
36	M21_lower	94%	4		1				5	35.0	61.1	81.8	142.9	5198	intertidal beach	Semak Daun

37	M22_upper		2	1	1				4	35.0	47.9	83.6	114.3	4158	reef crest	Semak Daun
38	M22_lower	90%	1						1	35.0	46.4	21.5	28.6	1040	reef crest	Semak Daun
39	M23_upper			2	1				3	35.0	46.8	64.1	85.7	3119	reef crest	Semak Daun
40	M23_lower		1	2	1				4	35.0	59.1	67.7	114.3	4158	reef crest	Semak Daun
41	M24_upper			2					2	35.0	48.1	41.6	57.1	2079	reef crest	Semak Daun
42	M24_lower	94%	2						2	35.0	48.5	41.3	57.1	2079	reef crest	Semak Daun
43	M25_upper		1	1					2	35.0	39.0	51.3	57.1	2079	reef crest	Panggang
44	M25_lower		2	1					3	35.0	38.2	78.5	85.7	3119	reef crest	Panggang
45	M26_upper		2	1					3	35.0	47.8	62.8	85.7	3119	reef crest	Panggang
46	M26_lower	84%		1				1	2	35.0	43.0	46.5	57.1	2079	reef crest	Panggang
47	M27_upper		1	1					2	35.0	58.9	33.9	57.1	2079	reef crest	Panggang
48	M27_lower		1						1	35.0	50.1	20.0	28.6	1040	reef crest	Panggang
49	M28_upper			2					2	35.0	49.9	40.1	57.1	2079	intertidal beach	Panggang
50	M28_lower	84%	1						1	35.0	68.7	14.5	28.6	1040	intertidal beach	Panggang
51	M29_upper		1						1	35.0	41.2	24.3	28.6	1040	intertidal beach	Panggang
52	M29_lower		1				1		2	35.0	50.3	39.7	57.1	2079	intertidal beach	Panggang
53	M30_upper								0	35.0	54.0	0.0	0.0	0	intertidal beach	Panggang
54	M30_lower	94%							0	35.0	46.4	0.0	0.0	0	intertidal beach	Panggang
	Mean	89%									46.5	59.2	69.8	2541		
	Total		48	56	20	5	2	1	132							